UNCLASSIFIED

AD NUMBER
AD477285
LIMITATION CHANGES
TO: **Approved for public release; distribution is unlimited.**
FROM: **Distribution authorized to U.S. Gov't. agencies and their contractors; Administrative/Operational Use; OCT 1965. Other requests shall be referred to Office of Naval Research Washington, DC.**
AUTHORITY
onr notice 27 jul 1971

THIS PAGE IS UNCLASSIFIED

S 256-2

AD 477285

FINAL REPORT

CONTRIBUTIONS TO THE MONO LAKE EXPERIMENTS

VOLUME I

PREDICTIONS OF THE WATER WAVES AND RUN-UP GENERATED BY TNT EXPLOSIONS IN MONO LAKE

nes

Contract No. Nonr 5006(00)
October 1965

NATIONAL ENGINEERING SCIENCE CO.

Prepared for
DEPARTMENT OF THE NAVY
Office of Naval Research
Washington 25, D. C.

FINAL REPORT

CONTRIBUTIONS TO THE MONO LAKE EXPERIMENTS

Research conducted for:

Department of the Navy
Office of Naval Research
Washington 25, D. C.

VOLUME I

PREDICTIONS OF THE WATER WAVES AND RUN-UP GENERATED BY TNT EXPLOSIONS IN MONO LAKE

Prepared by:

Bernard J. Le Méhauté
Robert W. Whalin
Lois M. Webb

October 1965

Contract No. Nonr 5006(00)

NESCO Report S-256-2

NATIONAL ENGINEERING SCIENCE COMPANY
711 South Fair Oaks Avenue
Pasadena, California 91106

FOREWORD

This is Volume I of the final report under Contract No. Nonr 5006(00). The predictions which were performed before the test (Interim Report No. SN 256-1) are contained in this volume together with some additional predictions that were omitted from the previous report because of new information on test conditions and because of insufficient time between contract reception and field test initiation. The method of prediction is described in this report, and Vols. II and III contain complete descriptions of the linear theories employed in these predictions. Volume II also contains some natural extensions of the linear constant depth theory which may prove very useful for further considerations.

It is interesting to note that since the work of wave prediction has been performed, two studies which are of direct interest to the Mono Lake project have been achieved under the sponsorship of ONR and SRI. They are "A Generalized Theory for Waves on a Slope" including nonlinear effects, bottom friction and wave reflection, and "A Synthesis of Theory and Experiments on Wave Run-up". This predicting work has only partly benefitted from these two studies, which will be published in the near future.

CONTENTS

ABSTRACT

The purpose of this project was to predict the water waves generated by the Mono Lake field tests. These tests consisted of detonating ten TNT explosions of approximately 9500 pounds each, and measuring the water waves and run-up produced by the detonations.

This volume of the final report contains these predictions and a brief description of the theoretical and empirical methods employed in performing the predictions. The predictions presented here are precisely those issued in Interim Report SN 256-1 prior to the field tests with the exception of the run-up on radial 2 where the slope of the deck was changed from 1/40 to 1/30. The run-up predictions for radial 2 have been altered to reflect this change and those for radial 3 have been eliminated since that run-up deck was eliminated during the field tests. This report gives an indication of the reliability of the predictions by inserting a maximum expected envelope for the deep water predictions. The addition of more predictions was deemed useless since all predictions will have to be altered slightly for correlation with the field test data so that they coincide with the precise charge weight and geometry at shot time. Any additional predictions necessary for correlation with the experimental data can be performed with maximum efficiency at that time.

1. INTRODUCTION

The purpose of this project was to perform predictions of the water waves, prior to the field tests, produced by TNT explosions in Mono Lake. This objective has been fulfilled with Interim Report SN 256-1 and this volume of the final report. Furthermore, Vols. II and III of the final report contain clear elucidations of the linear theories used to perform some of these predictions as well as extensions to a more generalized formulation of the linear theory. The results of this project and the experimental data from the field tests will form a firm basis upon which to evaluate the state of the art in performing such predictions, at least for relatively small high-explosive detonations.

The predictions were based on a preliminary experimental plan and a topographical map of Mono Lake. Slight alterations of the predictions will have to be performed prior to a correlation with the experimental data to account for variations from the original plan. The charge weight will not be precisely 9500 pounds and the measurement stations may vary slightly relative to ground zero (GZ). It was originally planned to extend the artificial run-up decks into the water in order to provide a constant slope from the point of breaking inception through the run-up. This was not accomplished and may have a non-negligible effect on the wave run-up. The planned run-up deck on radial 3 was eliminated and the slope of the deck on radial 2 was altered in the field. These changes are reflected in the predictions of this report. All these variations can be compensated for upon analyzing the field data for verification of the various methods employed in performing the predictions.

The predictions performed consist of amplitude time curves at every station on the constant depth radial. The computations were made from the initial assumption of a stationary symmetric water cavity with a lip, and the asymptotic solution was used at all measurement stations.

The use of the asymptotic solution at the nearest station is not warranted near the front of the wave train; however, this can be analyzed when the field data are available.

The theory of Roseau was used to compute the wave amplification over the area simulating the continental slope and this theory includes reflection as well as linear shoaling as a function of wave number. Each point of the wave envelope as computed by the axially symmetric constant depth linear theory was modified by an amplification factor from Roseau. The phase of the waves within the envelope was calculated from the former theory. It was found that the waves within the wave train should behave according to the linear shoaling theory and the reflection effect was negligible.

The wave propagation over the simulated continental shelf was again computed from the linear shoaling theory by calculating the amplification factor for each point of the wave envelope up to the point of breaking inception. No dispersion was predicted during the propagation over this area since the first envelope of the wave train consists of shallow water waves in this area (i.e., $\lambda >> 1d$). The effects of both viscous and turbulent friction were considered and nonlinear propagation effects were found to be negligible except in the near breaking area where they were included in a factor accounting for this effect.

Predictions of the wave run-up for the maximum waves were made from the curves of Saville. It was found that the maximum run-up should correspond to the waves of maximum amplitude. It was assumed that the bottom slope was constant and equal to the slope of the artificial run-up decks. A prediction of the run-up of each predicted wave from one shot at the 1/50 slope was performed. The curves of Saville were used for all but the leading wave which was computed from the theory of Le Méhauté for a solitary wave.

From preliminary reports of the run-up, it appears that all predictions were within 50 percent of the measured values; however, a true assessment of the validity of various theories will have to wait for a comprehensive correlation of the field data with the predictions.

2. SHOT GEOMETRY, WAVE INSTRUMENTATION, AND DESIRED PREDICTIONS

The primary purpose of the Mono Lake test series is to obtain reliable data from field tests which will allow an assessment of the various theories developed for the prediction of the surface water wave effects and wave run-up produced by underwater explosions. Accordingly, a preliminary experimental plan was established with the assistance of cognizant personnel involved in the DOD wave program. The Waterways Experiment Station at Vicksburg, Mississippi implemented this preliminary plan and carried out the field tests. This section of the report presents the shot geometry, experimental plan and desired predictions.

Figure 1 depicts Mono Lake with the depth contours and proposed instrumentation. The run-up decks indicated were changed after the predictions had been performed. The radial 1 run-up deck remained as planned, radial 3 was not instrumented for run-up, and the slope of the run-up deck on radial 2 was altered from 1/40 to 1/30. The artificial run-up decks were not extended into the water and the actual bottom profile near shore of radials 1 and 2 are shown in Fig. 2. These profiles were recorded one day before detonation of the first shot of the test series and were furnished by Dr. R. E. Kent.

The charges detonated were spherical TNT charges of approximately 9500 pounds, the precise charge weight being determined at the test site. Charge placement was performed with a triangular shaped surface float made of relatively light material having little effect upon the generation process. Table 1 shows the geometry of the detonations. Predictions were performed for shots 1 - 9. Shot 10 was a shallow water explosions which can be used to validate the nonsaturated breaker theory of Le Méhauté.

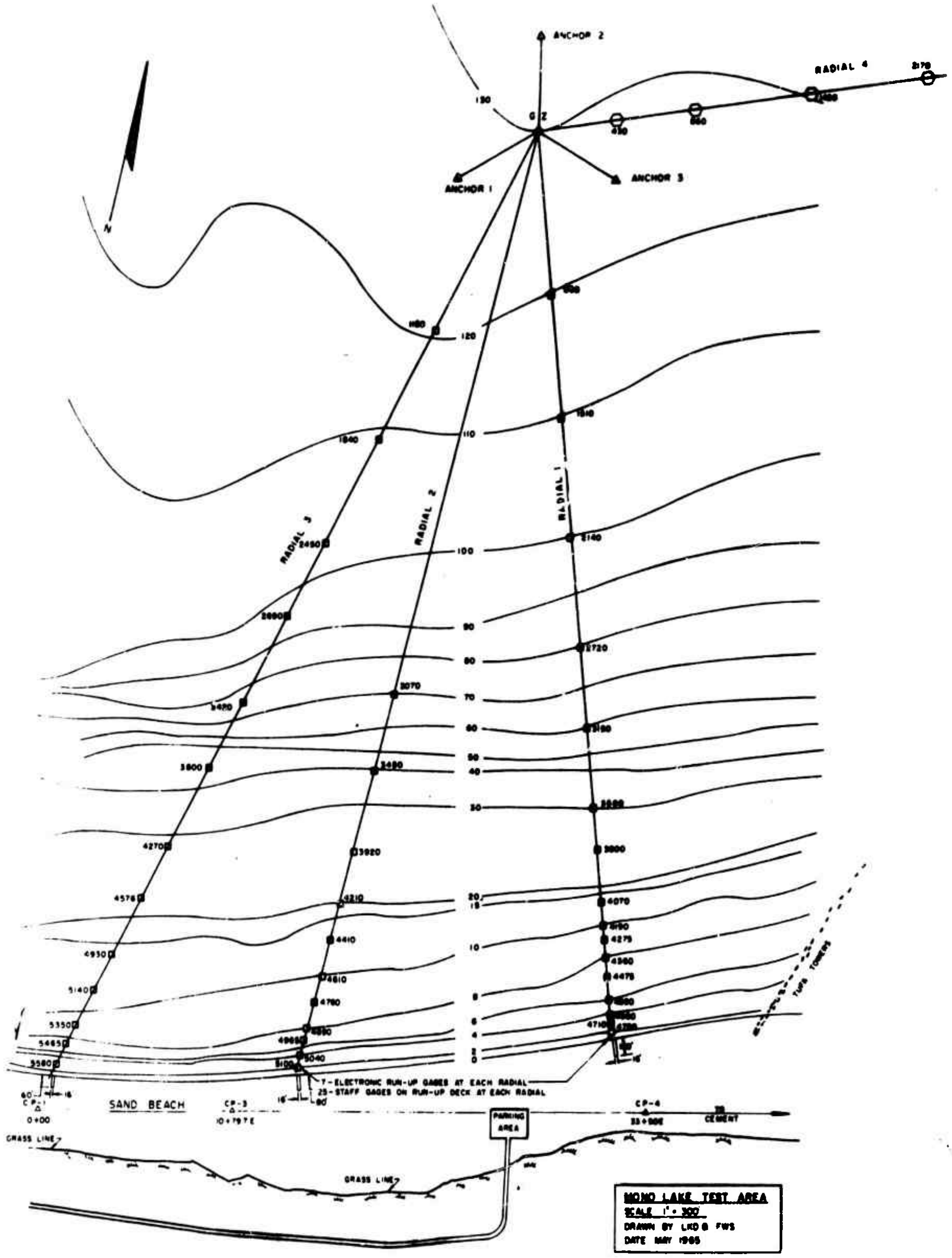

Figure 1

Mono Lake Bottom Topography and Planned Instrumentation

PC-3-7464

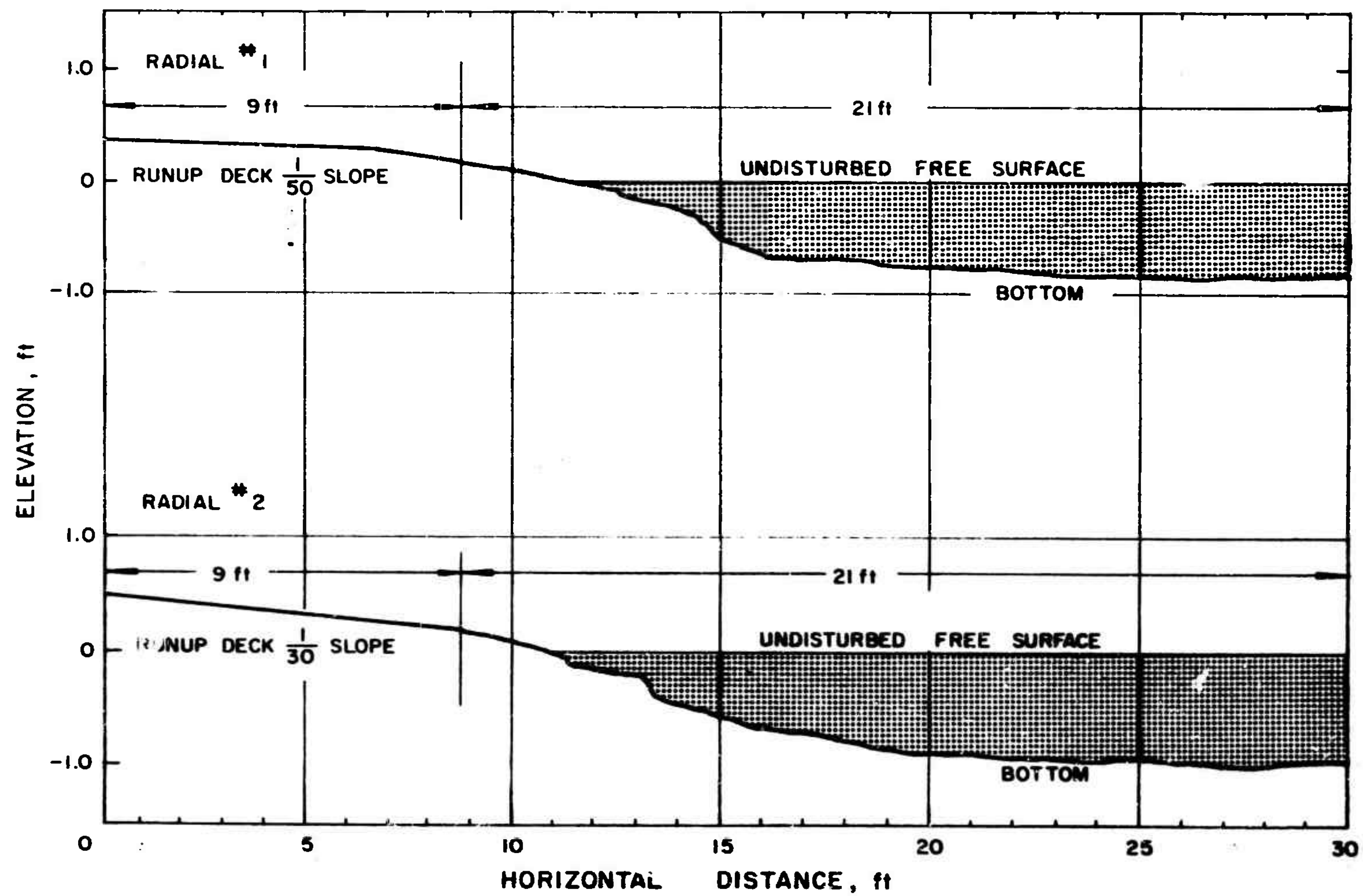

Figure 2

Near Shore Bottom Profiles One Day Prior to the Initial Detonation

PB-3-7465

TABLE 1

PLANNED SHOT GEOMETRY

Shot No.	Explosion Depth (z, ft.)	Reduced Depth ($z/W^{0.3}$)
1	- 8.64	-0.54
2	- 1.08	-0.07
3	-54.0	-3.41
4	- 4.32	-0.27
5	0.00	0.00
6	-43.2	-2.73
7	- 1.51	-0.10
8	-64.8	-4.08
9	- 0.65	-0.04
10	undecided	-----

Shots 1 - 9 detonated at GZ as shown in Fig. 1

Assumed W = 9500 lbs.

3. METHOD OF PREDICTION

The predictions involved the use of four methods, each of which is described below. The expected reliability of each method is discussed and indicated in the deep water predictions.

3.1 Generation Mechanism and Deep Water Predictions

The generation mechanism was simulated by a stationary symmetric water cavity with a lip such that the volume of water above the undisturbed free surface (lip volume) was equivalent to the volume of the water cavity. This condition conserves the mass of the fluid and, analytically speaking, removes the bore from the front of the wave train. Previous experimental results indicate that a bore does not precede the wave train. Figure 3 shows the initial deformation considered.

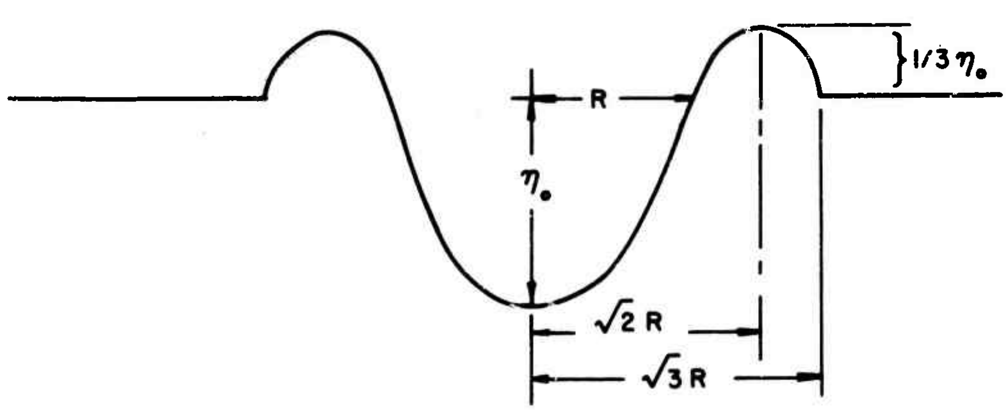

Figure 3
Representation of the Generation Mechanism

This initial deformation is represented by

$$\eta_o(r_o) = \begin{cases} \eta_o \left[\dfrac{r_o^4}{3R^4} - \dfrac{4r_o^2}{3R^2} + 1 \right] & r_o \leq \sqrt{3}\ R \\ 0 & r_o > \sqrt{3}\ R \end{cases}$$

The usual asymptotic solution (method of stationary phase, m. s. p.) was used to evaluate the integral obtained from the solution to the Laplace equation in cylindrical coordinates with the linearized free surface condition, the bottom condition for constant water depth, the above initial deformation and zero initial velocity distribution in the fluid. The wave amplitude is then expressed by

$$\eta(r,t) = \frac{1}{r} \sqrt{\frac{m\varphi(m)}{-\varphi'(m)}}\ \overline{\eta}_o(m) \cos\left(mr - \sqrt{m \tanh m}\ t\right)$$

where

$r = r'/d$ = dimensionless distance from the origin

$m = m'd$ = dimensionless wave number

$t = t'\sqrt{\frac{g}{d}}$ = dimensionless time after the detonation

$$\varphi(m) \equiv \frac{1}{2} \sqrt{\frac{\tanh m}{m}} + \frac{1}{2 \cosh^2 m} \sqrt{\frac{m}{\tanh m}} = \frac{r}{t}$$

and the prime variables are dimensional

$\overline{\eta}_o(m)$ = zero order Hankel transform of the initial deformation

$$\overline{\eta}_o(m) = \int_o^\infty \eta_o(r_o)\, J_o(mr_o) r_o\, dr_o = \frac{4\eta_o}{m^2}\ J_4(\sqrt{3}\ mR)$$

$\eta(r,t) = \eta'(r,t)/d$

d = water depth (constant)

g = gravitational acceleration

The above solution for the wave amplitude is developed in detail in Vol. II of this final report in which its relative merits and limitations are discussed. Such natural extensions within the scope of the linear constant depth theory are also discussed in that volume; especially those regarding a time dependent or asymmetrical initial deformation.

The evaluation of the parameters of the initial deformation, η_0 and R, is accomplished through the empirical relations (Whalin, 1965a) established from an analysis of WES test series. Table II shows various parameters at the maximum of the first envelope, all of which were computed from the empirical relationships that were derived from WES data.

The predictions on the constant depth radial, No. 4, appear in Appendix A. The uncertainty in the predictions is approximately ±20 percent. However, a maximum expected amplitude is represented on the predictions and the probability of any measurements exceeding this limit is small (approx. 0.02 - 0.05).

The arrival times at all proposed measurement stations were computed by using an average value, $\sqrt{g h}$, for the velocity of propagation of the wave front between each indicated depth contour of Fig. 1. These arrival times are given in Table III.

TABLE II

PARAMETERS AT THE MAXIMUM OF THE FIRST ENVELOPE (CONSTANT DEPTH)

Shot No.	$\eta'_{max}\, r'(ft^2)$	$k'_{max}\,(ft^{-1})$	λ'_{max} (ft)	T'_{max} (sec)
1	942	0.0291	216	6.5
2	1476	0.0337	187	6.1
3	1237	0.0291	216	6.5
4	956	0.0315	200	6.3
5	1265	0.0344	182	6.0
6	1251	0.0291	216	6.5
7	1336	0.0334	188	6.1
8	1054	0.0291	216	6.5
9	1547	0.0340	185	6.1

TABLE III

PREDICTED ARRIVAL TIMES AT ALL MEASUREMENTS

Station No.	Radial Distance from GZ (ft)	Arrival Time(sec)	Station No.	Radial Distance from GZ (ft)	Arrival Time(sec)
1-1	860	13.56	2-9	4965	127.44
1-2	1510	23.91	2-10	5040	133.07
1-3	2140	34.74	2-11	5100	139.18
1-4	2720	45.52	2-12	5140	146.23
1-5	3150	54.57			
1-6	3580	66.21	3-1	1180	18.56
1-7	3800	73.61	3-2	1840	29.41
1-8	4070	84.08	3-3	2450	39.85
1-9	4190	90.18	3-4	2890	47.61
1-10	4275	95.04	3-5	3420	57.69
1-11	4360	100.17	3-6	3800	66.42
1-12	4475	107.57	3-7	4270	80.20
1-13	4590	115.52	3-8	4576	90.88
1-14	4660	121.04	3-9	4930	105.45
1-15	4710	125.75	3-10	5140	115.72
1-16	4760	131.32	3-11	5350	127.18
1-17	4780	136.61	3-12	5465	134.26
			3-13	5580	143.38
2-1	3070	52.18	3-14	5655	153.69
2-2	3480	61.77			
2-3	3920	75.81	4-1	430	6.46
2-4	4210	86.58	4-2	860	13.29
2-5	4410	95.64	4-3	1420	21.95
2-6	4610	106.14	4-4	2170	33.54
2-7	4750	114.15	4-5	3230	49.92
2-8	4890	122.61			

3.2 Predictions at Stations over the Simulated Continental Slope

The general problem of determining the amplitude of a wave propagating over an uneven bottom is accomplished from the following formula for periodic waves extracted from a pending report on generalized theory for waves on a slope:

$$F_{av_t} = F_{av_i} \frac{r_o}{r} \left[1 - R_{(x)}^2 - \frac{1}{r_o F_{av_i}} \int_{r_o}^{r} r(D_f + D_p)\, dr \right]$$

where F_{av} is the energy flux, subscript t refers to the transmitted wave, and subscript i refers to the incident wave.

F_{av} is given by various formulas, depending upon the value of the Ursell parameter.

1) On the deep water side,

$$\frac{H}{L}\left(\frac{L}{d}\right)^3 \ll 1,$$

the linear theory can be used. Also, the principle of super-position is applied in such a way that R can be determined by application of the modified Roseau theory (assuming that nonlinear effects have a negligible influence on reflection).

2) On the shallow water side, the value of the transmission coefficient obtained from the Roseau theory does not always apply when

$$\frac{H}{L}\left(\frac{L}{d}\right)^3 \cong 1.$$

Then F_{av} must be expressed by nonlinear theory, such as the Stokes theory at the third order, or the cnoidal wave theory.

3) When

$$\frac{H}{L}\left(\frac{L}{d}\right)^3 >> 1,$$

a nonlinear theory must be applied. For the sake of simplicity, and due to the timing, the following value has been used for the case of shallow water:

$$\frac{1}{2}\rho g H^2 \sqrt{g (d + H)}$$

An exception must be made for a depth smaller than $1.3\ d_b$ (depth of breaking), in which case a more complex theory has to be used.

D_f and D_p are the dissipative functions due to bottom friction and permeability.

$$D_f = \frac{4}{3}\pi^2 \frac{\rho f H^3}{T^3 (\sinh k d)^3}, \quad f = \frac{2}{C_h^2} = 14.6 \frac{n^2}{d^{1/3}}$$

$$D_p = \frac{4\pi^2}{\nu T^2} \frac{\rho g p H^2}{\sinh 2 k d}, \quad k = \frac{2p}{\nu}$$

D_f has been calculated by assuming the shearing stress at the bottom to be quadratic and the friction factor to be $n = 0.03$. As a matter of fact, we may still be in a transitional regime. D_p was calculated by assuming the Darcy coefficient to be $K = 0.005$, which corresponds to the texture of the sand in Mono Lake insofar as it can be determined.

In practice, bottom friction effects have been neglected on the continental slope and wave reflection has been neglected on the continental shelf.

The problem of propagating the explosion-generated wave train over an uneven bottom, which resembles a continental slope, was solved approximately by the linear theory of the propagation of periodic waves over a continental slope (Vol. III of this report). This particular theory allows one to consider the propagation of periodic waves over a bottom contour of the shape shown in Fig. 4. The parameters of this bottom contour

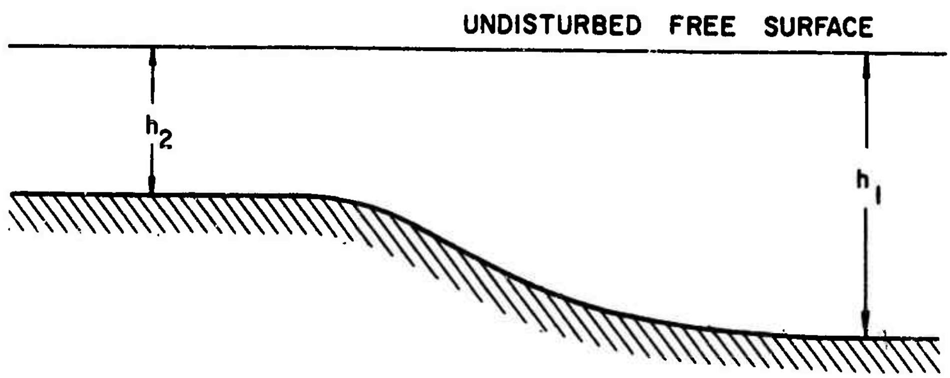

Figure 4
Roseau Bottom Contour

can be chosen so that it approximately fits a continental slope contour. The methods and Tables necessary for fitting these contours to various cases are given in Section 7, Vol. III of this report. The parameters $\rho = h_1/h_2 = 6$ and $\alpha = \pi/28$ were found for the Mono Lake radials. The reflection coefficient was negligible for Mono Lake in the period range $5 < T < 50$ seconds which includes, for all practical purposes, the entire first envelope of the wave train. The transmission coefficient is shown as function of period in Fig. 5.

In applying this theory one merely modifies the wave envelope by multiplying respective points on the envelope by the transmission coefficient given in Fig. 5. This factor gives the frequency modification due to linear shoaling and a linear reflection coefficient, where it must be assumed that the frequencies associated with respective points on the wave envelope behave in a similar manner to periodic progressive waves where the principle of conservation of energy flux is assumed. Initially, this may seem to be a drastic assumption for explosion-generated waves. However, if one computes the wave envelope from the linear constant depth theory and considers the values of d, T, and λ associated with various points of the envelope and plots these points on Fig. 6, then they all coincide very closely to line of linear wave shoaling. This indicates that the wave envelope should indeed behave in a linear manner consistent with the theory being applied. Actually, this should not come as a surprise since linear theories are being applied throughout both these phases of the wave propagation. Therefore, it is concluded that the frequency modification factor for the wave envelope, computed in this manner, should be reliable. Since the reflection coefficient is negligible, the end result is equivalent to applying the linear shoaling theory for periodic waves by using the method of conservation of energy flux. In addition, it also is equivalent to the geometrical optics method (Van Dorn, 1964) when applied to a radial which is normal to the bottom contours. The preceding three methods of computing a frequency modification factor for the wave envelope are equivalent under the specified conditions.

Appendix B contains amplitude time curves predicted at Mono Lake for one station on each radial where the wave envelope has been modified by the factor shown in Fig. 5. It is difficult to assess the reliability of this method in modifying the wave envelope, however, it is anticipated that the results will be reliable within ± 20 percent.

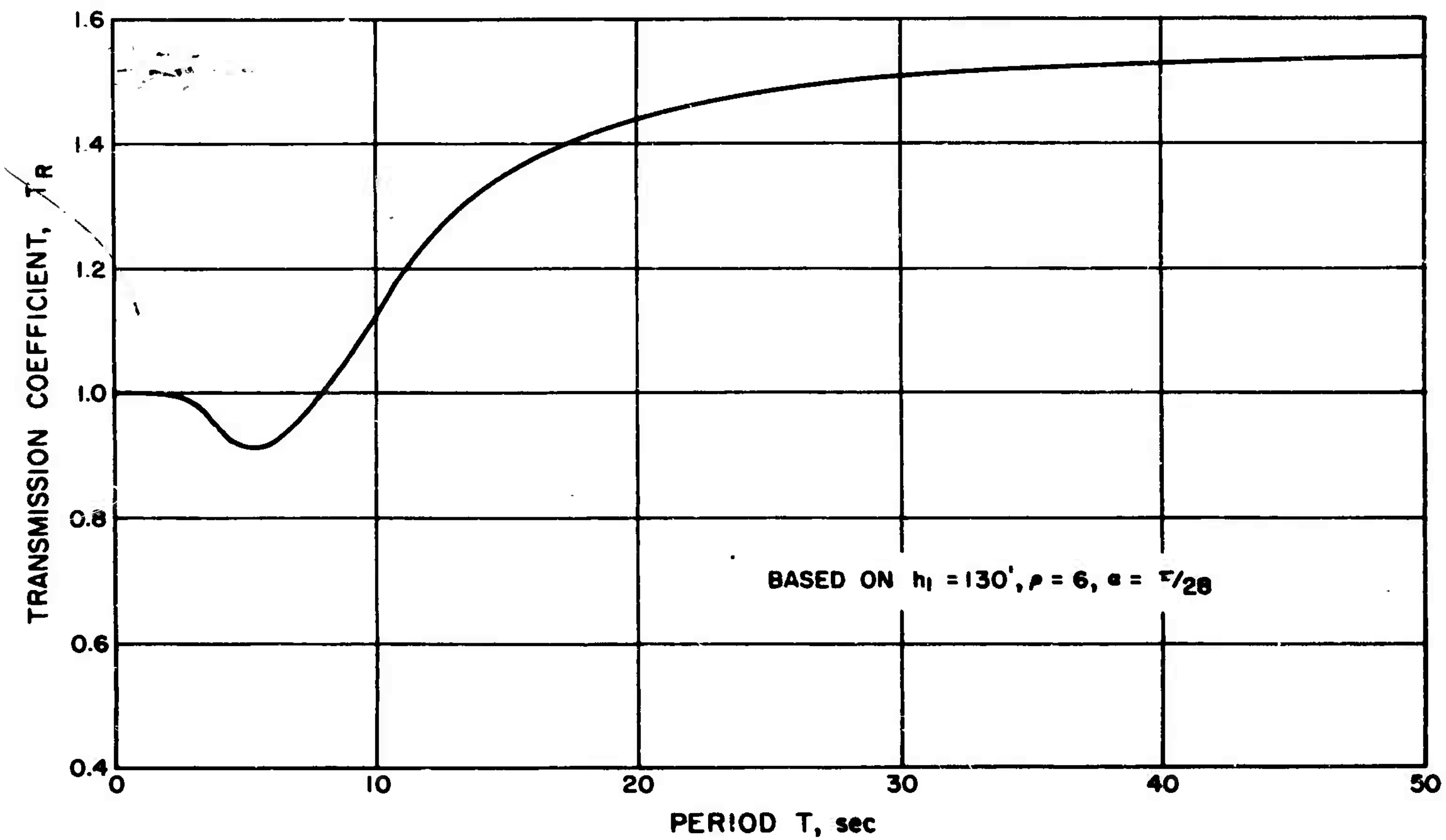

Figure 5

Transmission Coefficient as a Function of Period for the Mono Lake Bottom Contour

PA-3-7402

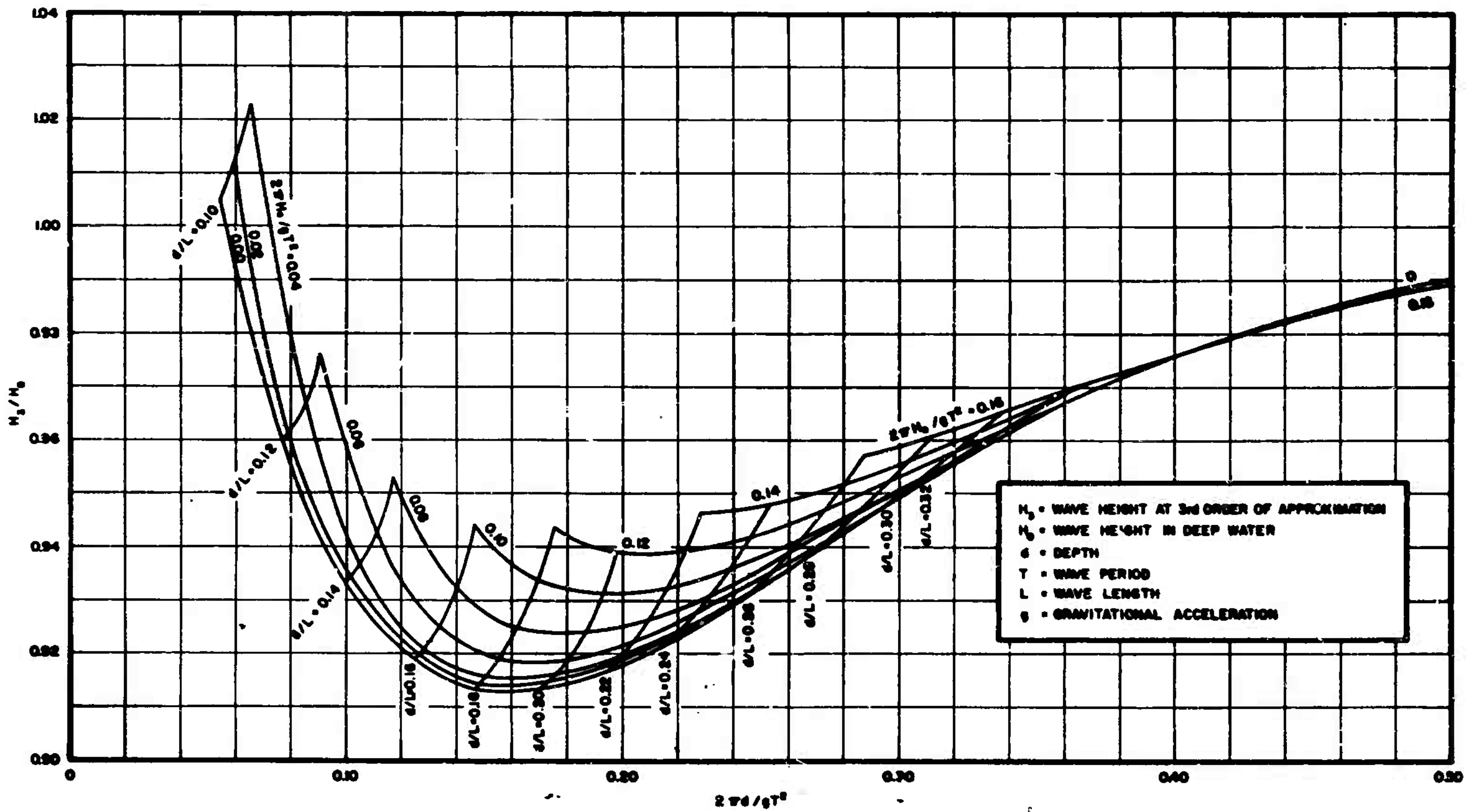

FIGURE 6

WAVE SHOALING CHARACTERISTICS AT THE THIRD ORDER OF APPROXIMATION

PC-3-7466

3.3 Wave Propagation on the Shelf

The wave propagation on the shelf and up to the point of breaking inception involved the consideration of the following phenomena:

a) Wave shoaling; should linear or nonlinear shoaling theory be used?

b) Wave damping due to both viscous and turbulent friction.

c) The wave height decay due to radial spreading. The distance from the explosion is not sufficient for this effect to be negligible.

d) The so-called "super elevation" of the waves just prior to breaking.

e) The increase in the number of waves in the first envelope due to dispersion.

As an input to this phase of the wave propagation, we have the amplitude time curves of Appendix B for each shot at a measurement station near the edge of the shelf. The question of dispersion (e) is the easiest one to resolve. From Appendix B one can observe that the wave heights are small and, from the periods associated with the wave train it is obvious that the wave lengths are sufficiently long that the waves are shallow water waves. Hence no dispersive effects are to be expected during the propagation over the shelf.

The next question to be considered is wave shoaling (a). From comparisons of the linear and nonlinear shoaling curves with the characteristics of the wave trains at the edge of the shelf, it was determined that the waves should behave in a linear manner, at least up to the near breaking point. Furthermore, computer runs were made where the effect of the nonlinear terms was considered and they were found to be negligible (less than 1 percent). Therefore, the linear shoaling theory is to be applied to each wave of the wave train and nonlinear effects are ignored up to the near-breaking point.

The effect of the radial spreading on the wave amplitude is compensated for by the usual term of $(R_1/R_2)^{1/2}$, R_1 being the distance from GZ to the stations at the edge of the shelf and R_2 the distance from GZ to the station where the wave amplitude is desired.

The friction effect is to be considered next. Both viscous and turbulent friction must be considered. The term that represents the friction and permeability effect for periodic waves is

$$\left[1 - \frac{2}{3\pi} \frac{f H \Delta x}{d^2} - \frac{4\pi}{T} \frac{K}{d} \Delta x\right]$$

where

- K = permeability coefficient
- H = wave height
- d = water depth
- Δx = distance of propagation
- f = $14.6\, n^2/d^{1/3}$ and
- n = the Manning coefficient, which is taken to be 0.03.

In the case of solitary waves, the term accounting for the friction effect becomes

$$\left[1 - \frac{8}{15} \frac{f H \Delta x}{d^2}\right]$$

This formulation is to be used for the leading wave.

Therefore, the computation of the wave height at a depth d_2 from the known height, a depth d_1 for periodic waves, is found from the formula

$$H_2 = H_s\left[1 - \frac{2}{3\pi} \frac{(14.6)\, n^2 H_1 (R_2 - R_1)}{\left(\frac{d_2 + d_1}{2}\right)^{7/3}} - \frac{4\pi}{T} \frac{K(R_2 - R_1)}{\left(\frac{d_1 + d_2}{2}\right)}\right]\left[\frac{R_1}{R_2}\right]^{1/2}$$

where nonlinear effects on the shoaling are negligible and H_s is the wave height obtained from tables of wave shoaling data. The computations were performed on the computer in a step-by-step procedure between each given depth contour until the breaking criteria of $H_b = 0.78\ d_b$ was exceeded. To account for the so-called "super-elevation" near the breaking depth the amplitude was computed at a depth $d_n = 1.3\ d_b$. This value of the wave height at breaking was then multiplied by the factor 1.4 to account for the "super elevation" which has been observed experimentally. That is, $H_b = 1.4\ H_{d_n}$. The reason for this discrepancy with the Airy theory is undoubtedly due to nonlinear effects in the near-breaking region as the wave transforms from a symmetrical wave which does conform to the Airy theory to a humped wave profile which conforms to the solitary wave regime. These computations of the breaking wave height result from a combination of theoretical and experimental research and are deemed to provide the best reliability in performing predictions.

In order to obtain predictions at any station on the shelf one merely applies the linear shoaling theory to the predictions of Appendix B and corrects these by the factors accounting for friction and radial spreading. For the leading waves, predictions at any station on the shelf can be obtained from Figs. 7, 8, and 9, which show the wave modification on the shelf as a function of the distance from GZ for various initial wave amplitudes along radials 1, 2, and 3 respectively. The modification of wave amplitudes not depicted on these graphs can be performed by a linear interpolation between the given lines.

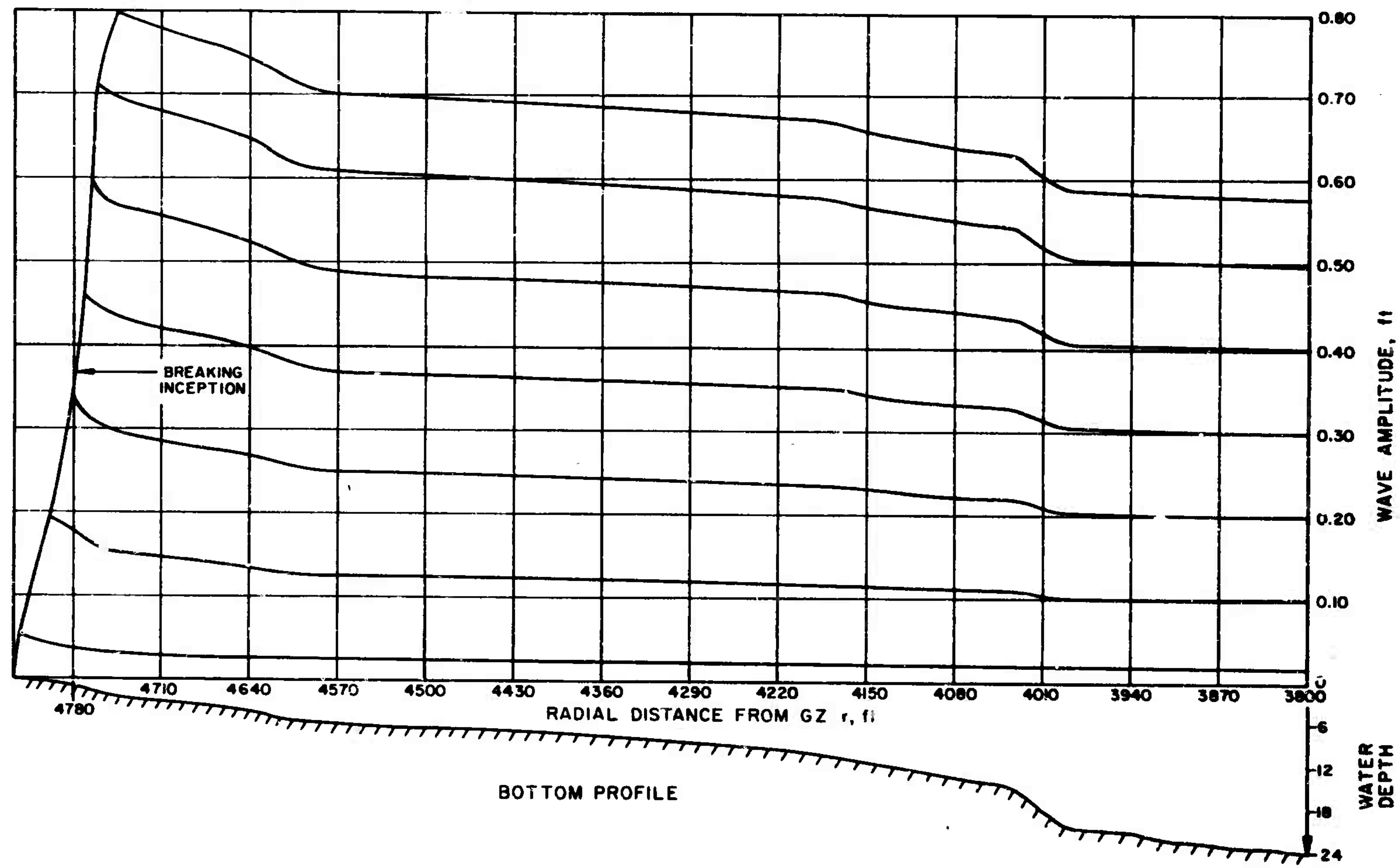

Figure 7
Wave Modification over the Shelf for Leading Waves (T >9 sec) Radial 1

PB-3-7467

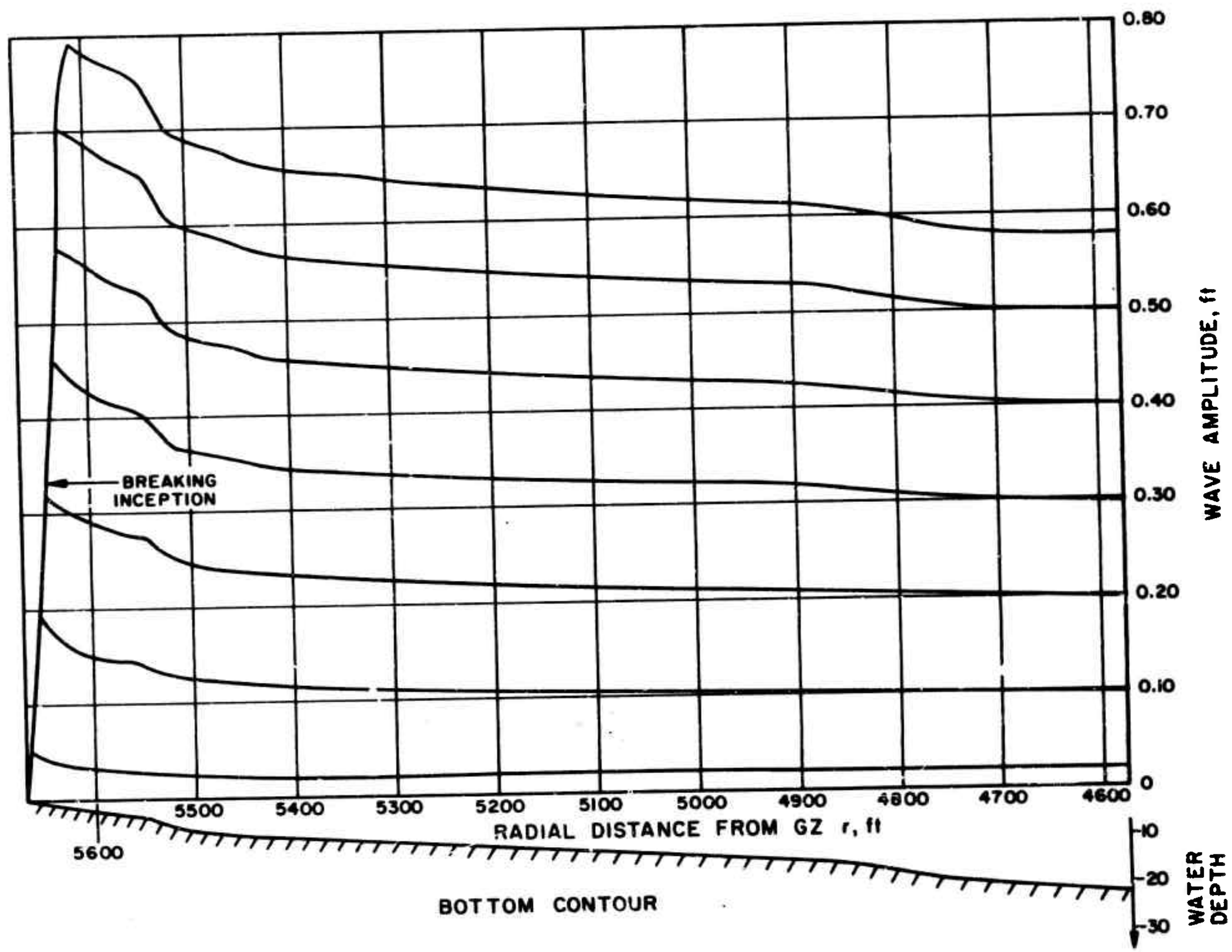

Figure 8
Wave Modification over the Shelf for Leading Waves (T > 9 sec) Radial 2

PB-3-7468

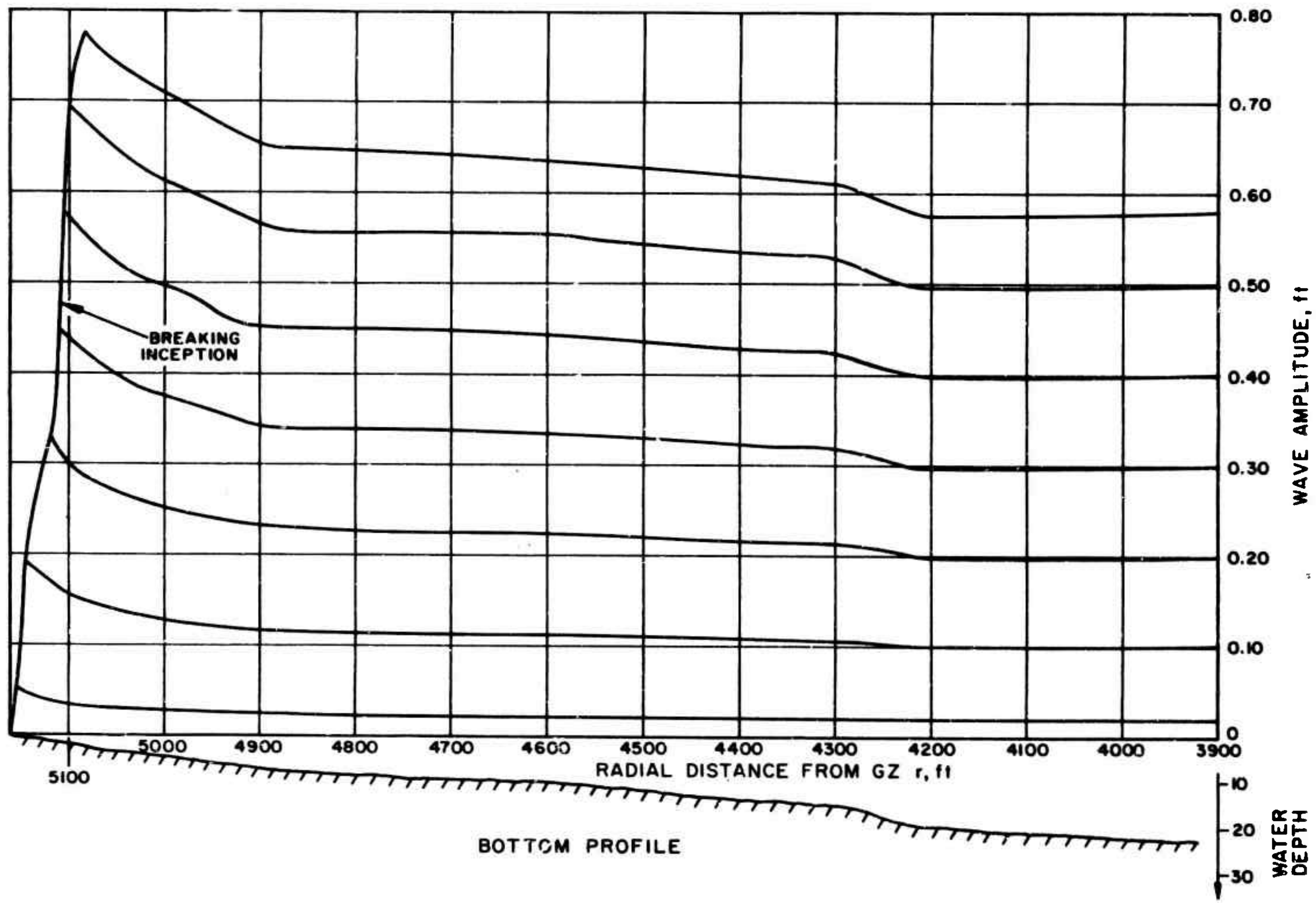

Figure 9
Wave Modification over the Shelf for Leading Waves (T > 9 sec) Radial 3

PB-3-7469

3.4 Run-up Predictions

The prediction of the wave run-up involves the assumption that three-dimensional effects are negligible and the determination of the type of wave present. That is, the following questions must be considered:

a) Are three-dimensional effects important?

b) Is the wave which is causing the run-up a breaking or a non-breaking wave?

c) If the wave is a breaking wave, is it

   1. a non-saturated breaker?

   2. a plunging breaker?

   3. an intermediate type of breaker?

d) Does the backwash have a non-negligible effect on the run-up of successive waves?

The shoreline contours at Mono Lake are very regular and three-dimensional effects on the wave run-up were considered negligible, especially on the artificial run-up decks where the predictions were performed.

It was determined that all but the leading wave and perhaps the second and third waves were breaking waves, probably of an intermediate type, where the backwash would have a non-negligible influence on the run-up. Therefore, the run-up prediction was performed from the curves of Saville (1961) where the wave height H_o' is determined from

$$H_o' = \frac{2.66}{T} H_b^{3/2}$$

and the breaking wave height, H_b, is determined from the previous section. The period to be assumed is that period associated with the successive waves of the wave train shown in Appendix B at stations near the edge of the shelf. Figure 10 shows the curves from Saville (1961) which were used to determine the wave run-up.

Table IV gives the predicted wave run-up for the maximum waves of the envelope, which also corresponds to the maximum wave run-up of any wave. It is also predicted which wave of the wave train gives the maximum run-up. The run-up predictions of Table IV are the same for radial 1 as in the Interim Report SN 256-1. However, the run-up predictions for radial 2 are different because:

a) Radials 2 and 3 have been reversed in the nomenclature from the interim report (i.e., radial 2 is now the middle radial and was formerly numbered 3).

b) The run-up deck planned on radial 3 was eliminated.

c) The slope on radial 2 was changed from 1/40 to 1/30, given in the experimental plan upon which the predictions of the interim report were based.

Figure 11 shows the predicted run-up on radial 1 for each wave of the first envelope from Shot 2. The run-up for the leading wave is predicted by the assumption that it is a solitary wave; the method and curves of Le Méhauté (1964) were used for this prediction. It is not obvious which method to use for predicting the wave run-up of the second, third and fourth waves; this is indicated by the broken line in Fig. 11. Analysis of the data will greatly assist in performing future predictions for the leading waves.

Detailed predictions for each wave of the wave train for every shot were not performed. These predictions were deemed to be inefficient, since they will have to be repeated during the analysis phase to conform to the actual field conditions and geometry existing at shot time.

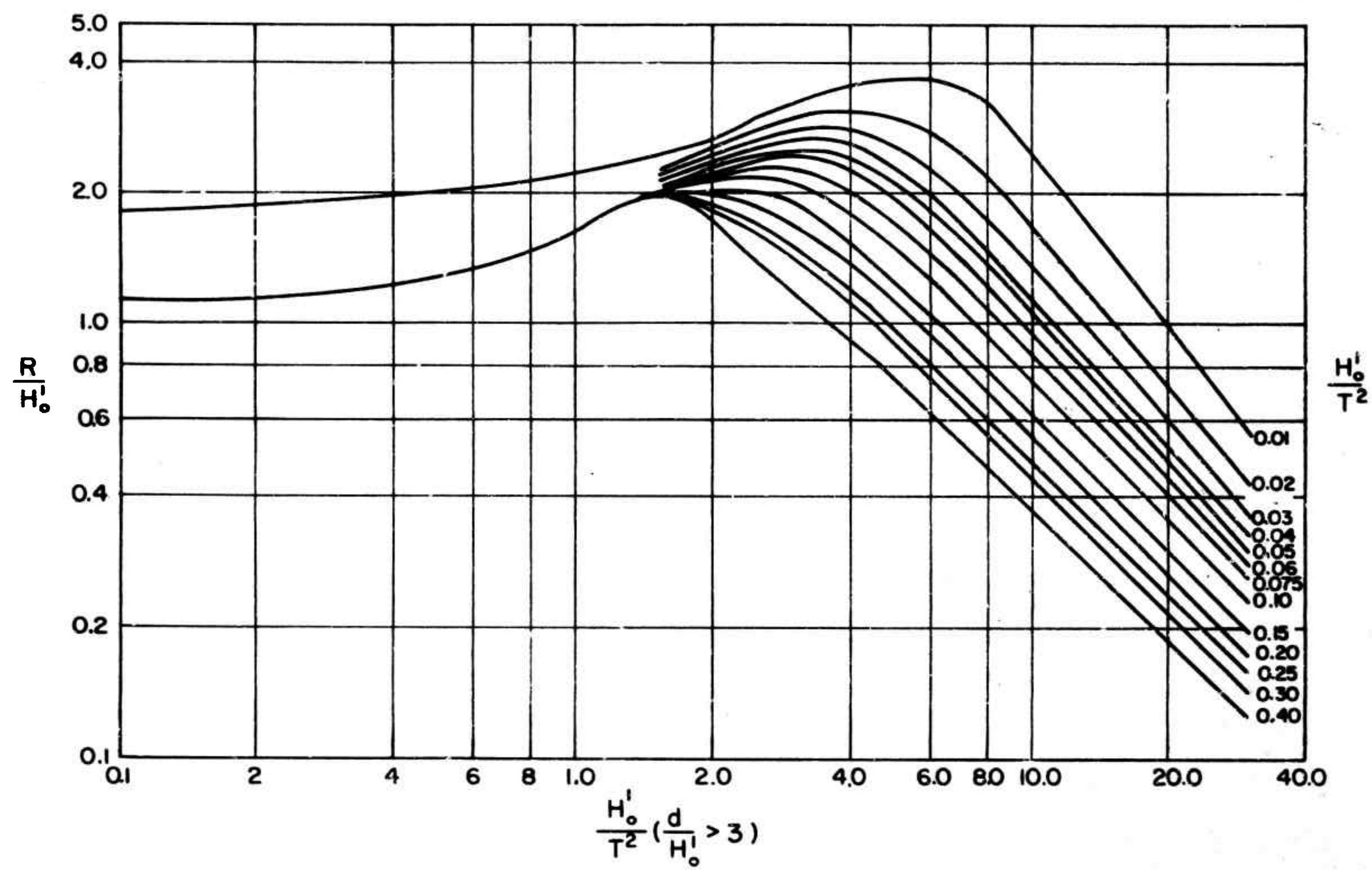

Figure 10
Saville Curves for Determining the Wave Run-up $\left(\frac{d}{H_o'} > 3\right)$

PA-3-7570

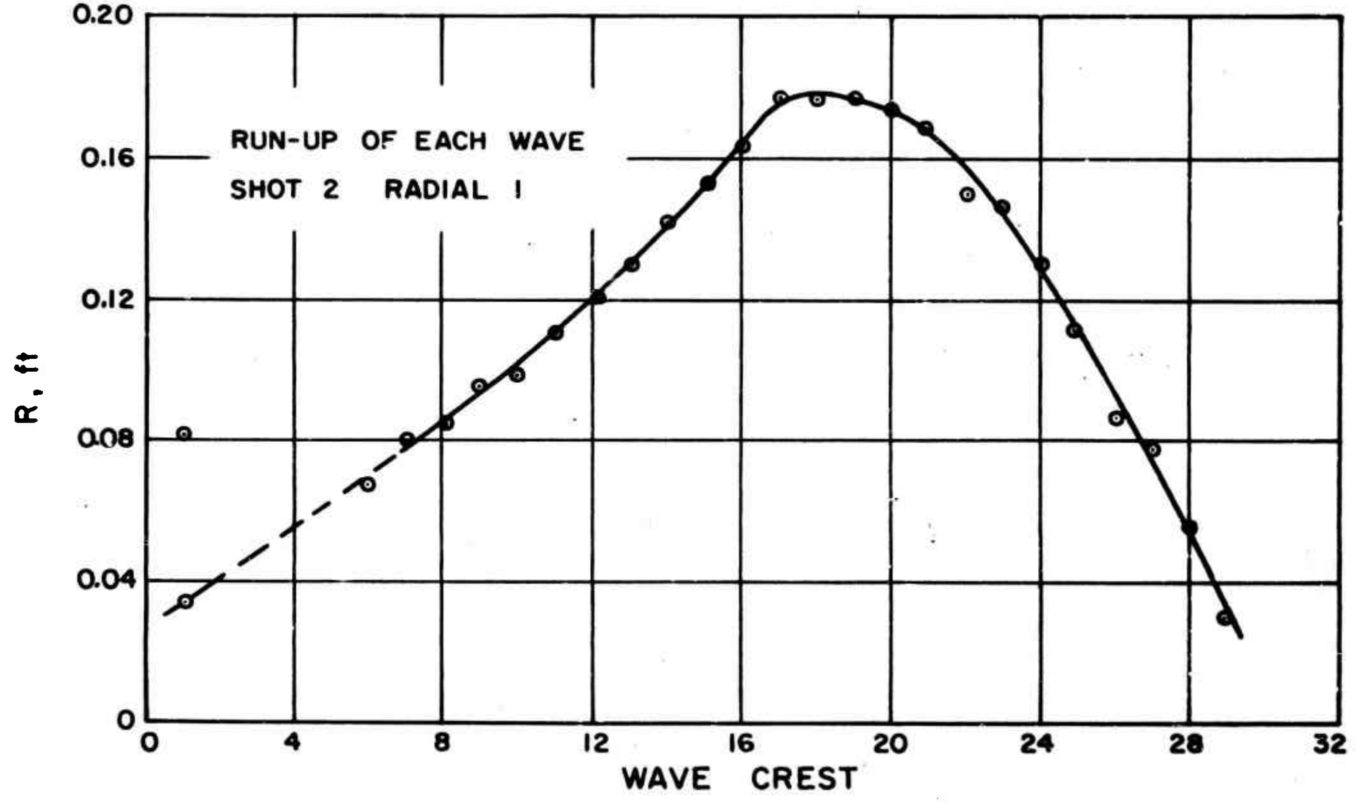

Figure 11
Predicted Run-up on Radial 1 for Each Wave from Shot 2

PA-3-7571

TABLE IV

RUN-UP PREDICTIONS FOR THE MAXIMUM WAVES OF EACH SHOT

Shot No.	Radial	R (ft.)	Wave
1	1	0.12	17
2	1	0.18	19
3	1	0.15	17
4	1	0.12	18
5	1	0.15	19
6	1	0.17	17
7	1	0.16	19
8	1	0.13	17
9	1	0.18	19
1	2	0.22	17
2	2	0.32	19
3	2	0.28	17
4	2	0.22	18
5	2	0.29	20
6	2	0.28	17
7	2	0.30	20
8	2	0.24	17
9	2	0.33	20

4. DISCUSSION OF THE PREDICTIONS AND THE EXPECTED WAVE SPECTRUM

The predictions for the Mono Lake Experiment were considered to be performed from the most reliable methods available to fit the geometry and field conditions at Mono Lake. The predictions along the constant depth radial are relatively straightforward and involved an application of the methods developed by Whalin (1965a, 1965b, 1965c, 1964). The reliability of these predictions is assumed to be ± 20 for most cases, and any improvement in this reliability without major new developments will have to come from the natural extensions to the linear theory which is indicated in Vol. II of this report.

The methods used on the slope and the shelf are considered to be reliable within ± 10 to 20 percent. The predictions for these areas are considered reliable within 30 to 40 percent when the uncertainty in the deep water linear constant depth theory is considered.

The computations of the breaking wave height were made from a combination of theoretical methods and empirical data which indicated the existence of the "super-elevation" phenomena. The run-up computations performed from the curves of Saville for the majority of the wave train and the curves of Le Méhauté for the leading wave are considered to be reliable with ± 20 to 30 percent.

In the final analysis, when the uncertainty in each phase of the wave propagation is considered, the run-up predictions are expected to have a reliability of ± 50 to 70 percent for most cases. It can be expected that unexplained anomalies may exist in the run-up measurements. These would be in the form of an unusually large or small run-up for one particular wave of the wave train in relation to the preceeding and succeeding wave. Anomalies of this type can be a result of the particular period of that wave and its phase in relation to the backwash and the background waves present in Mono Lake.

The run-up predictions were based upon the preliminary experimental plan that called for extending the slope of the artificial run-up decks into the water so the topography from the point of breaking inception was that of a constant slope of 1/50 and 1/30 for radials 1 and 2 respectively. Since this was not the case, it could have a non-negligible effect on the run-up. Other factors which will affect the predictions are the exact charge weight, assumed to be 9,500 lbs, and the distances from the actual G Z to the various measurement stations and run-up decks. All these factors must be considered when correlating the experimental data with the predictions. At that time the predictions will be revised to account for all these slight variations from the experimental plan.

5. CONCLUSIONS

The desired conclusion of assessing the validity of these predictions performed for the Mono Lake Experiment will have to wait for a comprehensive analysis of the data in relation to the predictions and the actual field conditions. However, the objective of the project was fulfilled through Interim Report SN 256-1 and this volume of the Final Report. Volumes II and III of the Final Report present a complete and detailed account of the linear theories which were employed in performing some of these predictions. These two volumes fill a gap which has existed in the literature. Specific conclusions are related to each method.

5.1 Deep Water Constant Depth Predictions

These predictions are expected to be accurate within ± 20 percent; any consistent deviation beyond this would necessitate a revision in the prediction method for future detonations. There are several natural extensions to the linear constant depth theory which should be investigated and which may increase the reliability of future predictions. The prediction at Station 4-1 was performed from the asymptotic solution which is not too reliable at a station this close to GZ. The method of Whalin (1965b) should be applied to this station, and the data from this station should provide an excellent opportunity of evaluating the validity of the linear theory relatively near GZ. The reason for not applying the integration method developed for areas near the source in these predictions is that it is relatively expensive to run the computer program. The program would have to be rerun during the analysis phase when the precise charge weight and instrumentation geometry were known. The correlation of these predictions with the data will enable us to increase the reliability of future predictions.

5.2 Predictions of the Effect of the Slope

The reflection effect of the slope on the wave train was predicted to be negligible and any deviation in this would be very unexpected. Therefore, it is expected that these predictions, in conjunction with the experimental data, will afford an excellent basis upon which to evaluate the applicability of the linear shoaling theory to this phase of the propagation. The predictions will also enable one to determine and evaluate the dispersion in the wave train as it propagates over the slope.

5.3 Wave Propagation on the Shelf

The linear shoaling theory, corrected for the radial spreading of energy and viscous and turbulent friction effects, was applied to this phase of the wave propagation. Although the friction effect was small, it was not negligible (on the order of 5 percent). The analysis of the data will enable us to determine the applicability of the principle of conservation of energy flux and linear shoaling theory to the prediction of the propagation of non-breaking explosion waves on the shelf. In addition, we should gain an insight into the method of treating the leading waves, i.e., can the leading wave or waves be treated as solitary waves or long waves up to breaking inception?

Depending upon the comprehensiveness of the instrumentation in the breaking area, which should have been adequate, we will be able to estimate the "super-elevation" effect and determine the validity of our methods of computing the wave height at breaking inception.

Shot 10, being a shallow shot, should afford one case for evaluating the non-saturated breaker theory of Le Méhauté, and, in addition, should yield valuable information on the prediction of the generation and propagation characteristics of shallow water explosions.

5.4 Run-up Predictions

The run-up predictions are expected to be reliable within 50 percent with the exception of unexplained anomalies as previously mentioned. This experiment will yield data on the run-up of explosion waves, data relatively nonexistent under the controlled conditions present at Mono Lake. These data should prove most beneficial in evaluating the relatively unproven methods of predicting the run-up of explosion-generated water waves.

In summary, the performance of these predictions prior to the field tests will provide a firm basis upon which to evaluate the present methods of predicting all phases of the wave propagation and run-up generated by underwater explosions in deep water. Although some effects were found to be negligible, such as reflection from the slope and nonlinear effects on the shelf prior to breaking, it is anticipated that upon completion of the analysis of experimental results, the objectives of the overall program will be fulfilled, and extensions and modifications of the presently used methods will increase the reliability of future predictions.

6. REFERENCES

1. Carrier, G. F., and H. P. Greenspan, "Water Waves of Finite Amplitude on a Sloping Beach," Journal of Fluid Mechanics, No. 4, 1958, pp. 97-109.

2. Eagleson, Peter S., "Laminar Damping of Oscillatory Waves," Journal of Hydraulics Division, American Society of Civil Engineers, May 1962.

3. Greenspan, H. P., "On the Breaking of Water Waves of Finite Amplitude on a Sloping Beach," Journal of Fluid Mechanics, No. 4, 1958, pp. 330-334.

4. Ho, D. V., and R. E. Meyer, "Climb of a Bore on a Beach," Division of Applied Mathematics, Brown University Technical Report No. 47 [562(07)/47], March 1962, 40 pages.

5. Ho, D. V., R. E. Meyer, M. C. Shen, "Long Surf," Technical Report No. 4 [562(34)/4], Division of Applied Mathematics, Brown University, March 1963, 17+ pages.

6. Isaacson, E., "Waves Against an Overhanging Cliff," Comm. Pure and Applied Mathematics, Vol. 1, pp. 201-209, 1948.

7. Kajiura, Kinjiro, "The Leading Wave of a Tsunami," Bulletin of the Earthquake Research Institute, Vol. 41, 1963, pp. 535-571.

8. Kaplan, Kenneth, "Generalized Laboratory Study of Tsunami Run-up," Technical Memorandum No. 70, Beach Erosion Board, Corps of Engineers, January 1955.

9. Keller, H. B., D. A. Levine, and G. B. Whitham, "Motion of a Bore over a Sloping Beach," Journal of Fluid Mechanics, No. 7, 1960, pp. 302-316.

10. Keller, H. B., "Tsunamis -- Water Waves Produced by Earthquakes," Tsunami Hydrodynamics Conference, Honolulu, 1961, IUGG Monograph No. 24.

11. Kiski, Tsutomu, "The Breaking and Run-up of the Solitary Wave on a Sloping Beach," Note for the Seminar on Wave Run-up, Sapporo, Japan, April 1965.

12. Koh, R., and B. Le Méhauté, "Wave Shoaling (At a Fifth Order of Approximation)", publication pending in Journal of the Geophysical Union.

13. Kranzer, H. E., and J. B. Keller, "Water Waves Produced by Explosions," Journal of Applied Physics, 30, 398 (1959), NYU-IMS Research Report No. 222, September 1955.

14. Laitone, E. V., "Higher Approximations to Nonlinear Water Waves and the Limiting Heights of Cnoidal, Solitary, and Stokes' Waves," Technical Memorandum No. 133, Beach Erosion Board, Corps of Engineers, February 1963, 106 pages.

15. Le Méhauté, B., "Gravity Waves on Bottom Slopes and Wave Run-up," Final Report, DASA-1543, National Engineering Science Company, 26 June 1964.

16. Le Méhauté, B., "Wave Breakers on a Beach and Surge on a Dry Bed," Journal of Hydraulics Division, American Society of Civil Engineers, March 1964, pp. 187-216 (with J. Freeman).

17. Le Méhauté, B., "New Theoretical Development on Surge on a Dry Bed and the Wave Run-up," publication pending in Journal of the Hydraulics Division, American Society of Civil Engineers.

18. Le Méhauté, B., and M. Moore, "Theoretical Results on the Breaking of a Solitary Wave and Wave Run-up," publication pending in Journal of the Hydraulics Division, American Society of Civil Engineers.

19. Le Méhauté, B., and R. Koh, "A Theoretical Study of Waves Breaking at an Angle with a Shoreline (at a Fifth Order of Approximation)," publication pending in Journal of the Geophysical Union.

20. Le Méhauté, B., and L. Webb, "Periodic Gravity Waves on a Gentle Slope at a Third Order of Approximation," IX Conference on Coastal Engineering, Lisbon, 1964.

21. Meyer, R. E., and A. D. Taylor, "On the Equations of Surf," Technical Report No. 5 [562(34)/5], Division of Applied Mathematics, Brown University, July 1963, 11 pages.

22. Munk, Walter H., "Increase in the Period of Waves Traveling over Large Distances: With Applications to Tsunamis, Swell, and Seismic Surface Waves," Transactions, American Geophysical Union, Vol. 28, No. 2, April 1947.

23. Shen, M. C., and R. E. Meyer, "Asymptotic Bore Development on Beaches of Non-uniform Slope," Technical Report No. 2 [562(34)/2], Division of Applied Mathematics, Brown University, October 1962, 14 pages.

24. Shen, M. C., and R. E. Meyer, "Wave Run-up on Beaches," Technical Report No. 3, [562(34)/3], Division of Applied Mathematics, Brown University, October 1962, 36 pages.

25. Stoker, J. J., "Water Waves," Interscience Publishers, Inc., New York, 1957.

26 Van Dorn, W. G., "Explosion-generated Waves in Water of Variable Depth," Journal of Marine Research, Sears Foundation, V. 22, No. 2, 15 May 1964, pp. 123-141.

27. Van Dorn, W. B., and W. Montgomery, "Water Waves from 10,000 lb High Explosive Charges," S.I.O. Rep. 63-20, 1963.

28. Whalin, R. W., "Water Waves Produced by Impulsive Energy Sources. Part V: Propagation," NMC-IEC, September 1965c.

29. Whalin, R. W., and R. E. Kent, "Water Waves Produced by Impulsive Energy Sources. Part VI: Data Analysis," NMC-IEC, January 1964. SECRET.

30. Whalin, R. W., "Water Waves Produced by Underwater Explosions: Propagation Theory for the Area Near the Explosion," Journal of Geophysical Research, Vol. 70, No. 22, November 15, 1965b.

31. Whalin, R. W., "Research on the Generation and Propagation of Water Waves Produced by Underwater Explosion. Part II: A Prediction Method," NMC-IEC, 1965a.

32. Whitham, G. B., "Mass Momentum and Energy Flux in Water Waves," Journal of Fluid Mechanics, Vol. 12, Part 1, pp. 135-147, 1962.

33. "Shore Protection Planning and Design," Technical Report No. 4, Beach Erosion Board, Corps of Engineers, 1961 (Run-up Curves of Saville).

APPENDIX A

PREDICTIONS FOR DEEP WATER STATIONS

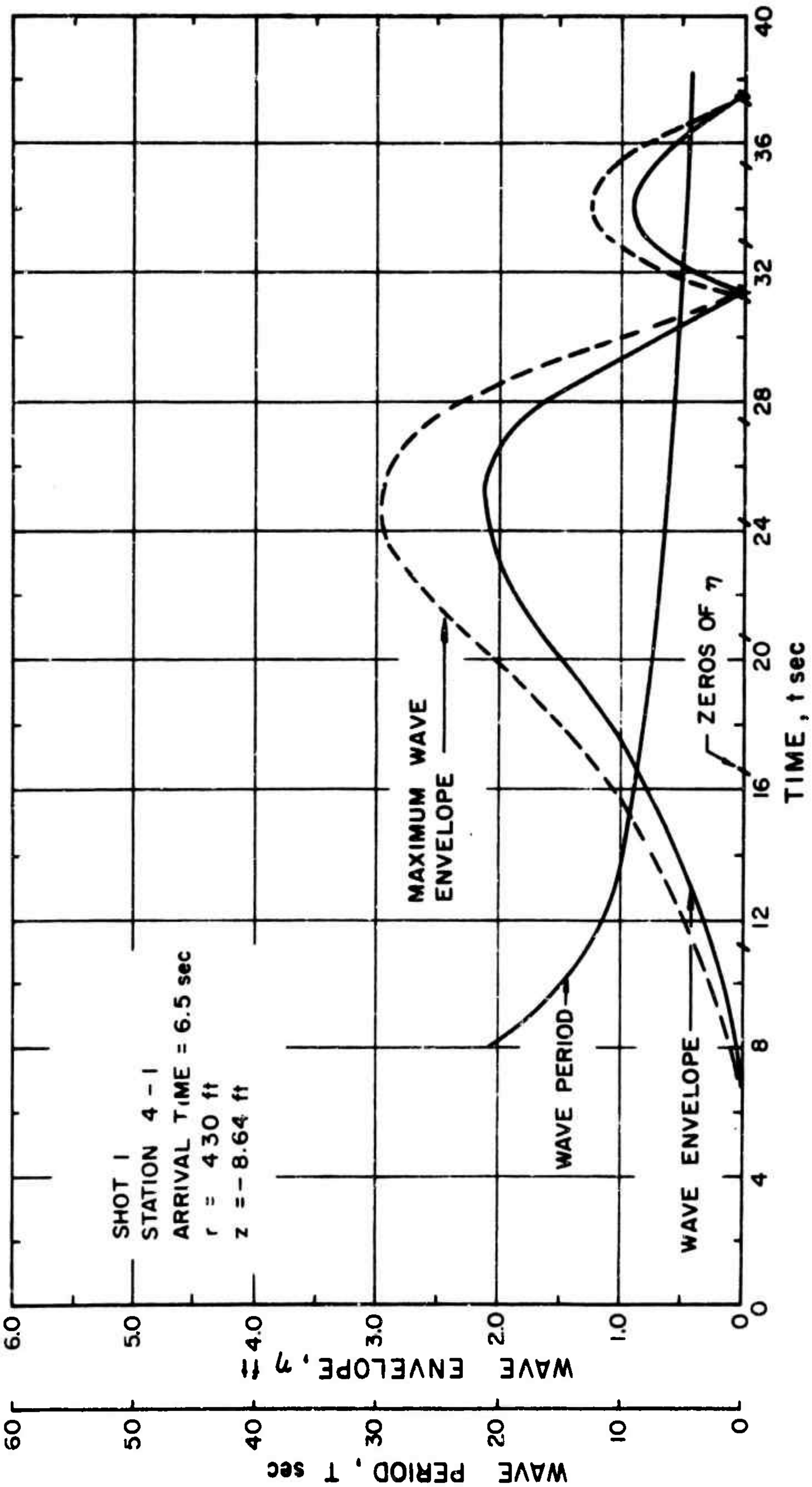
SHOT I
STATION 4 - I
ARRIVAL TIME = 6.5 sec
r = 430 ft
z = -8.64 ft
MAXIMUM WAVE ENVELOPE
WAVE PERIOD
WAVE ENVELOPE
ZEROS OF η
TIME, t sec
WAVE ENVELOPE, η ft
WAVE PERIOD, T sec
0
4
8
12
16
20
24
28
32
36
40
0
1.0
2.0
3.0
4.0
5.0
6.0
10
20
30
40
50
60

PA-3-7770

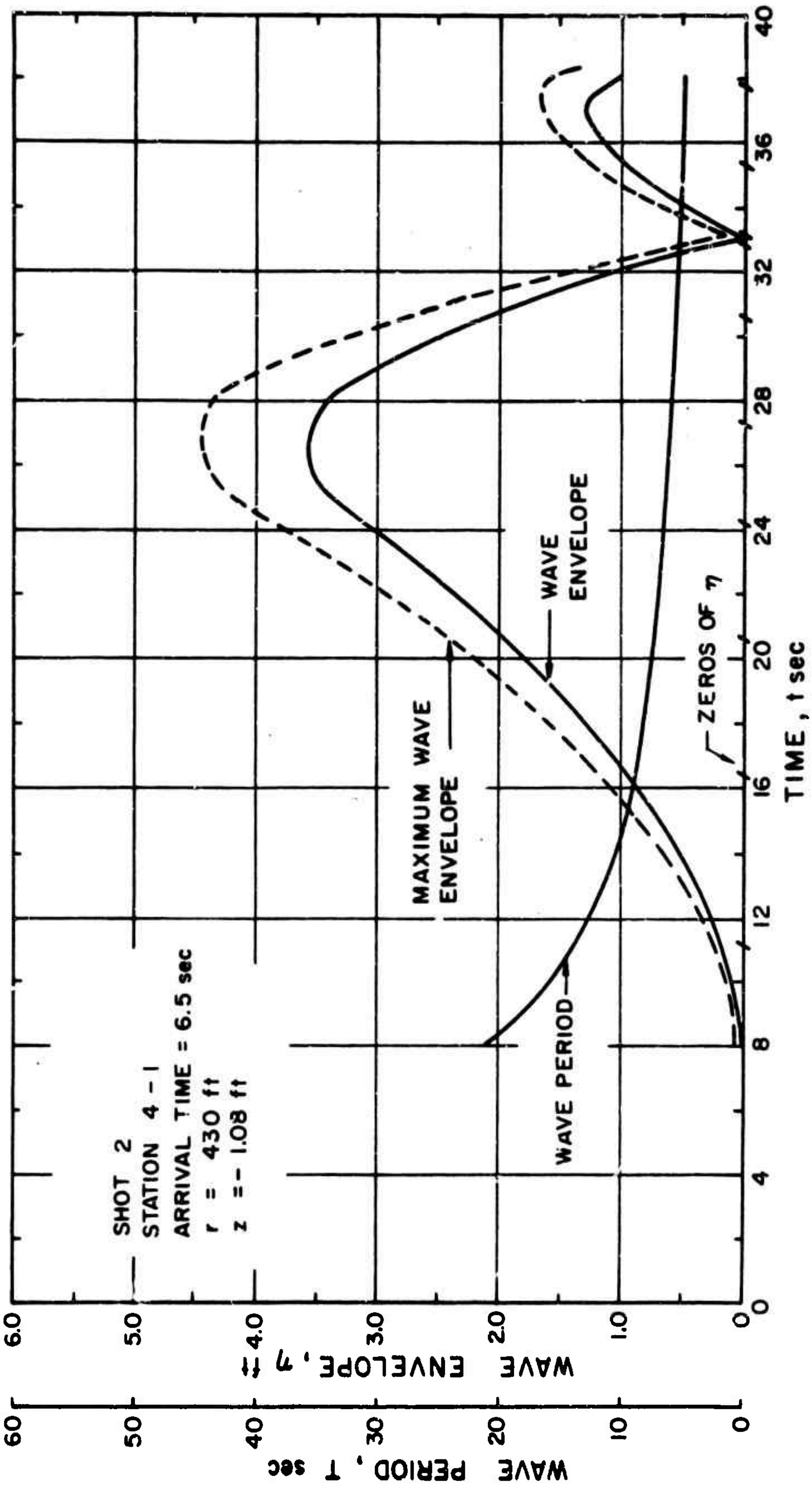
SHOT 2
STATION 4 - I
ARRIVAL TIME = 6.5 sec
r = 430 ft
z = - 1.08 ft
MAXIMUM WAVE ENVELOPE
WAVE ENVELOPE
WAVE PERIOD
ZEROS OF η
TIME, t sec
WAVE ENVELOPE, η ft
WAVE PERIOD, T sec
0
4
8
12
16
20
24
28
32
36
40
0
1.0
2.0
3.0
4.0
5.0
6.0
0
10
20
30
40
50
60
PA-3-777

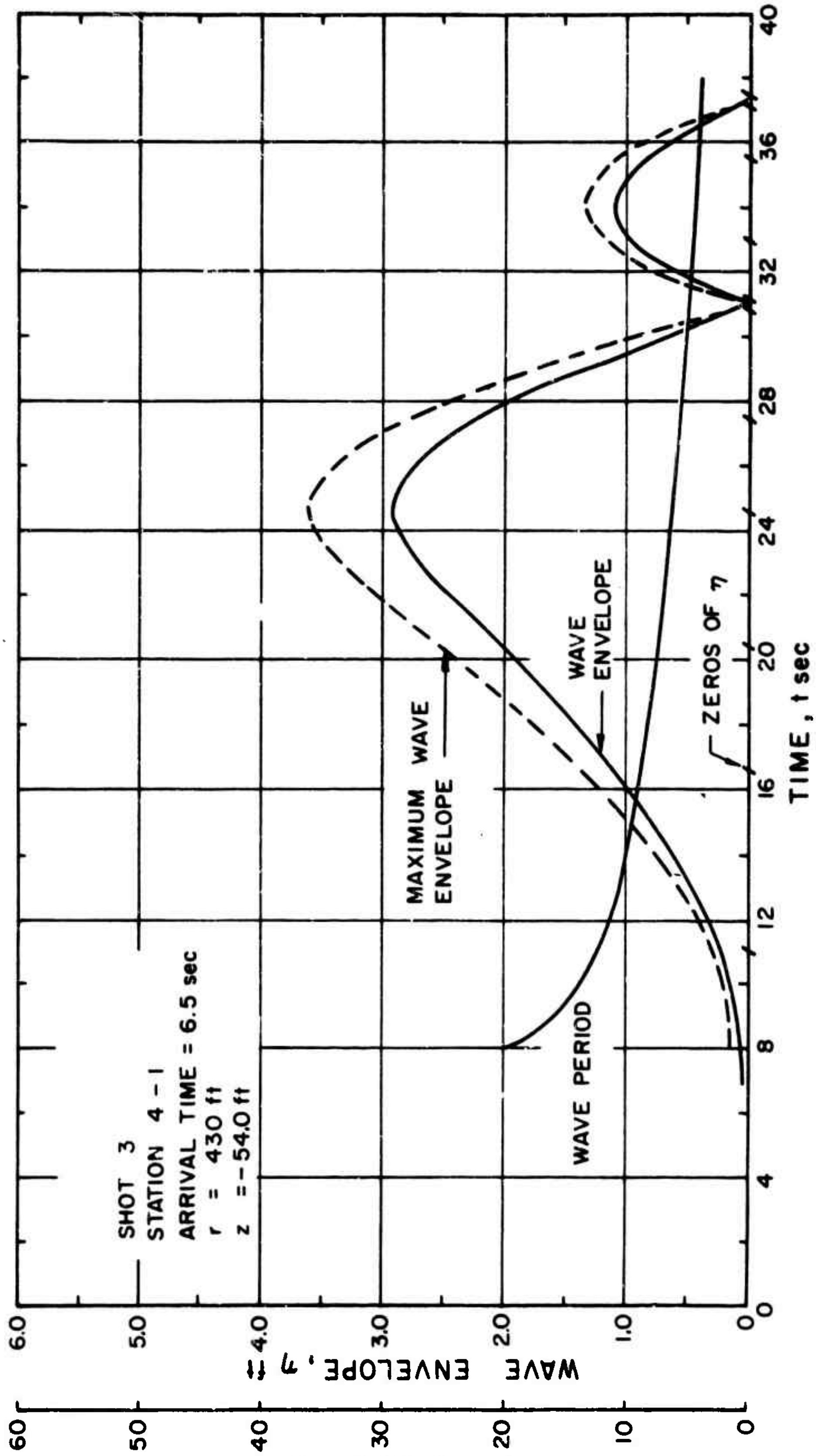
SHOT 3
STATION 4 - 1
ARRIVAL TIME = 6.5 sec
r = 430 ft
z = -54.0 ft
WAVE PERIOD
MAXIMUM WAVE ENVELOPE
WAVE ENVELOPE
ZEROS OF η
TIME, t sec
WAVE ENVELOPE, η ft
WAVE PERIOD, T sec
0
4
8
12
16
20
24
28
32
36
40
0
1.0
2.0
3.0
4.0
5.0
6.0
0
10
20
30
40
50
60

PA-1-7772

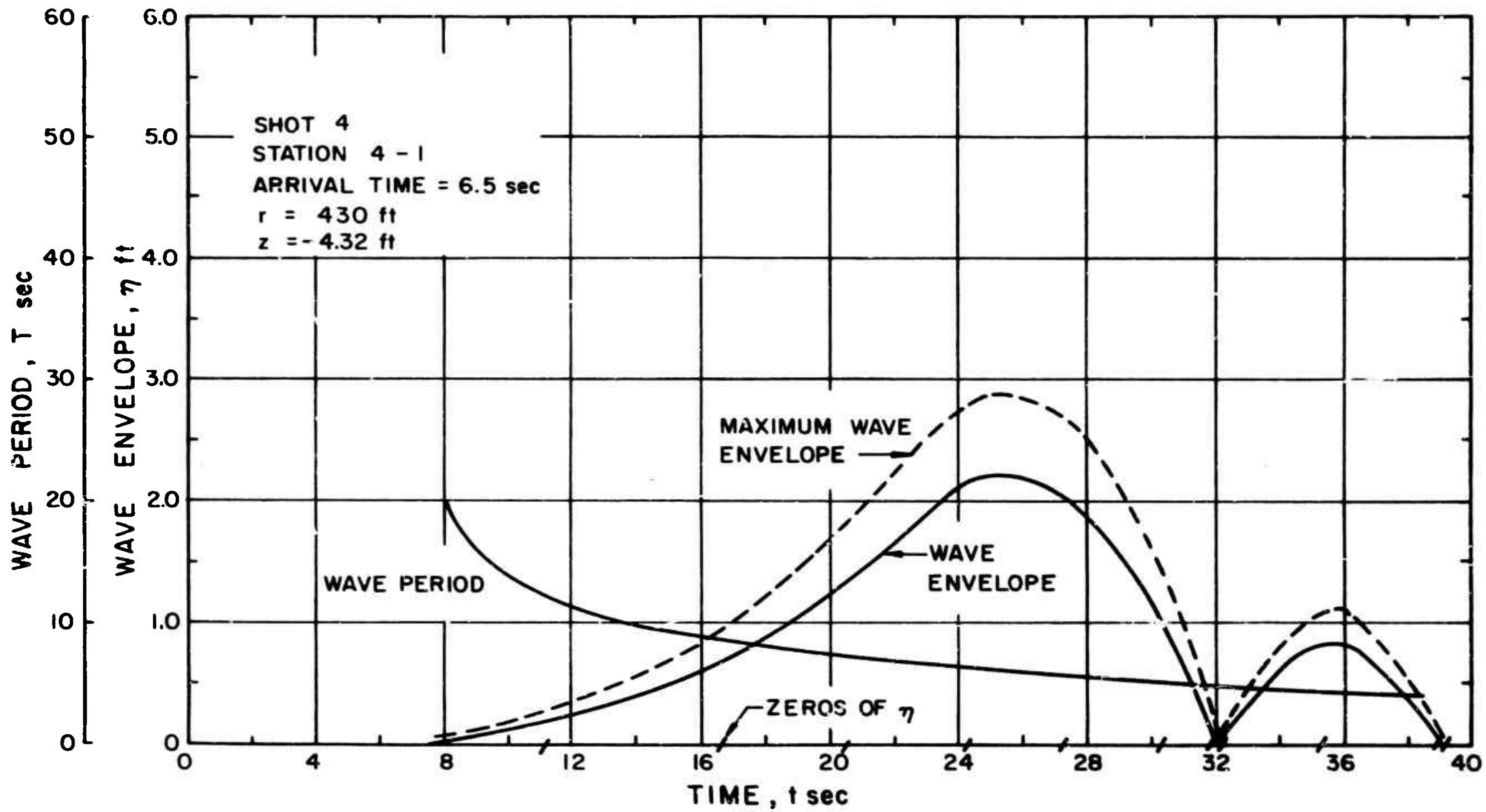
SHOT 4
STATION 4 - I
ARRIVAL TIME = 6.5 sec
r = 430 ft
z =-4.32 ft
MAXIMUM WAVE ENVELOPE
WAVE ENVELOPE
WAVE PERIOD
ZEROS OF η
WAVE PERIOD, T sec
WAVE ENVELOPE, η ft
TIME, t sec
0
4
8
12
16
20
24
28
32
36
40
0
10
20
30
40
50
60
0
1.0
2.0
3.0
4.0
5.0
6.0

PA-3-7773

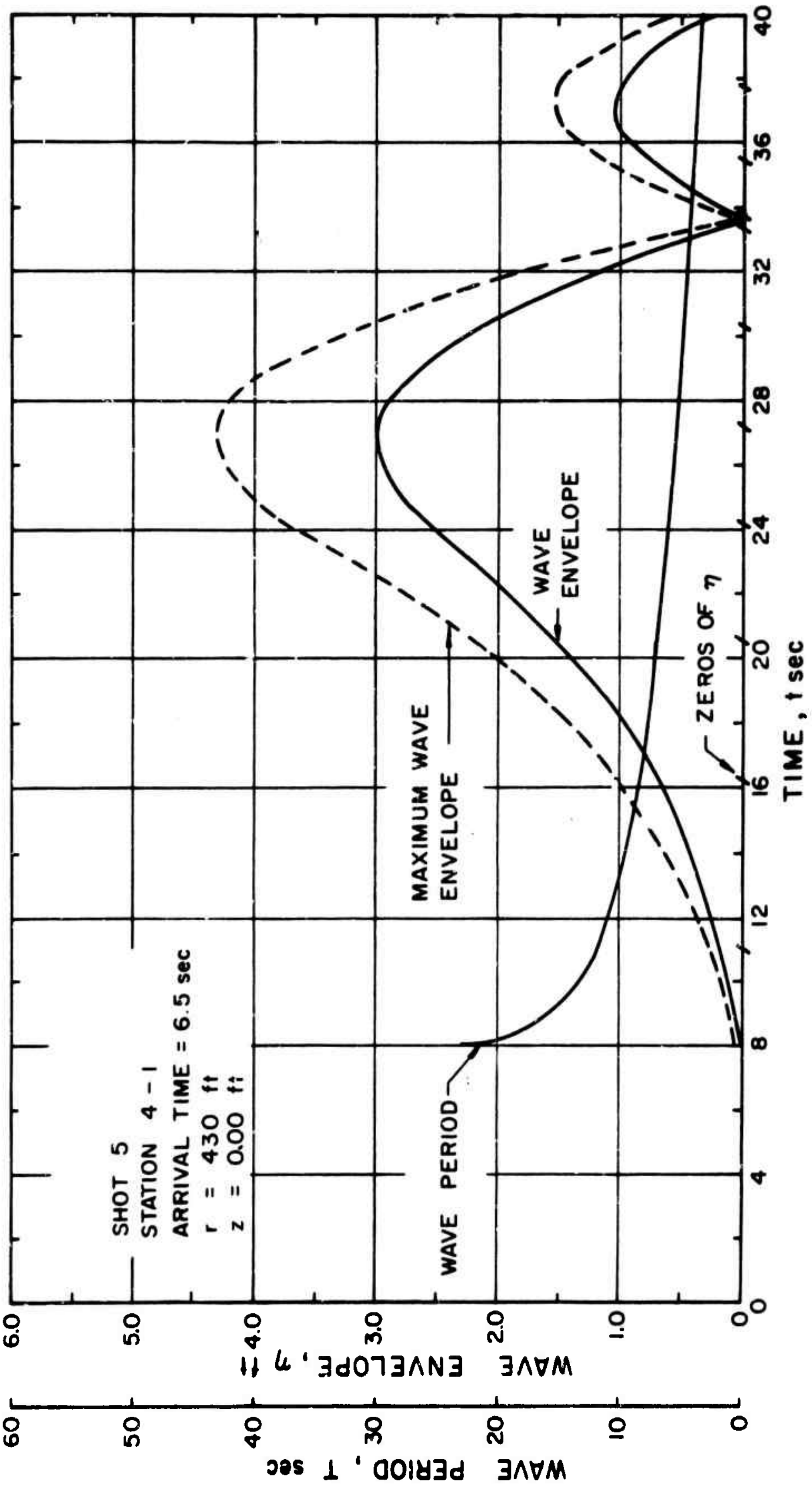
SHOT 5
STATION 4 - I
ARRIVAL TIME = 6.5 sec
r = 430 ft
z = 0.00 ft
WAVE PERIOD
MAXIMUM WAVE ENVELOPE
WAVE ENVELOPE
ZEROS OF η
TIME, t sec
0 4 8 12 16 20 24 28 32 36 40
WAVE ENVELOPE, η ft
0 1.0 2.0 3.0 4.0 5.0 6.0
WAVE PERIOD, T sec
0 10 20 30 40 50 60

PA-3-7774

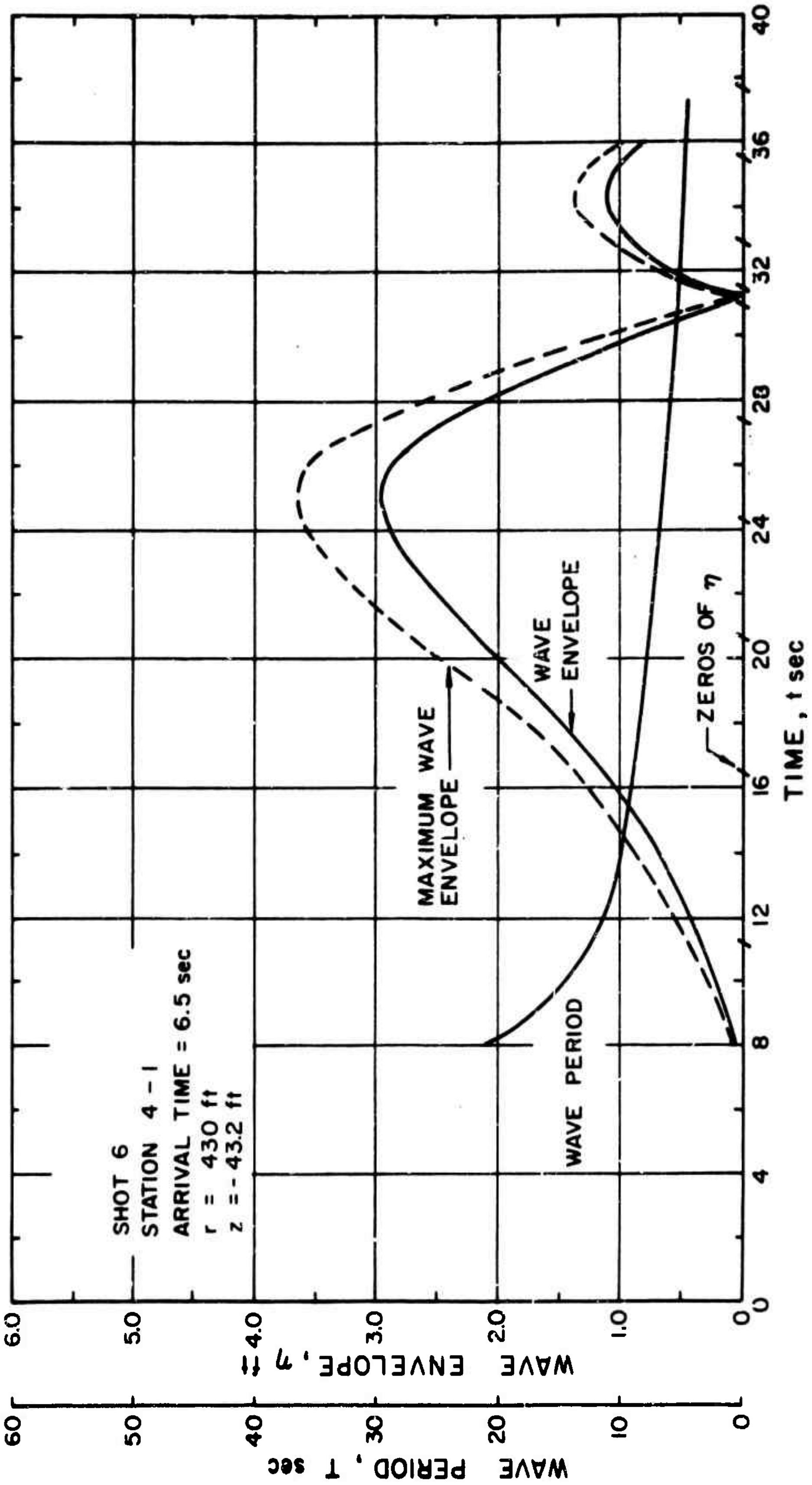
SHOT 6
STATION 4 - I
ARRIVAL TIME = 6.5 sec
r = 430 ft
z = - 43.2 ft
WAVE PERIOD
MAXIMUM WAVE ENVELOPE
WAVE ENVELOPE
ZEROS OF η
TIME , t sec
WAVE ENVELOPE , η ft
WAVE PERIOD , T sec
0
4
8
12
16
20
24
28
32
36
40
0
1.0
2.0
3.0
4.0
5.0
6.0
0
10
20
30
40
50
60

PA-1-7775

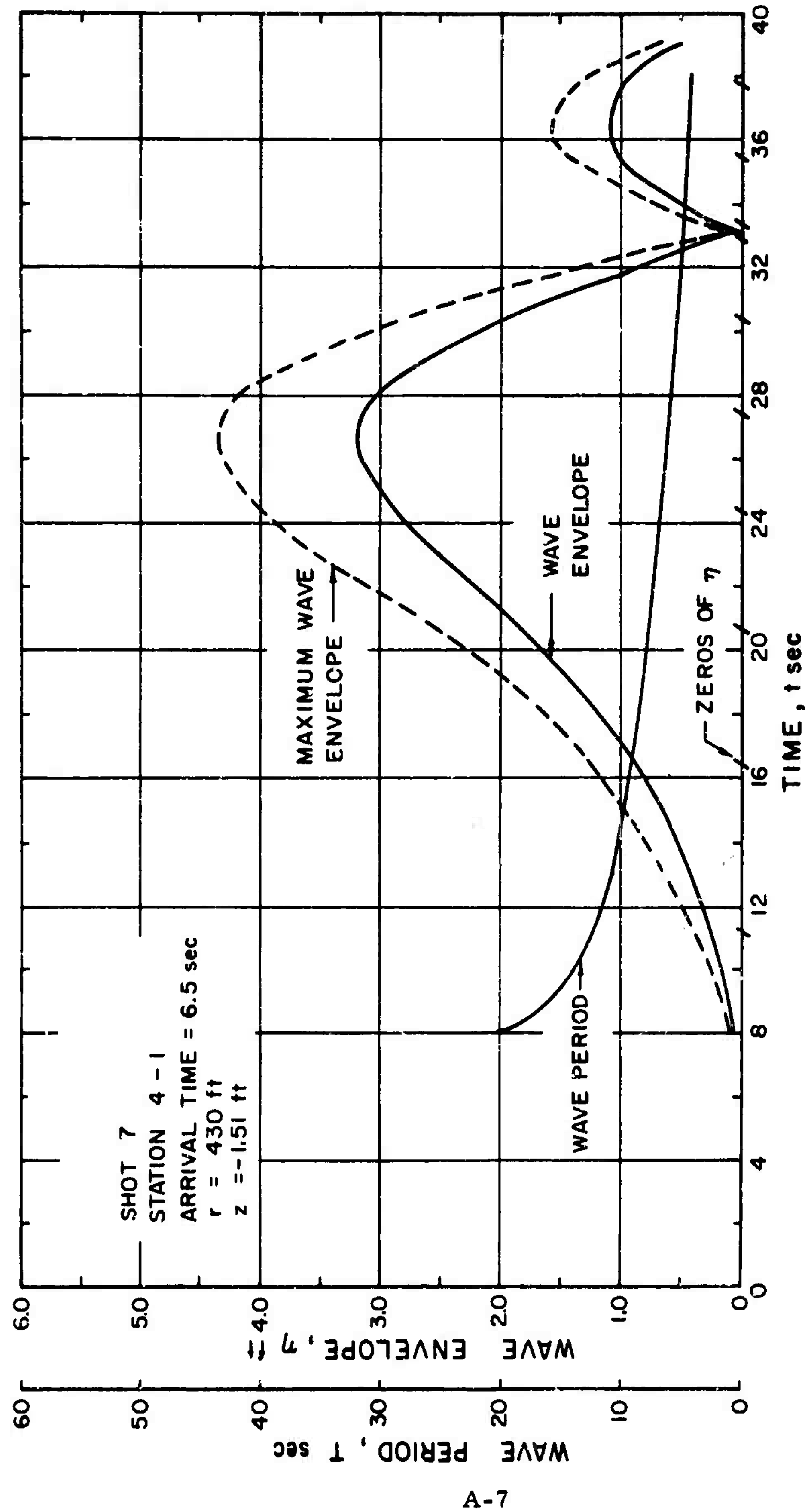

SHOT 7
STATION 4 - I
ARRIVAL TIME = 6.5 sec
r = 430 ft
z = -1.51 ft
MAXIMUM WAVE ENVELCPE
WAVE ENVELOPE
WAVE PERIOD
ZEROS OF η
TIME , t sec
WAVE ENVELOPE , η ft
WAVE PERIOD , T sec
0
4
8
12
16
20
24
28
32
36
40
1.0
2.0
3.0
4.0
5.0
6.0
10
20
30
40
50
60

PA-3-7776

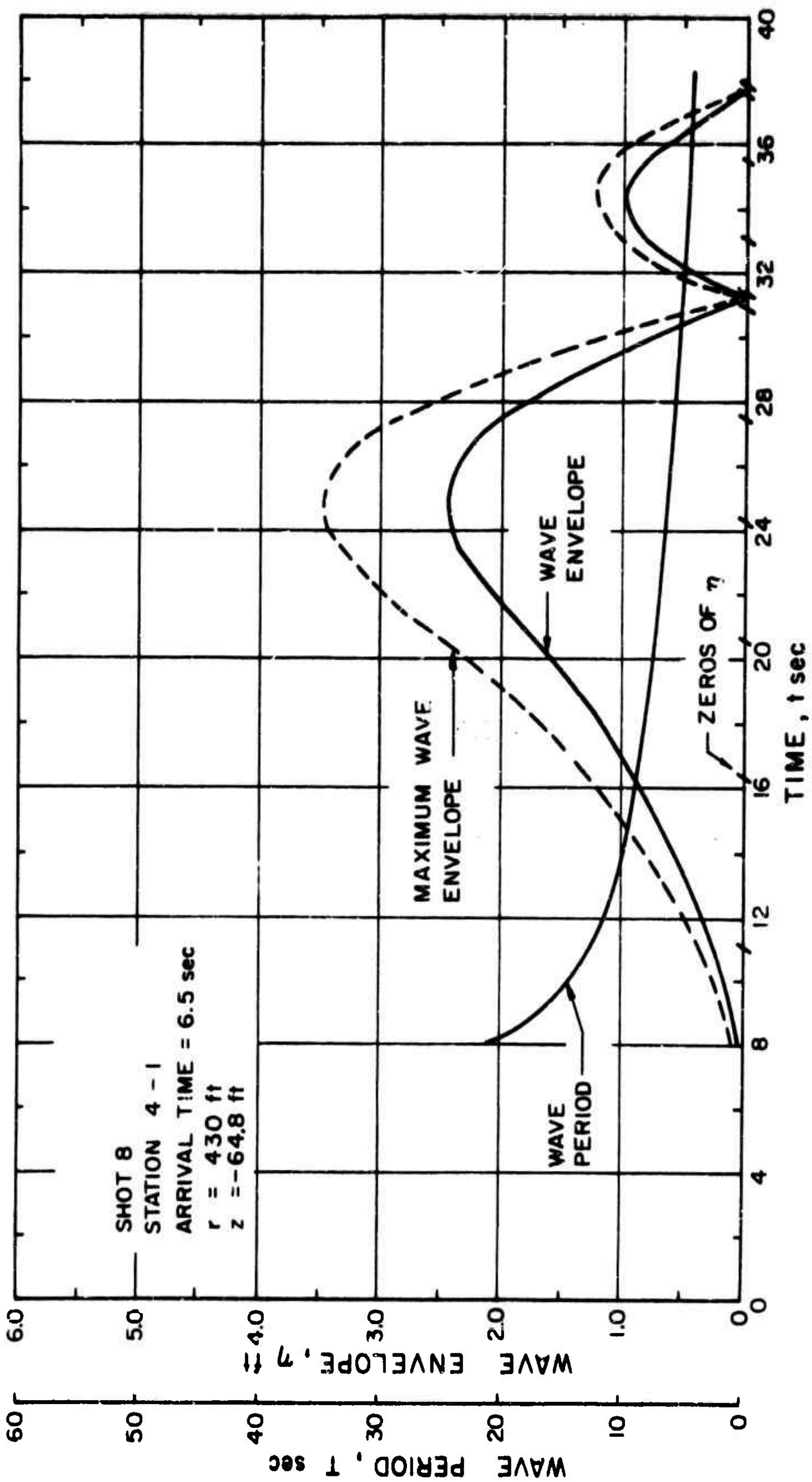
SHOT 8
STATION 4 - 1
ARRIVAL TIME = 6.5 sec
r = 430 ft
z = -64.8 ft
MAXIMUM WAVE ENVELOPE
WAVE ENVELOPE
WAVE PERIOD
ZEROS OF η
TIME, t sec
WAVE ENVELOPE, η ft
WAVE PERIOD, T sec
0
4
8
12
16
20
24
28
32
36
40
1.0
2.0
3.0
4.0
5.0
6.0
10
20
30
40
50
60

PA-3-7777

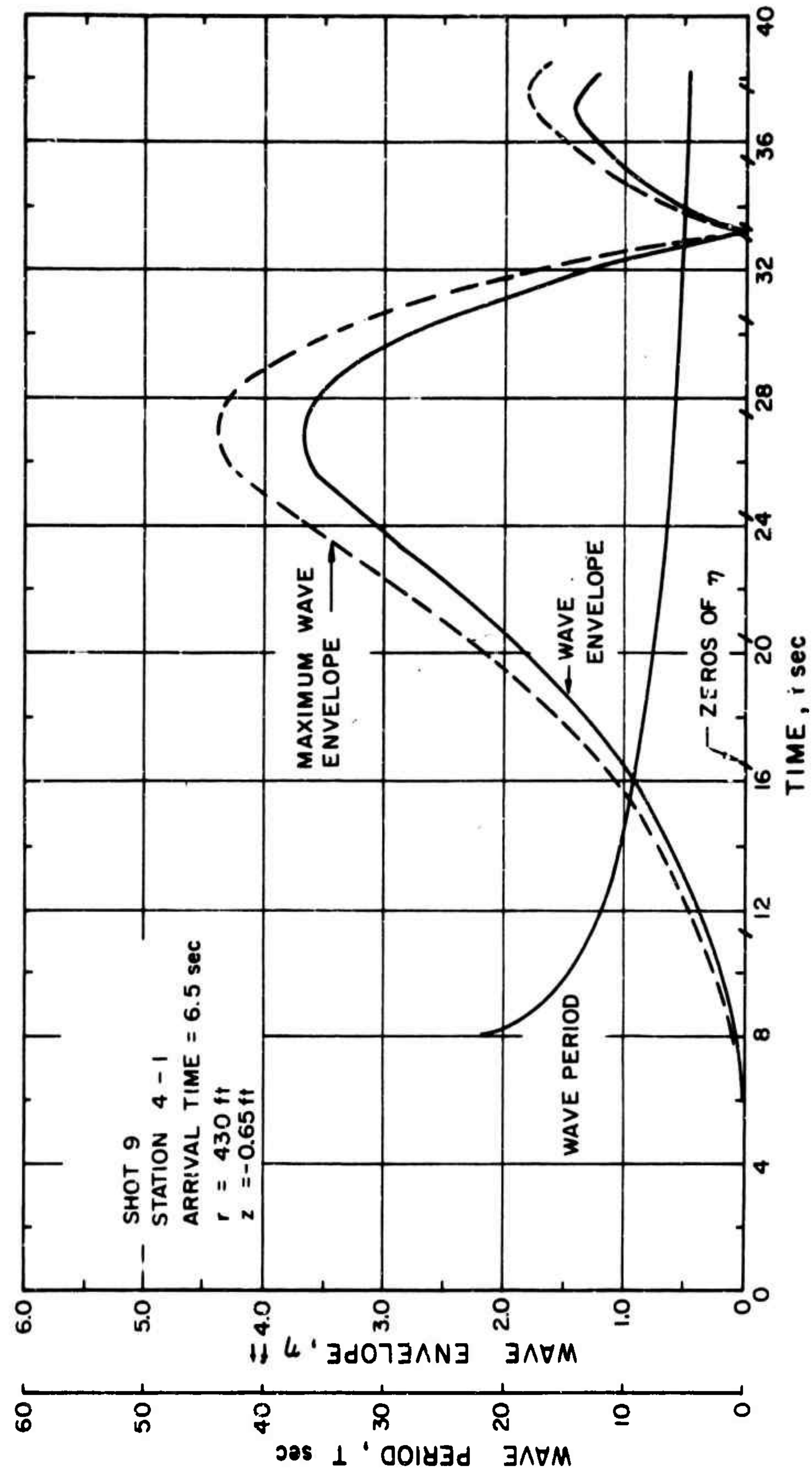
SHOT 9
STATION 4 - 1
ARRIVAL TIME = 6.5 sec
r = 430 ft
z = -0.65 ft
MAXIMUM WAVE ENVELOPE
WAVE ENVELOPE
ZEROS OF η
WAVE PERIOD
TIME, t sec
WAVE ENVELOPE, η ft
WAVE PERIOD, T sec

PA-5-7775

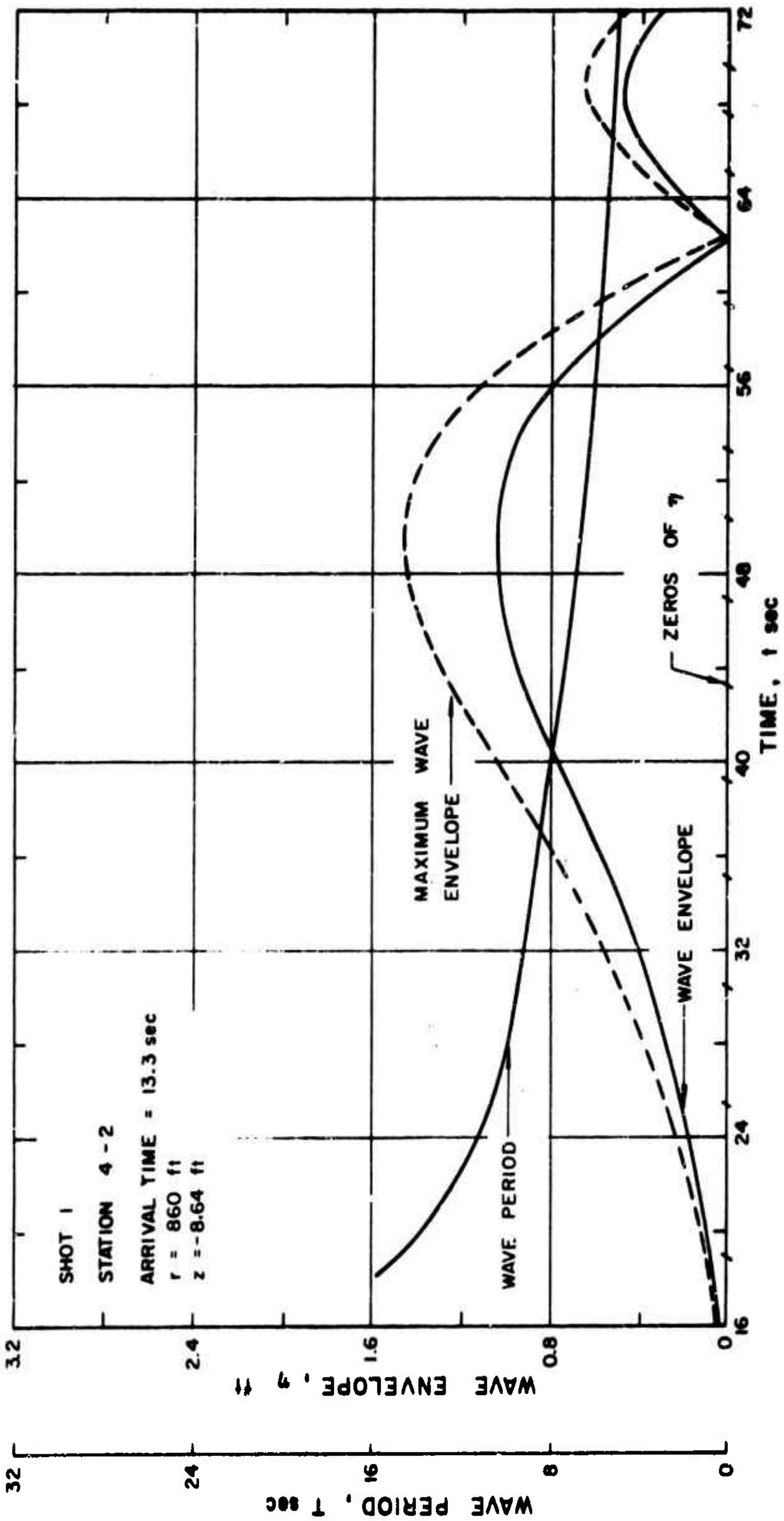

SHOT 1
STATION 4-2
ARRIVAL TIME = 13.3 sec
r = 860 ft
z = -8.64 ft
WAVE PERIOD
WAVE ENVELOPE
MAXIMUM WAVE ENVELOPE
ZEROS OF η
TIME, t sec
16
24
32
40
48
56
64
72
WAVE ENVELOPE, η ft
0
0.8
1.6
2.4
3.2
WAVE PERIOD, T sec
0
8
16
24
32

PB-3-7779

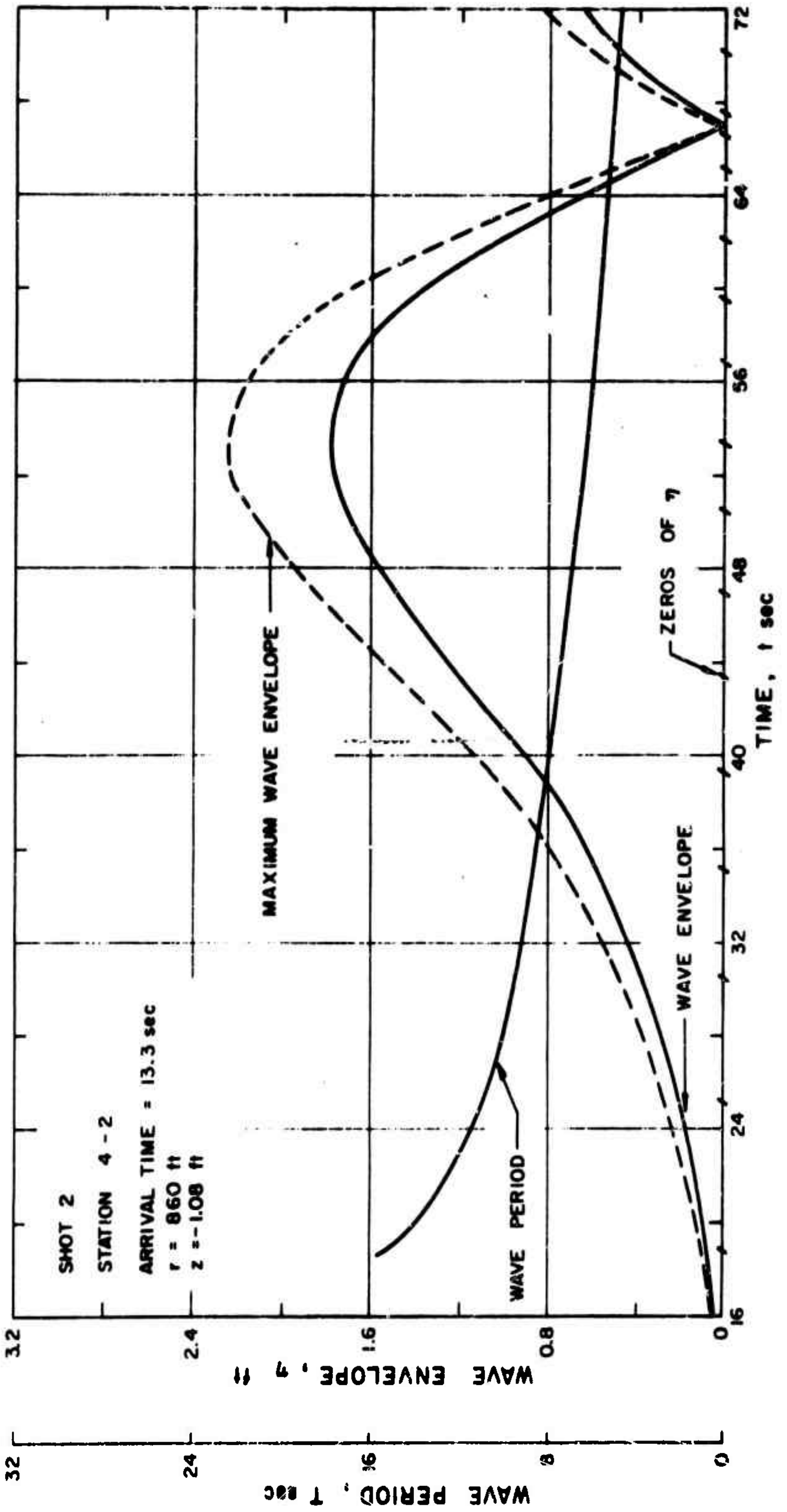

SHOT 2
STATION 4 - 2
ARRIVAL TIME = 13.3 sec
r = 860 ft
z = -1.08 ft
MAXIMUM WAVE ENVELOPE
WAVE ENVELOPE
WAVE PERIOD
ZEROS OF η
TIME, t sec
WAVE ENVELOPE, η ft
WAVE PERIOD, T sec
16
24
32
40
48
56
64
72
0
0.8
1.6
2.4
3.2
0
8
16
24
32

PB-3-7780

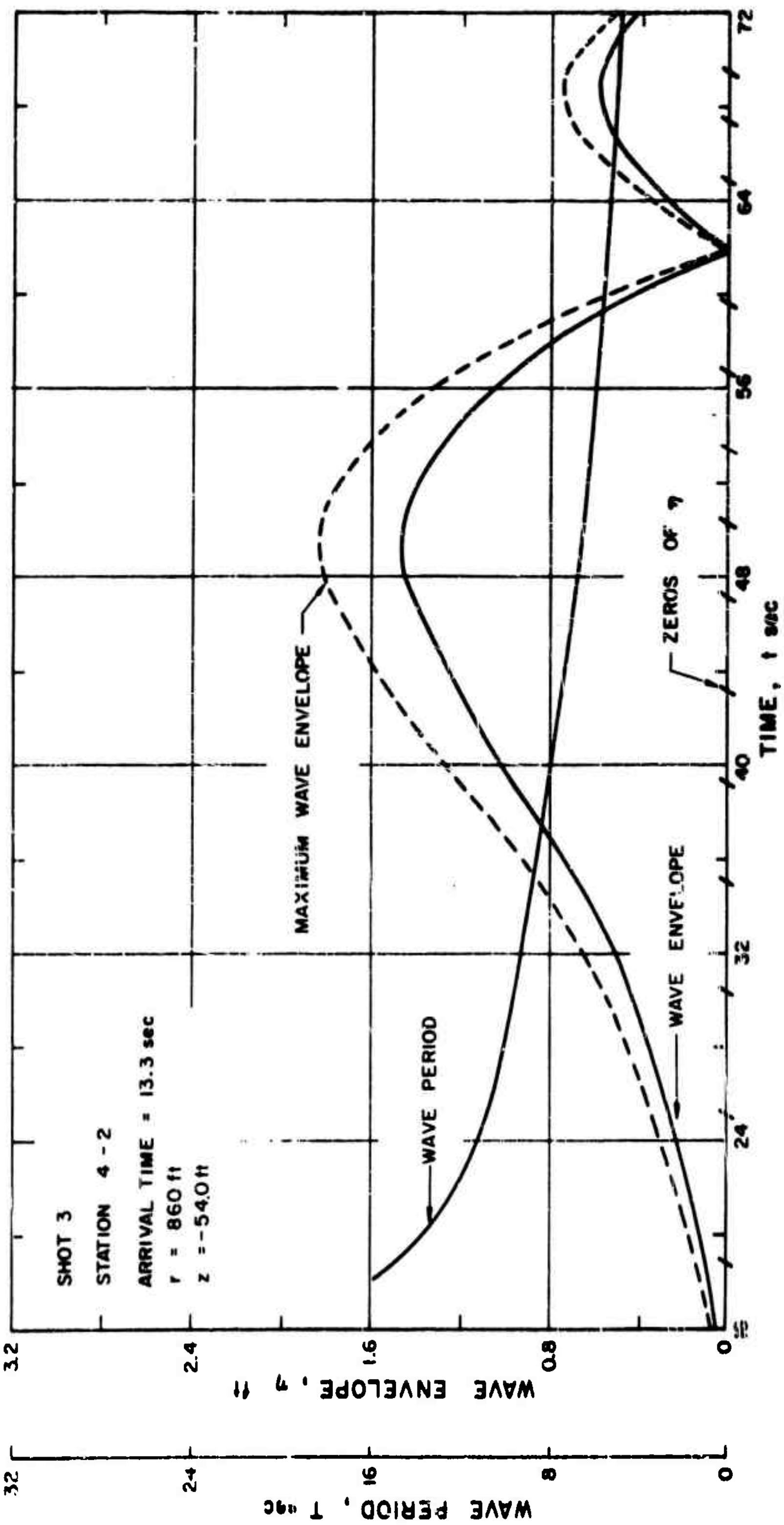
SHOT 3
STATION 4 - 2
ARRIVAL TIME = 13.3 sec
r = 860 ft
z = -54.0 ft
WAVE PERIOD
WAVE ENVELOPE
MAXIMUM WAVE ENVELOPE
ZEROS OF η
TIME, t sec
24
32
40
48
56
64
72
WAVE ENVELOPE, η ft
0
0.8
1.6
2.4
3.2
WAVE PERIOD, T sec
0
8
16
24
32

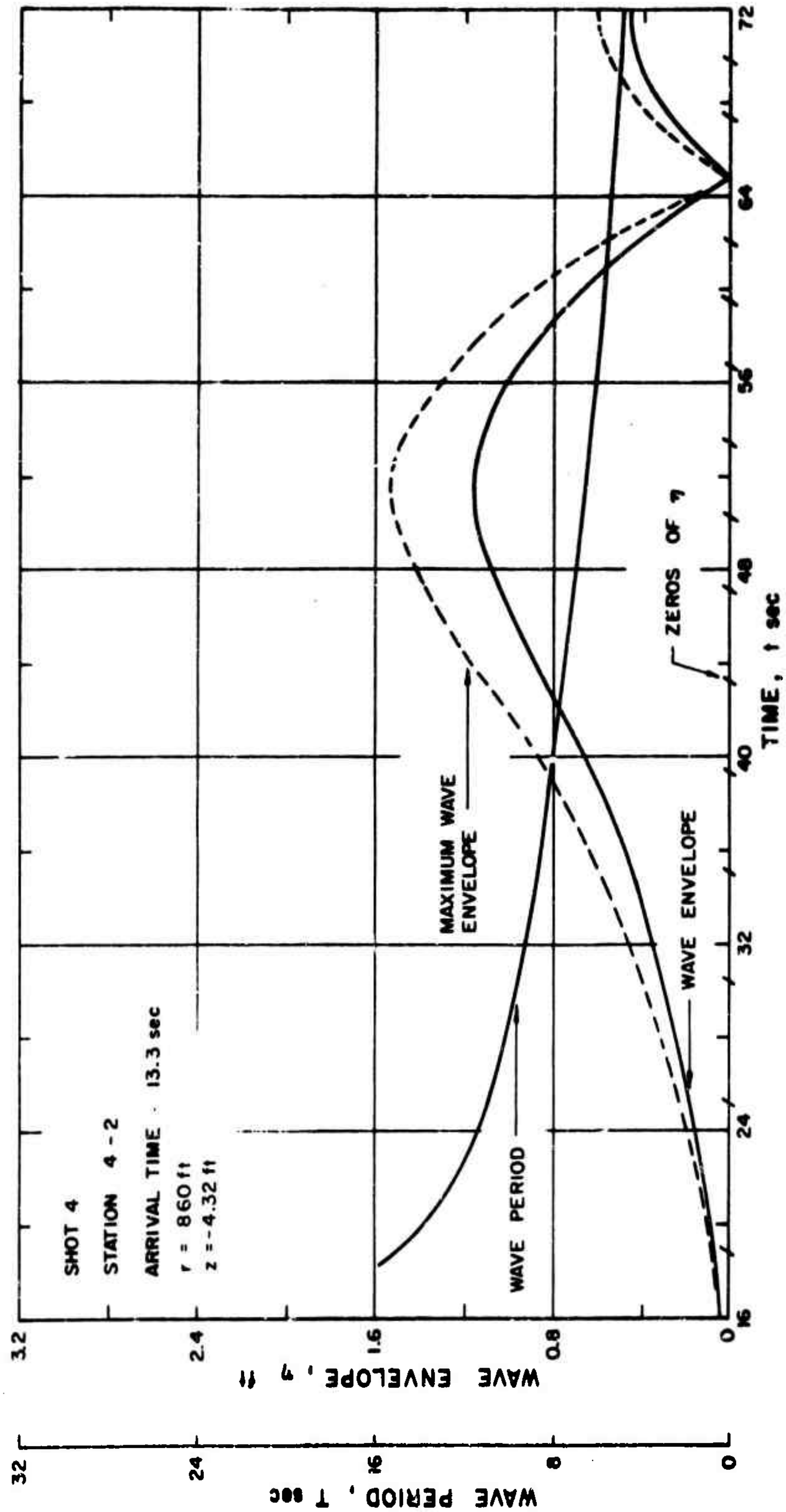
SHOT 4
STATION 4-2
ARRIVAL TIME · 13.3 sec
r = 860 ft
z = -4.32 ft
WAVE PERIOD
WAVE ENVELOPE
MAXIMUM WAVE ENVELOPE
ZEROS OF η
TIME, t sec
16
24
32
40
48
56
64
72
WAVE ENVELOPE, η ft
0
0.8
1.6
2.4
3.2
WAVE PERIOD, T sec
0
8
16
24
32

PB-1-7782

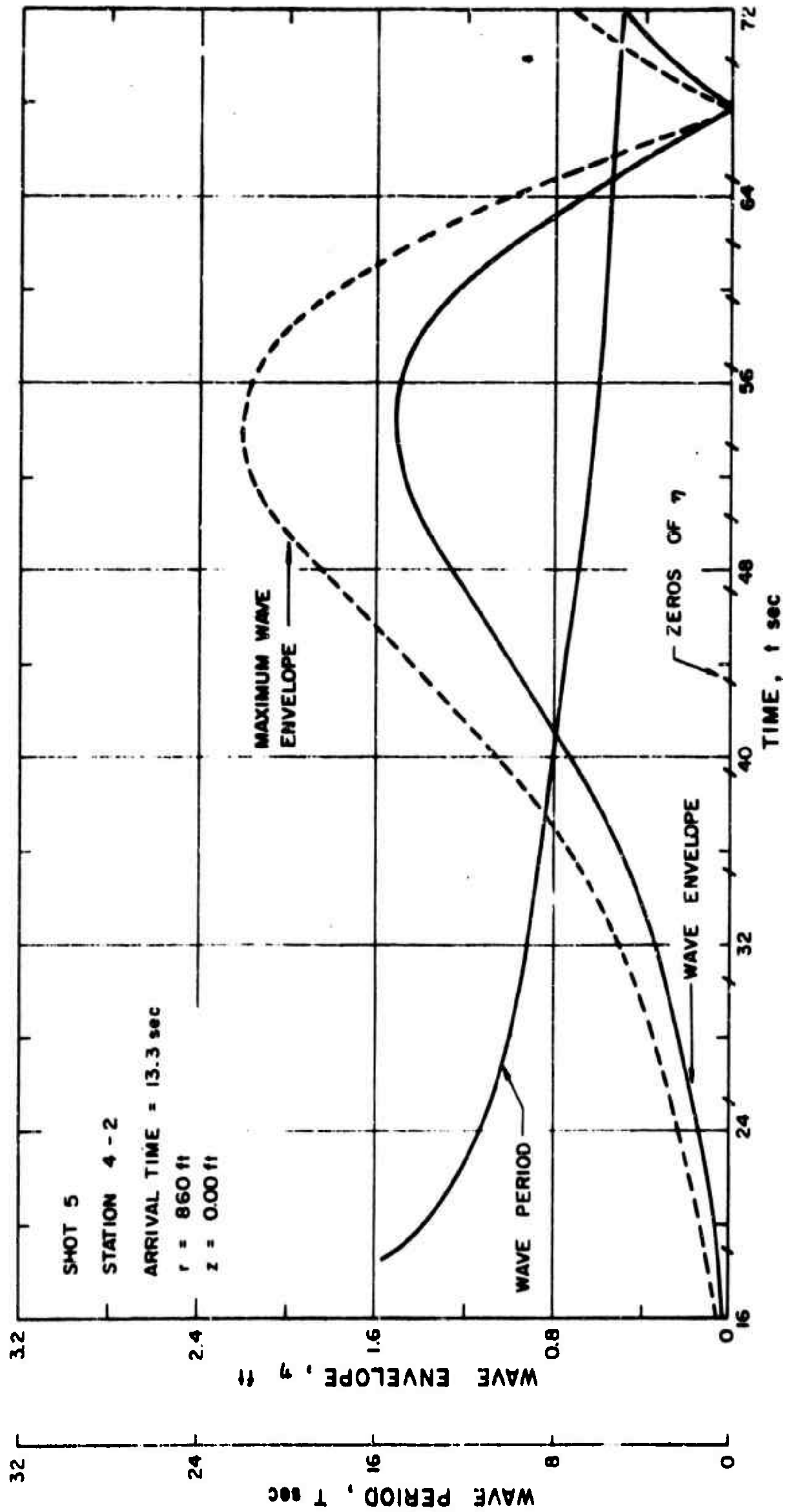

SHOT 5
STATION 4-2
ARRIVAL TIME = 13.3 sec
r = 860 ft
z = 0.00 ft
WAVE PERIOD
WAVE ENVELOPE
MAXIMUM WAVE ENVELOPE
ZEROS OF η
TIME, t sec
16 24 32 40 48 56 64 72
WAVE ENVELOPE, η ft
0 0.8 1.6 2.4 3.2
WAVE PERIOD, T sec
0 8 16 24 32

PB-3-7713

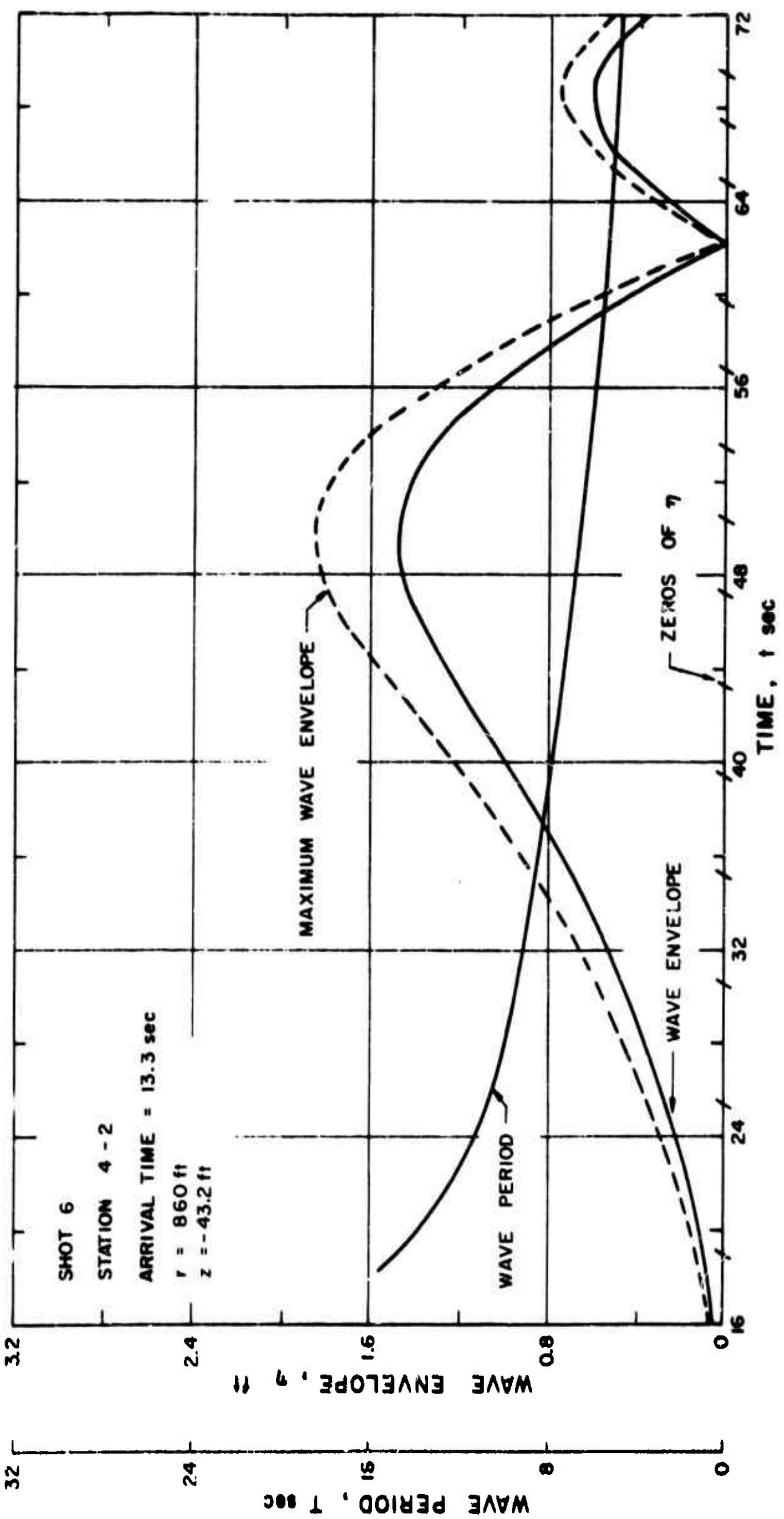
SHOT 6
STATION 4-2
ARRIVAL TIME = 13.3 sec
r = 860 ft
z = -43.2 ft
WAVE PERIOD
WAVE ENVELOPE
MAXIMUM WAVE ENVELOPE
ZEROS OF η
TIME, t sec
16
24
32
40
48
56
64
72
WAVE ENVELOPE, η ft
0
0.8
1.6
2.4
3.2
WAVE PERIOD, T sec
0
8
16
24
32

PB-3-7784

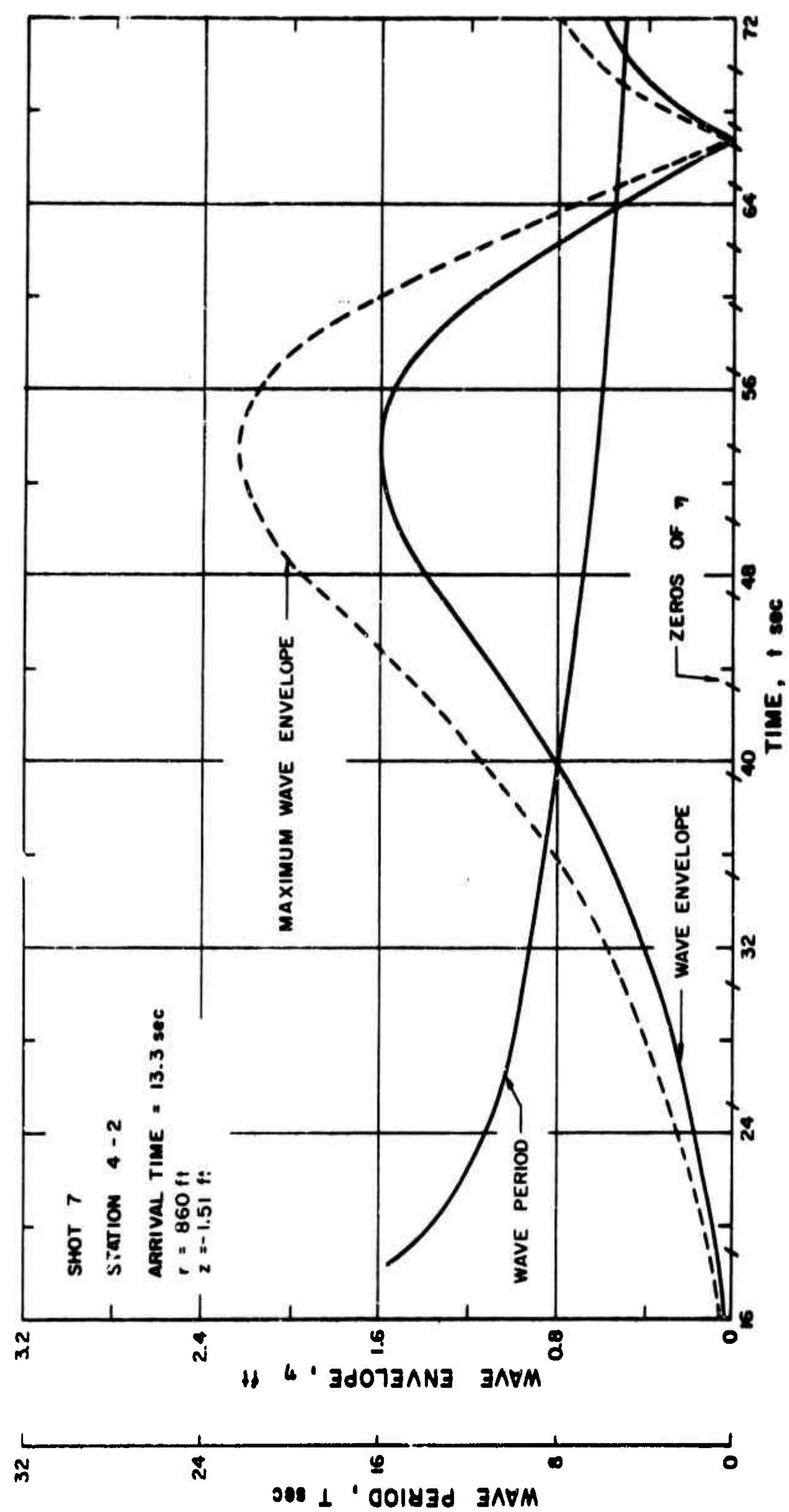
SHOT 7
STATION 4 - 2
ARRIVAL TIME = 13.3 sec
r = 860 ft
z = -1.51 ft
WAVE PERIOD
WAVE ENVELOPE
MAXIMUM WAVE ENVELOPE
ZEROS OF η
TIME, t sec
16
24
32
40
48
56
64
72
WAVE ENVELOPE, η ft
0
0.8
1.6
2.4
3.2
WAVE PERIOD, T sec
0
8
16
24
32

PB-3-7785

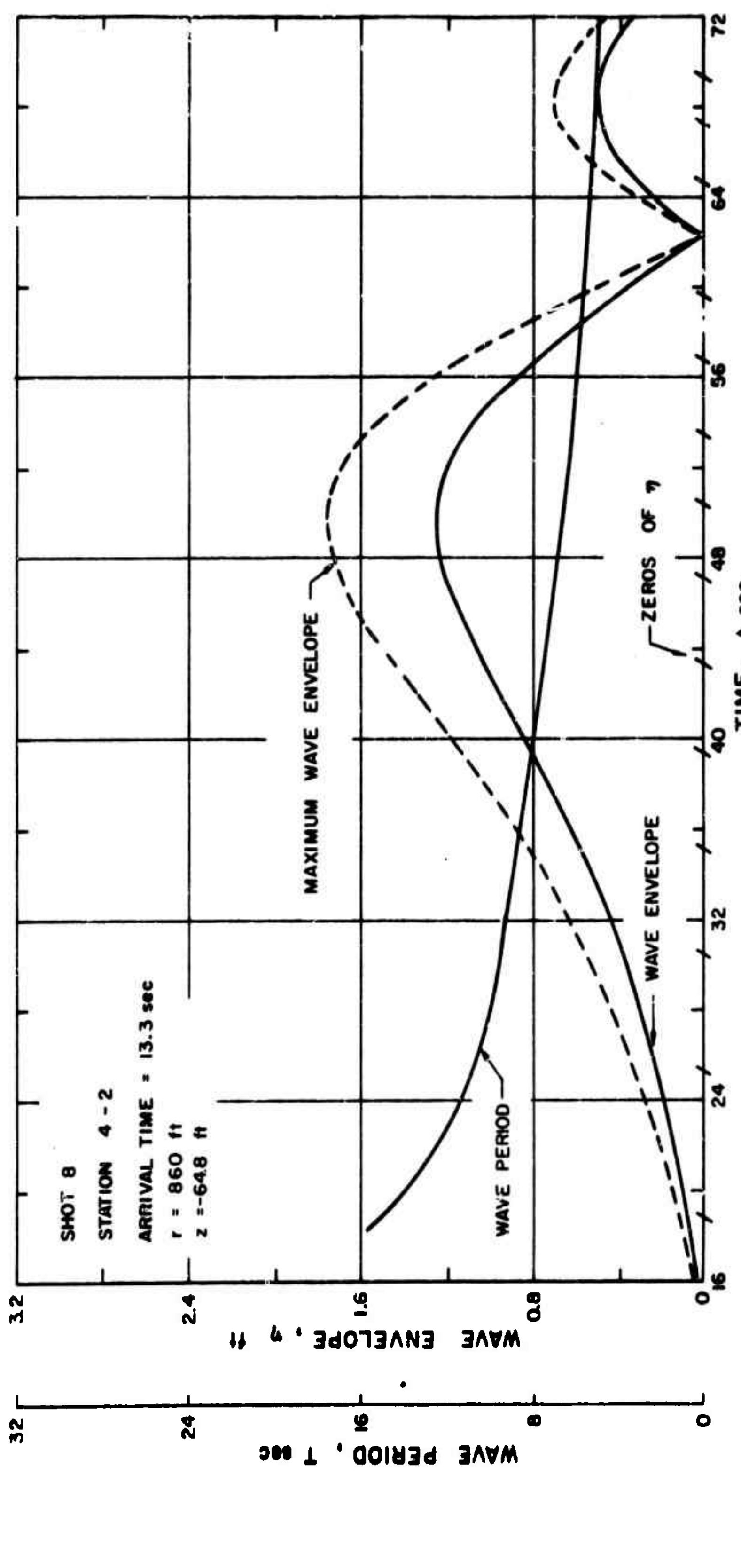
SHOT 8
STATION 4 - 2
ARRIVAL TIME = 13.3 sec
r = 860 ft
z = -64.8 ft
WAVE PERIOD
WAVE ENVELOPE
MAXIMUM WAVE ENVELOPE
ZEROS OF η
TIME, t sec
WAVE ENVELOPE, η ft
WAVE PERIOD, T sec
16
24
32
40
48
56
64
72
0
0.8
1.6
2.4
3.2
0
8
16
24
32

PB-3-7786

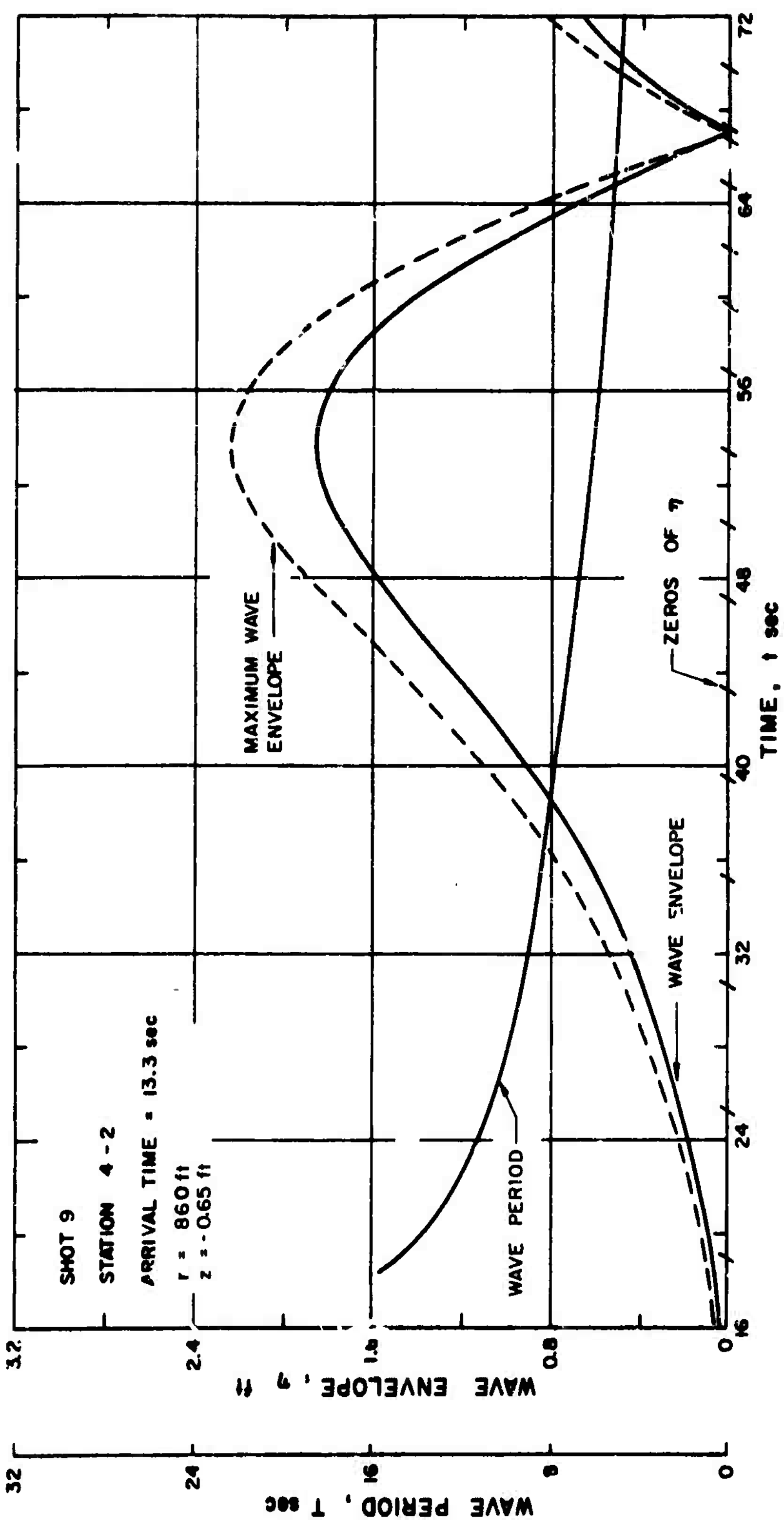
SHOT 9
STATION 4-2
ARRIVAL TIME = 13.3 sec
r = 860 ft
z = -0.65 ft
WAVE PERIOD
WAVE ENVELOPE
MAXIMUM WAVE ENVELOPE
ZEROS OF η
TIME, t sec
WAVE ENVELOPE, η ft
WAVE PERIOD, T sec

PB-1-7787

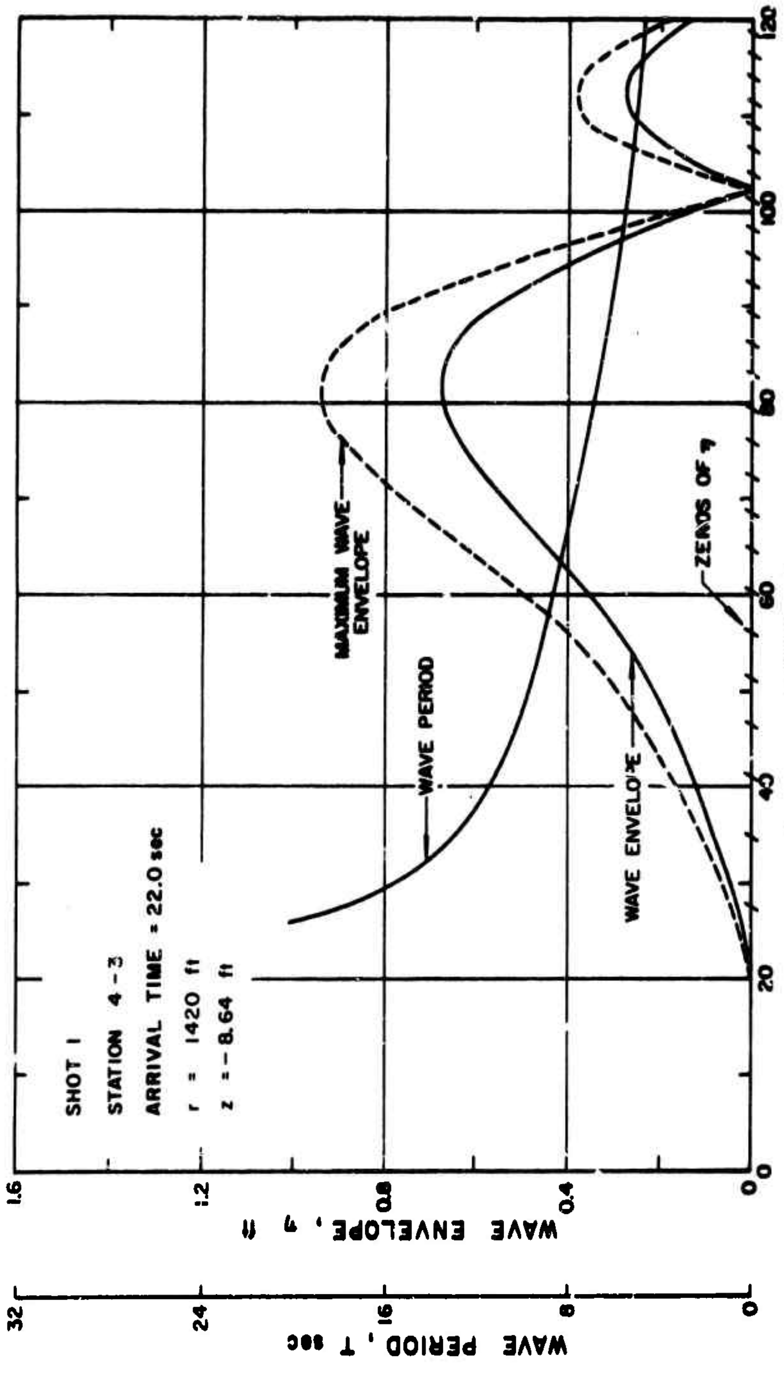
SHOT I
STATION 4-3
ARRIVAL TIME = 22.0 sec
r = 1420 ft
z = -8.64 ft
WAVE PERIOD
WAVE ENVELOPE
MAXIMUM WAVE ENVELOPE
ZEROS OF η
TIME, t sec
WAVE ENVELOPE, η ft
WAVE PERIOD, T sec

PB-3-7788

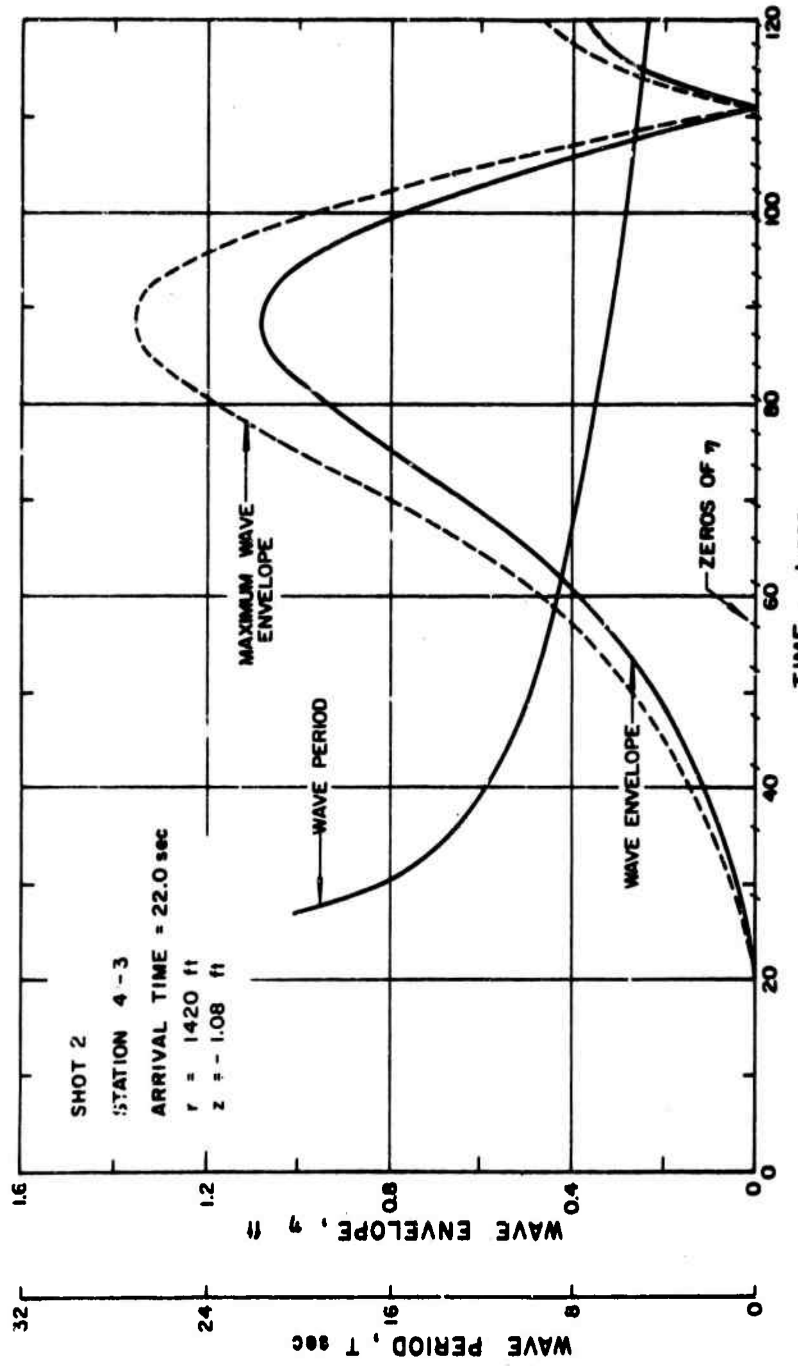
SHOT 2
STATION 4-3
ARRIVAL TIME = 22.0 sec
r = 1420 ft
z = - 1.08 ft
WAVE PERIOD
MAXIMUM WAVE ENVELOPE
WAVE ENVELOPE
ZEROS OF η
TIME , t sec
WAVE ENVELOPE , η ft
WAVE PERIOD , T sec
0
20
40
60
80
100
120
0.4
0.8
1.2
1.6
8
16
24
32

PB-3-7789

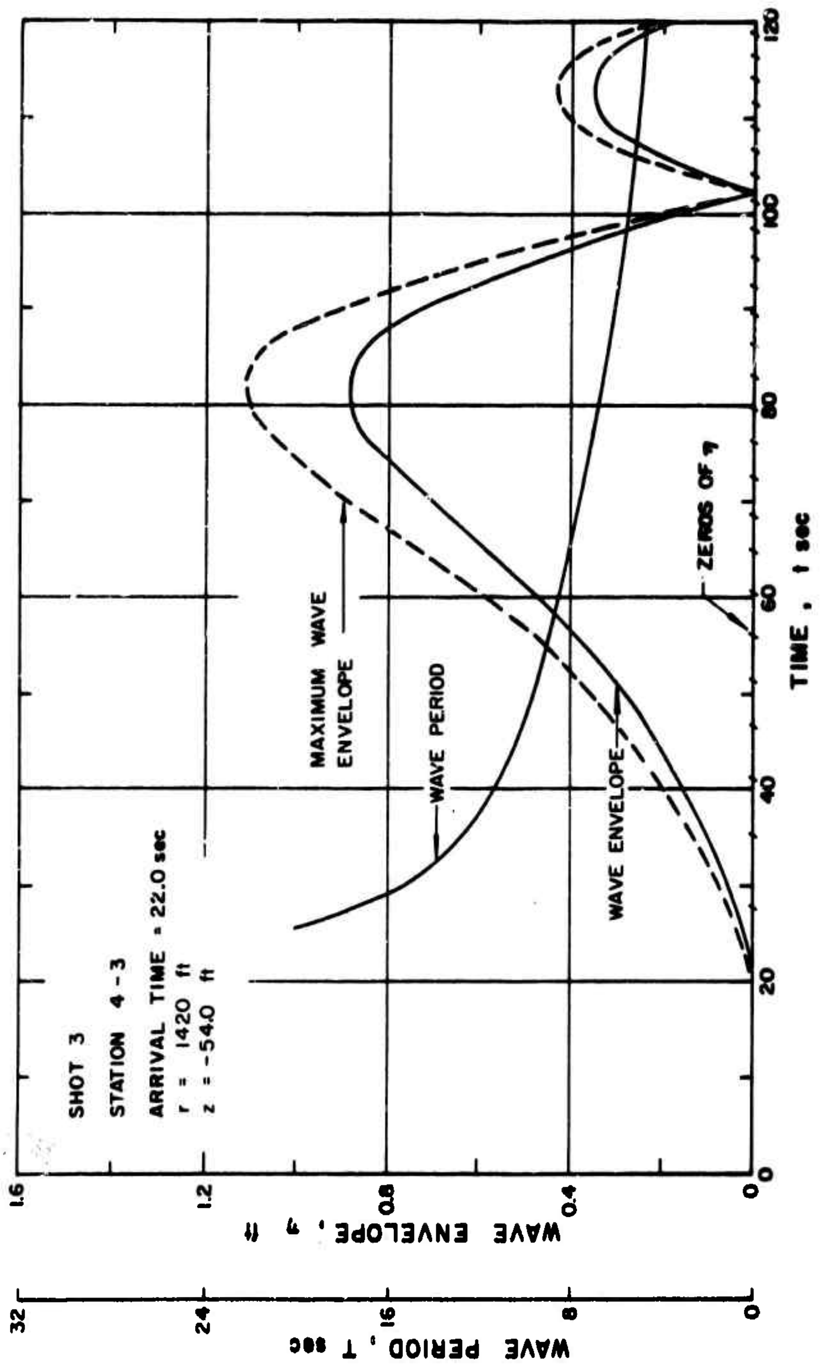

SHOT 3
STATION 4-3
ARRIVAL TIME = 22.0 sec
r = 1420 ft
z = -54.0 ft
MAXIMUM WAVE ENVELOPE
WAVE PERIOD
WAVE ENVELOPE
ZEROS OF η
TIME , t sec
0
20
40
60
80
100
120
WAVE ENVELOPE , η ft
0
0.4
0.8
1.2
1.6
WAVE PERIOD , T sec
0
8
16
24
32

PB-3-7790

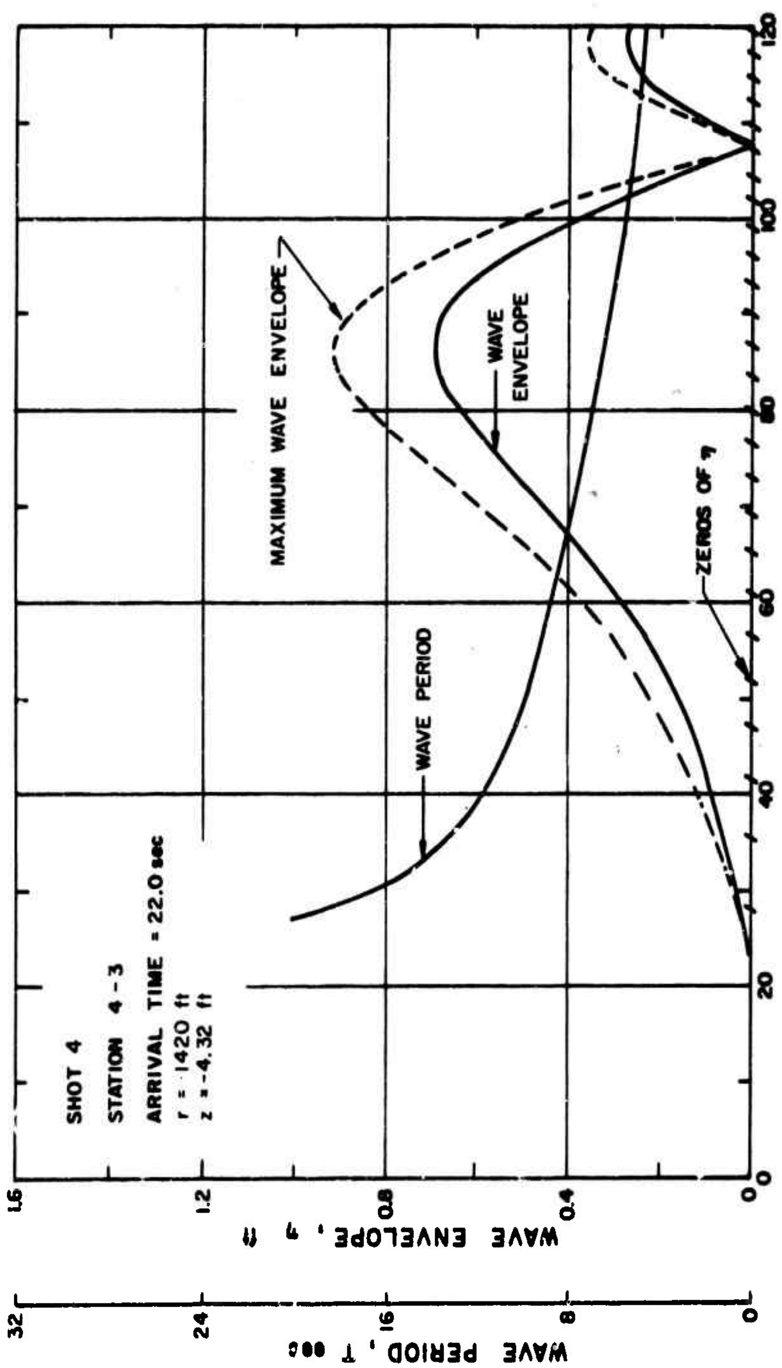
SHOT 4
STATION 4-3
ARRIVAL TIME = 22.0 sec
r = 1420 ft
z = -4.32 ft
MAXIMUM WAVE ENVELOPE
WAVE ENVELOPE
WAVE PERIOD
ZEROS OF η
TIME, t sec
WAVE ENVELOPE, η ft
WAVE PERIOD, T sec
0
20
40
60
80
100
120
0
0.4
0.8
1.2
1.6
0
8
16
24
32

PB-3-7791

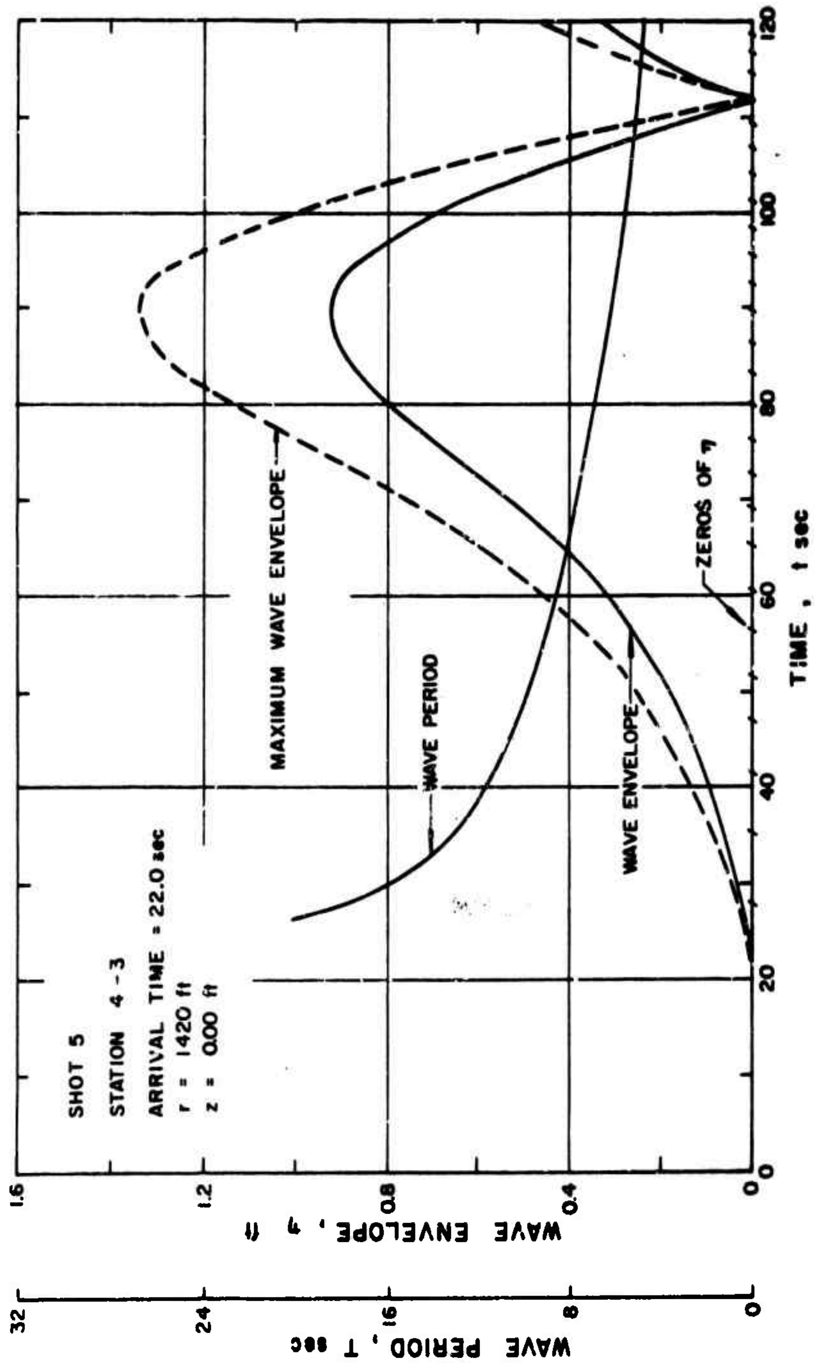
SHOT 5
STATION 4-3
ARRIVAL TIME = 22.0 sec
r = 1420 ft
z = 0.00 ft
MAXIMUM WAVE ENVELOPE
WAVE PERIOD
WAVE ENVELOPE
ZEROS OF η
TIME , t sec
WAVE ENVELOPE , η ft
WAVE PERIOD , T sec
0
20
40
60
80
100
120
0.4
0.8
1.2
1.6
8
16
24
32

PB-3-7792

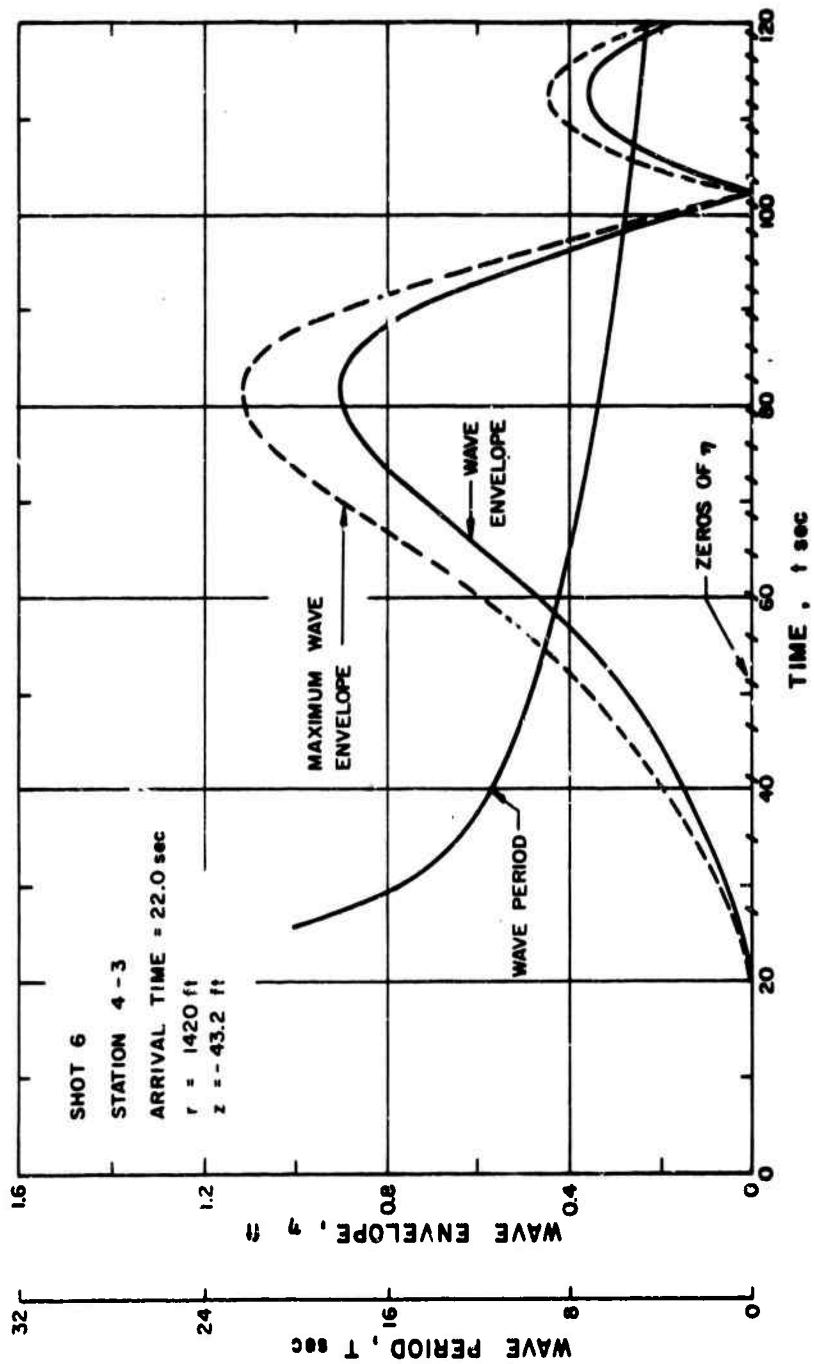
SHOT 6
STATION 4-3
ARRIVAL TIME = 22.0 sec
r = 1420 ft
z = -43.2 ft
MAXIMUM WAVE ENVELOPE
WAVE ENVELOPE
WAVE PERIOD
ZEROS OF η
TIME, t sec
WAVE ENVELOPE, η ft
WAVE PERIOD, T sec
0
20
40
60
80
100
120
0
0.4
0.8
1.2
1.6
0
8
16
24
32

PB-3-7791

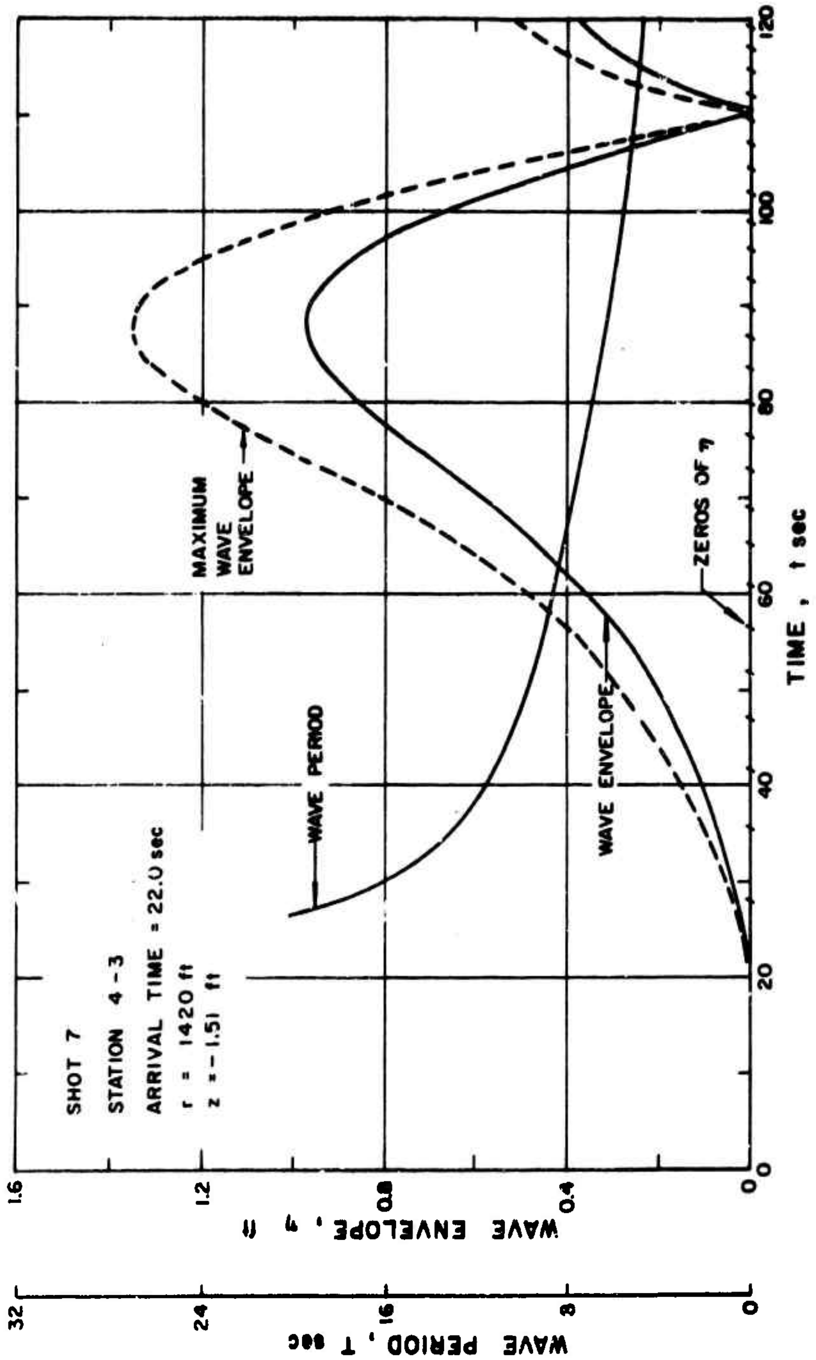
SHOT 7
STATION 4-3
ARRIVAL TIME = 22.0 sec
r = 1420 ft
z = -1.51 ft
WAVE PERIOD
WAVE ENVELOPE
MAXIMUM WAVE ENVELOPE
ZEROS OF η
TIME, t sec
WAVE ENVELOPE, η ft
WAVE PERIOD, T sec
0
20
40
60
80
100
120
0.4
0.8
1.2
1.6
8
16
24
32

PB-3-7794

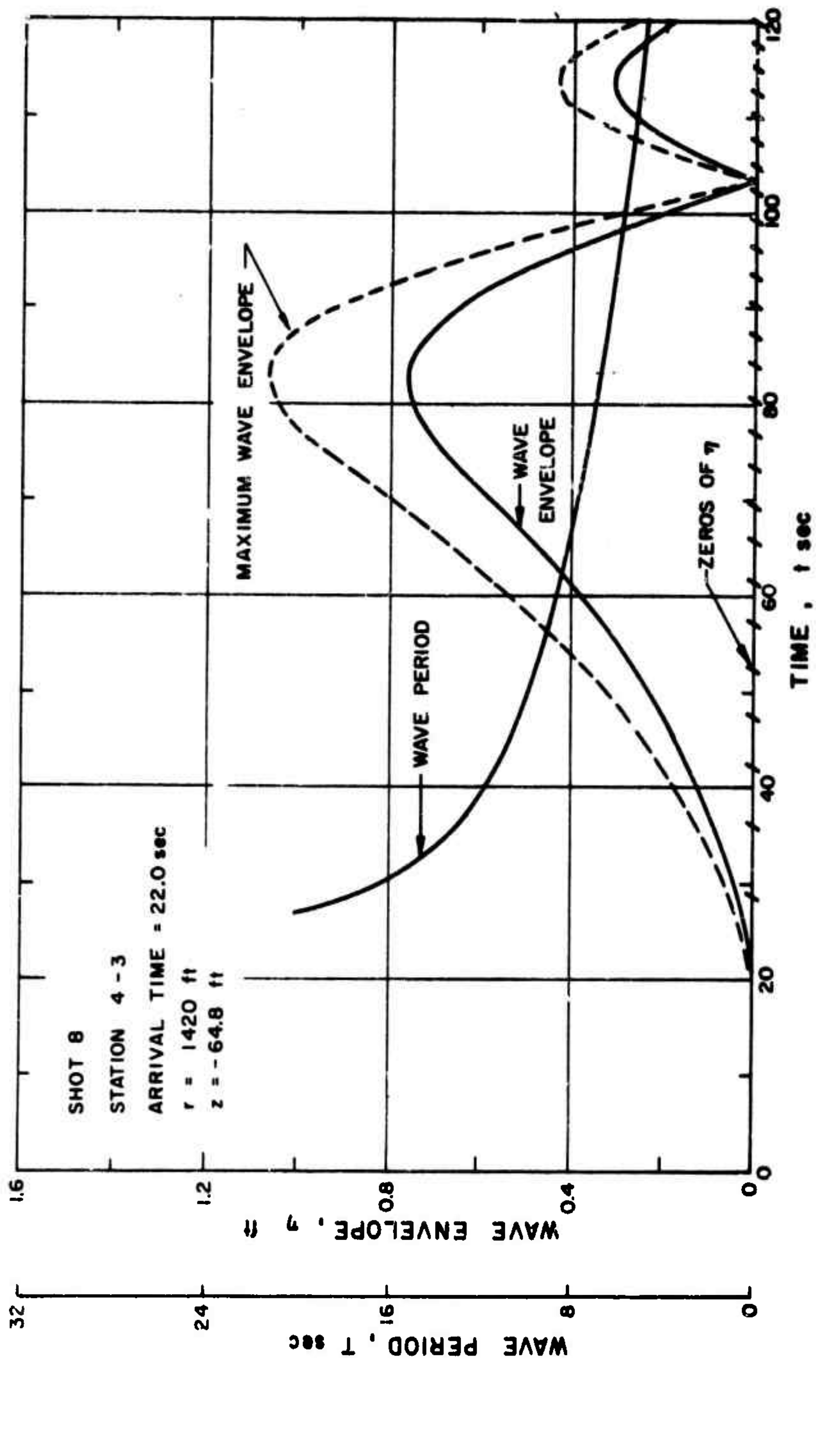
SHOT 8
STATION 4 - 3
ARRIVAL TIME = 22.0 sec
r = 1420 ft
z = -64.8 ft
MAXIMUM WAVE ENVELOPE
WAVE ENVELOPE
WAVE PERIOD
ZEROS OF η
TIME , t sec
WAVE ENVELOPE , η ft
WAVE PERIOD , T sec
0
20
40
60
80
100
120
0.4
0.8
1.2
1.6
8
16
24
32

PN-3-7795

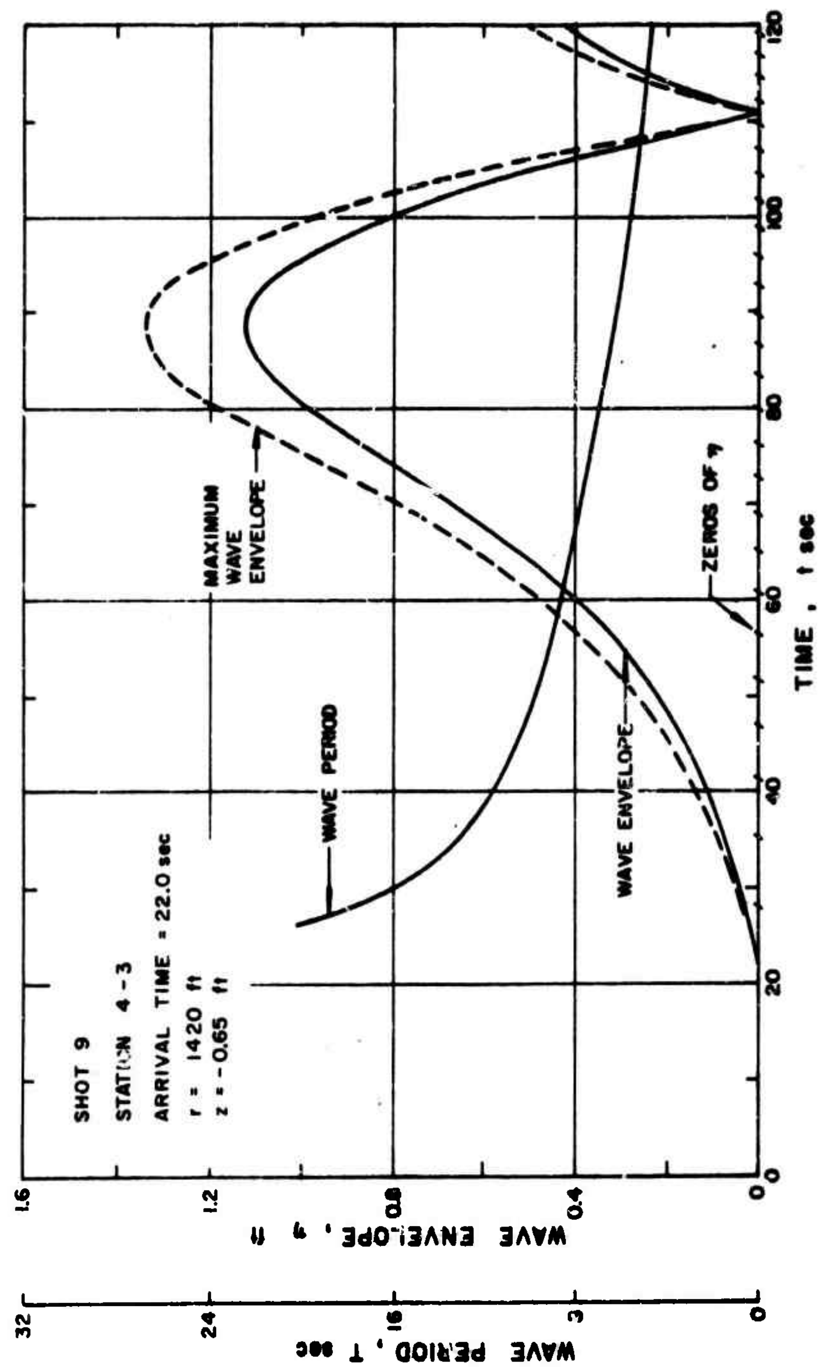
SHOT 9
STATION 4-3
ARRIVAL TIME = 22.0 sec
r = 1420 ft
z = -0.65 ft
WAVE PERIOD
WAVE ENVELOPE
MAXIMUM WAVE ENVELOPE
ZEROS OF η
TIME, t sec
WAVE ENVELOPE, η ft
WAVE PERIOD, T sec
0
20
40
60
80
100
120
0.4
0.8
1.2
1.6
8
16
24
32

PB-3-7796

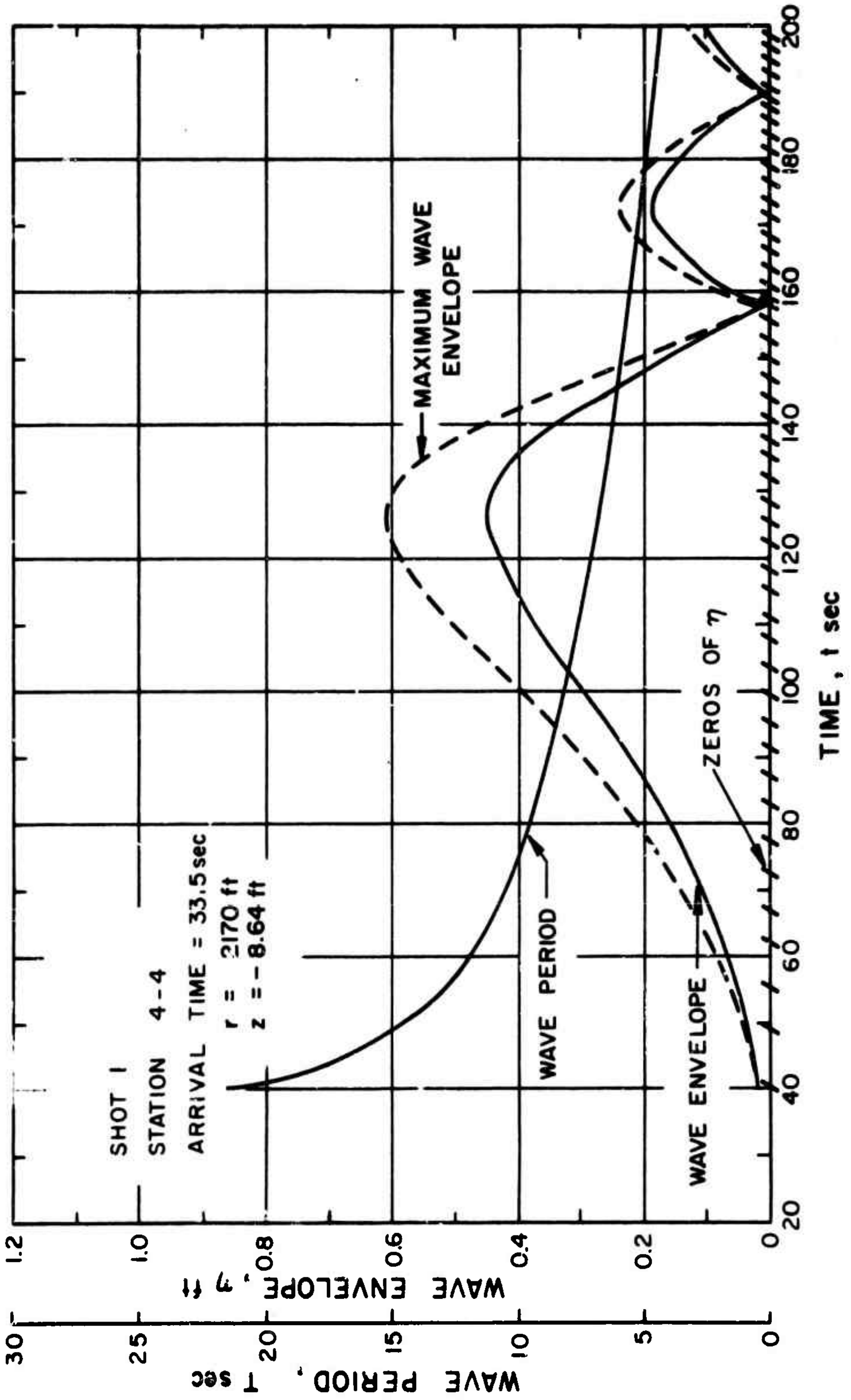
SHOT I
STATION 4-4
ARRIVAL TIME = 33.5 sec
r = 2170 ft
z = - 8.64 ft
MAXIMUM WAVE ENVELOPE
WAVE PERIOD
WAVE ENVELOPE
ZEROS OF η
TIME, t sec
WAVE ENVELOPE, η ft
WAVE PERIOD, T sec
0
20
40
60
80
100
120
140
160
180
200
0.2
0.4
0.6
0.8
1.0
1.2
5
10
15
20
25
30

PA-3-7797

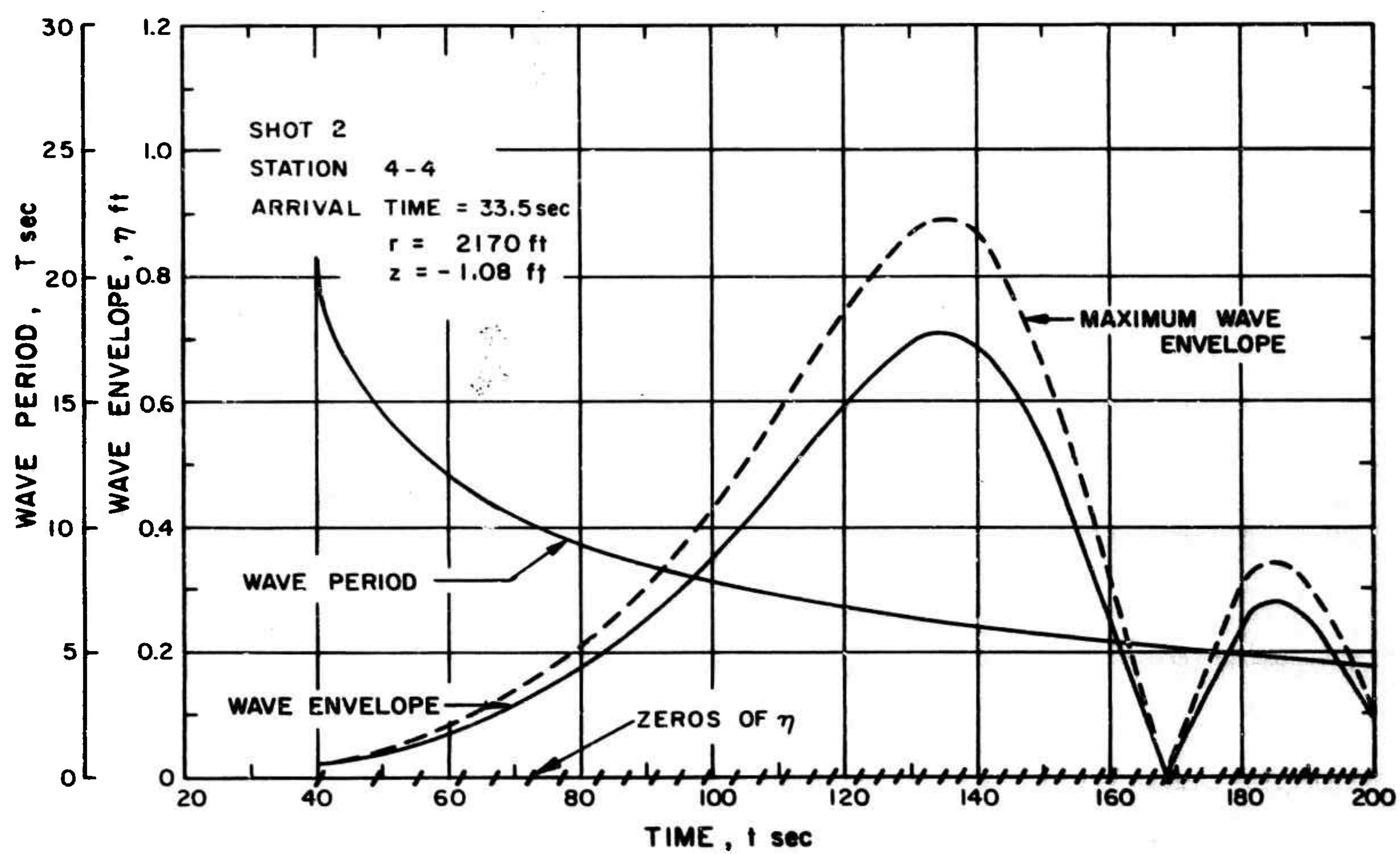
SHOT 2
STATION 4-4
ARRIVAL TIME = 33.5 sec
r = 2170 ft
z = -1.08 ft
MAXIMUM WAVE ENVELOPE
WAVE PERIOD
WAVE ENVELOPE
ZEROS OF η
WAVE PERIOD, T sec
WAVE ENVELOPE, η ft
TIME, t sec
0
5
10
15
20
25
30
0
0.2
0.4
0.6
0.8
1.0
1.2
20
40
60
80
100
120
140
160
180
200

PA-3-7798

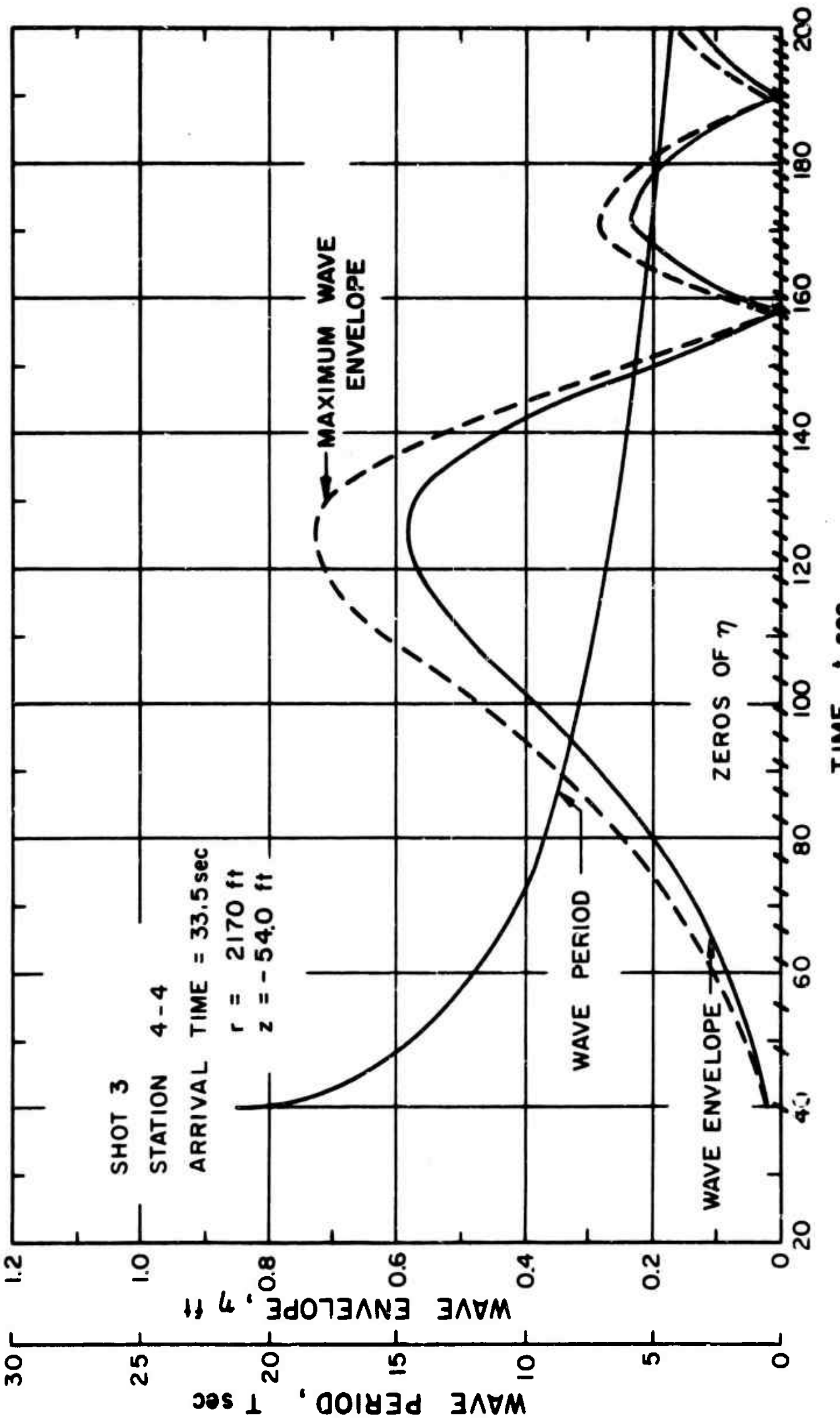
SHOT 3
STATION 4-4
ARRIVAL TIME = 33.5 sec
r = 2170 ft
z = -54.0 ft
MAXIMUM WAVE ENVELOPE
WAVE PERIOD
WAVE ENVELOPE
ZEROS OF η
TIME, t sec
WAVE ENVELOPE, η ft
WAVE PERIOD, T sec

PA-3-7799

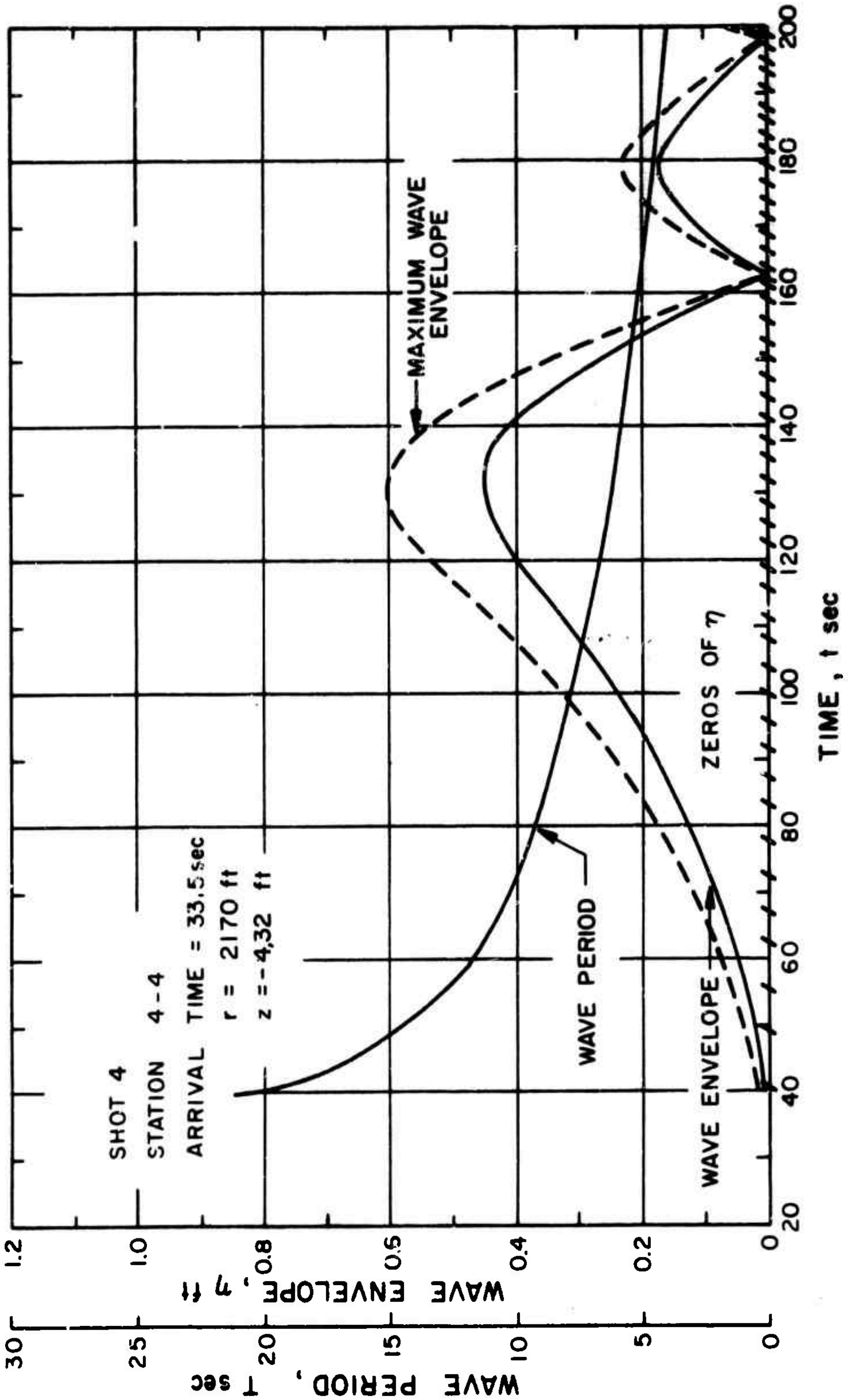
SHOT 4
STATION 4-4
ARRIVAL TIME = 33.5 sec
r = 2170 ft
z = -4.32 ft
WAVE PERIOD
WAVE ENVELOPE
MAXIMUM WAVE ENVELOPE
ZEROS OF η
TIME, t sec
WAVE ENVELOPE, η ft
WAVE PERIOD, T sec
20
40
60
80
100
120
140
160
180
200
0
0.2
0.4
0.6
0.8
1.0
1.2
0
5
10
15
20
25
30

PA-3-7800

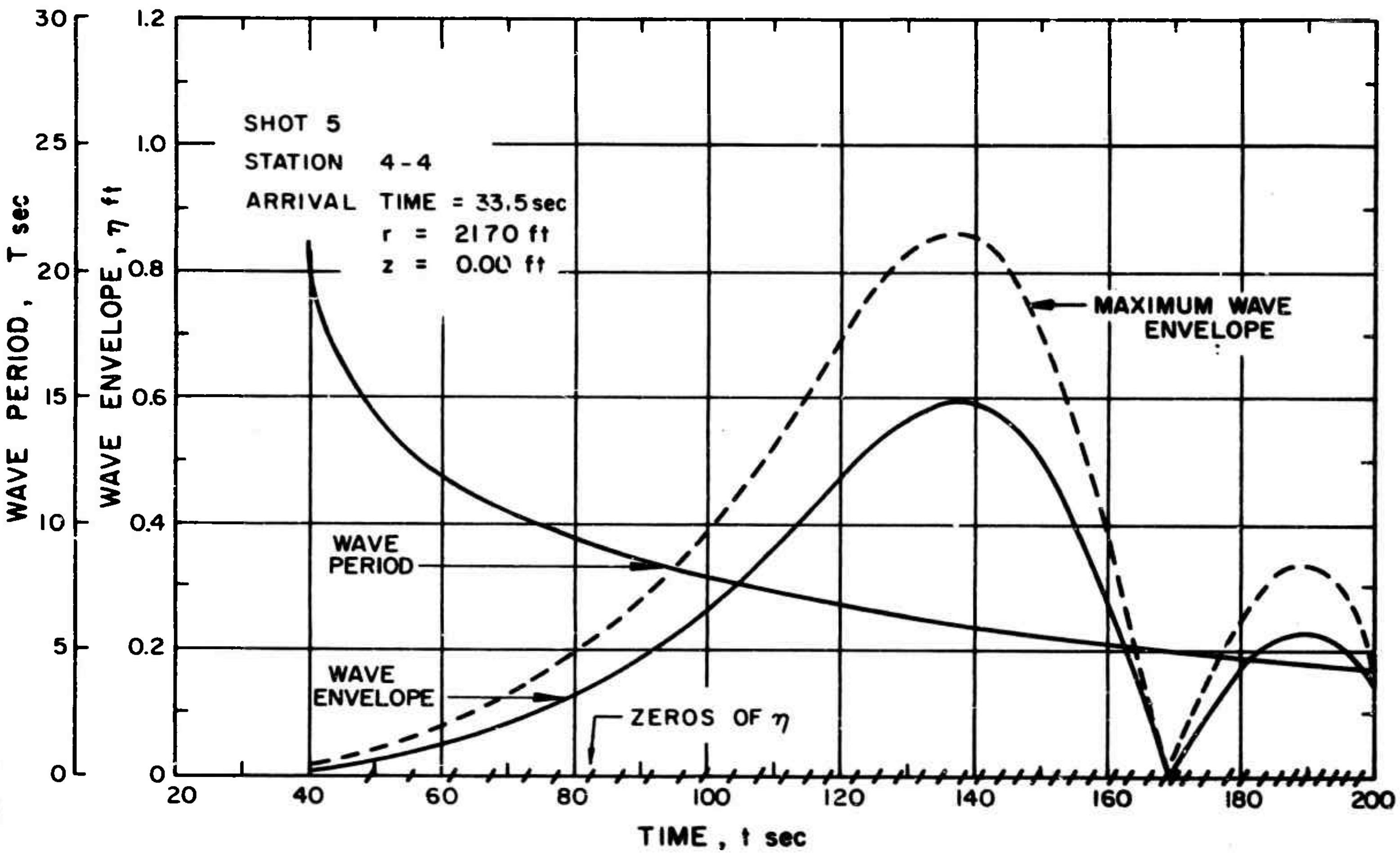
SHOT 5
STATION 4-4
ARRIVAL TIME = 33.5 sec
r = 2170 ft
z = 0.00 ft
MAXIMUM WAVE ENVELOPE
WAVE PERIOD
WAVE ENVELOPE
ZEROS OF η
TIME, t sec
WAVE PERIOD, T sec
WAVE ENVELOPE, η ft
0
5
10
15
20
25
30
0
0.2
0.4
0.6
0.8
1.0
1.2
20
40
60
80
100
120
140
160
180
200

PA-3-7801

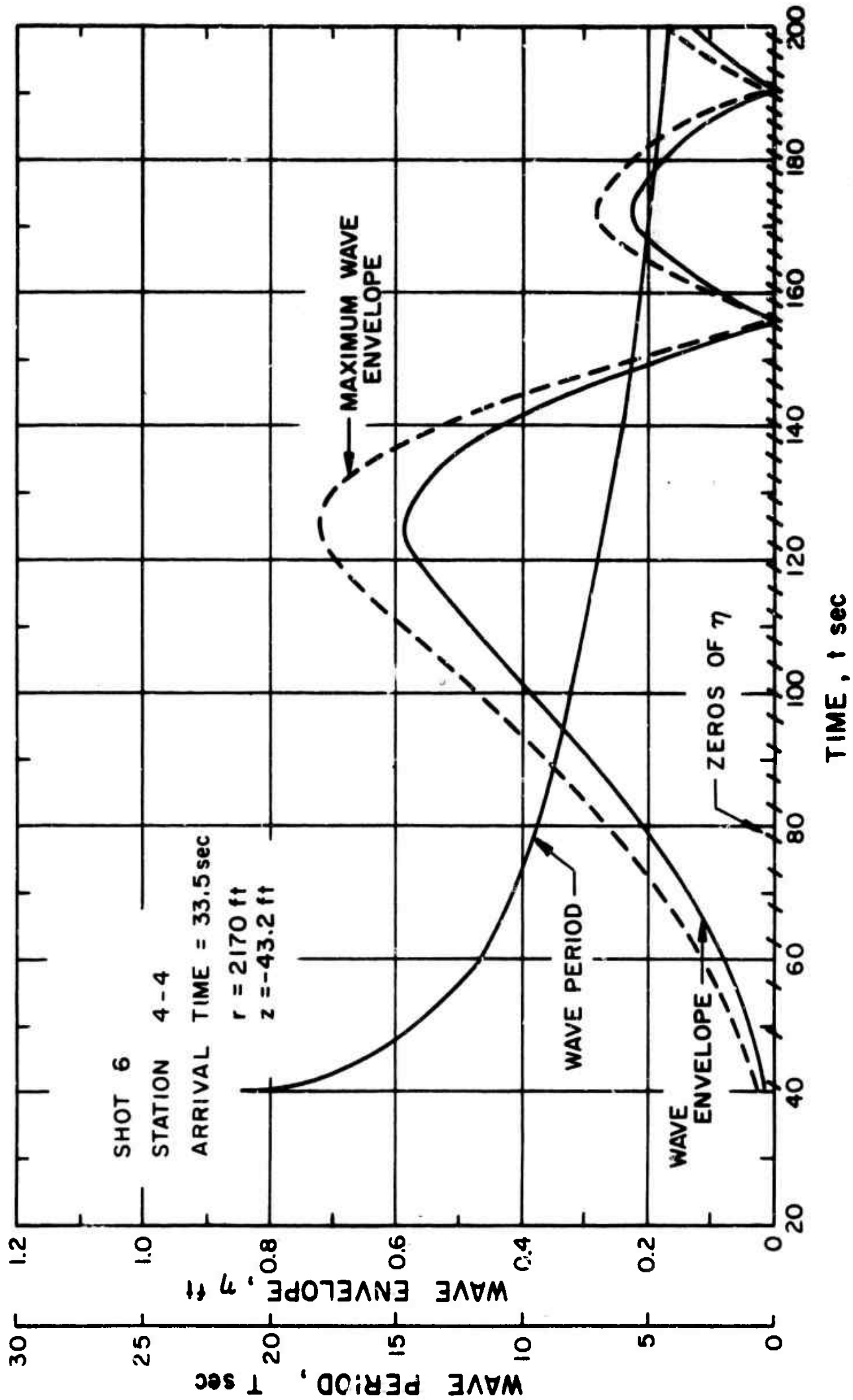
SHOT 6
STATION 4-4
ARRIVAL TIME = 33.5 sec
r = 2170 ft
z = -43.2 ft
MAXIMUM WAVE ENVELOPE
WAVE PERIOD
WAVE ENVELOPE
ZEROS OF η
TIME, t sec
WAVE ENVELOPE, η ft
WAVE PERIOD, T sec

PA-3-7802

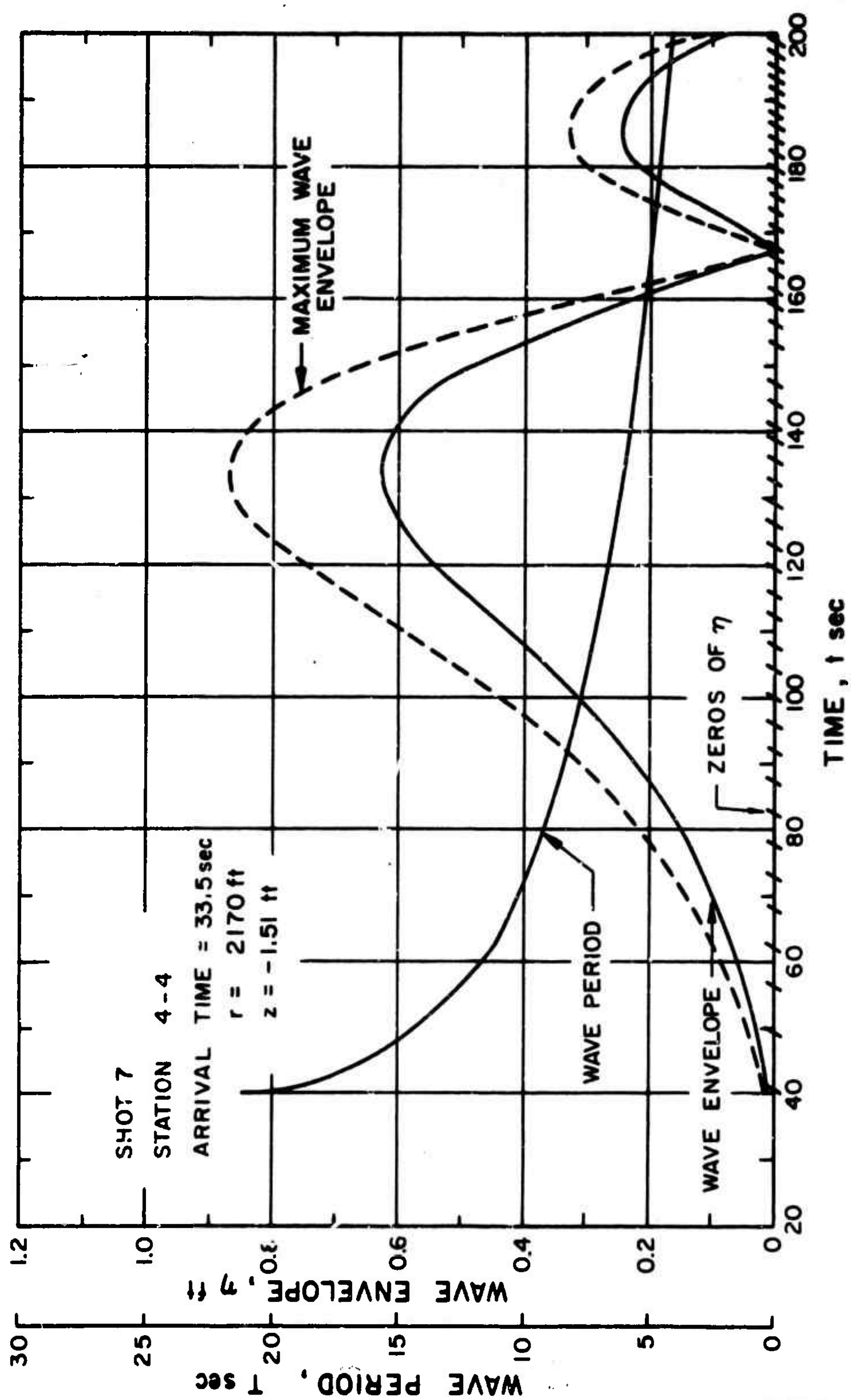
SHOT 7
STATION 4-4
ARRIVAL TIME = 33.5 sec
r = 2170 ft
z = -1.51 ft
MAXIMUM WAVE ENVELOPE
WAVE PERIOD
WAVE ENVELOPE
ZEROS OF η
TIME, t sec
WAVE ENVELOPE, η ft
WAVE PERIOD, T sec
20
40
60
80
100
120
140
160
180
200
0
0.2
0.4
0.6
0.8
1.0
1.2
0
5
10
15
20
25
30

PA-3-7803

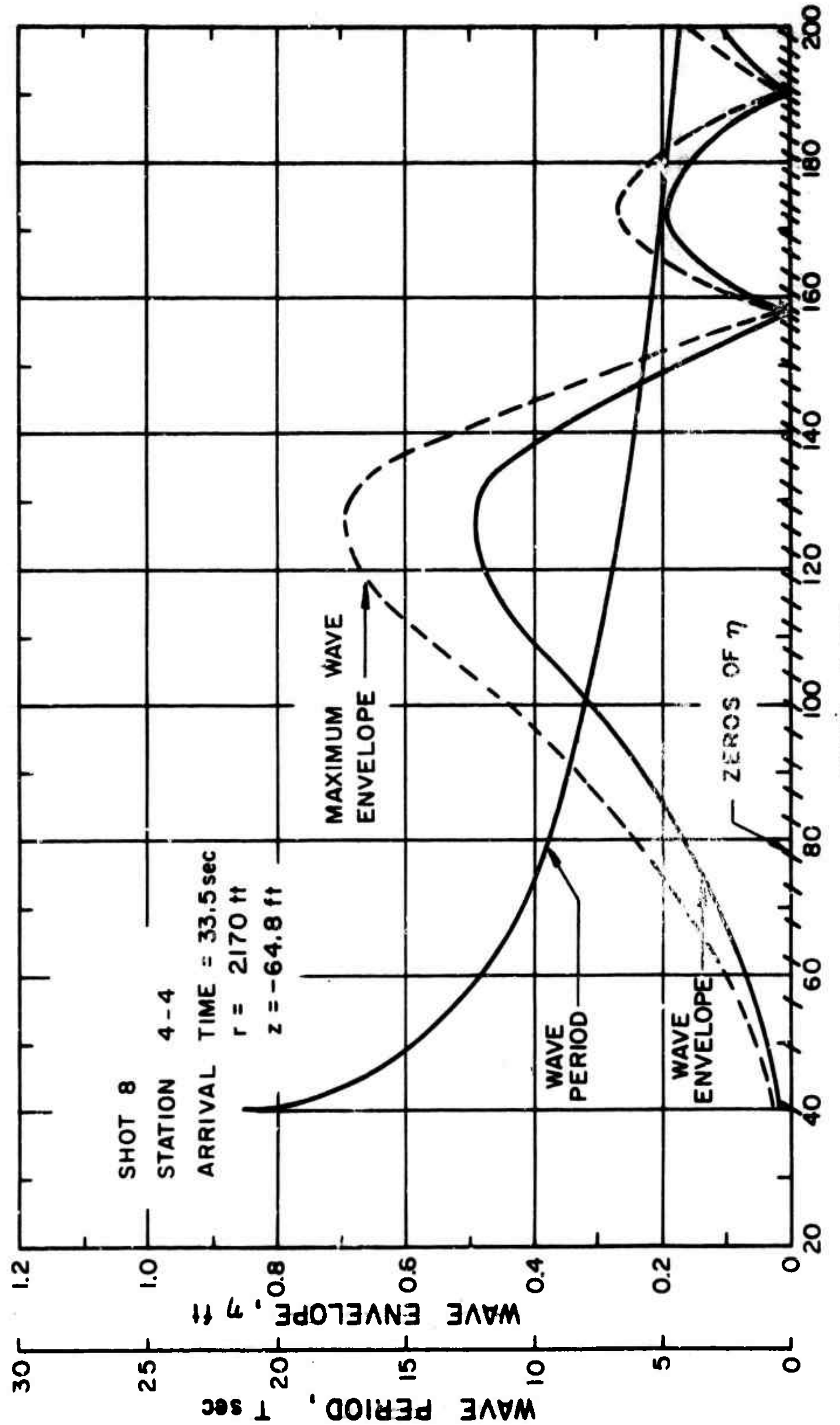

SHOT 8
STATION 4-4
ARRIVAL TIME = 33.5 sec
r = 2170 ft
z = -64.8 ft
WAVE PERIOD
WAVE ENVELOPE
MAXIMUM WAVE ENVELOPE
ZEROS OF η
TIME, t sec
WAVE ENVELOPE, η ft
WAVE PERIOD, T sec

PA-3-7804

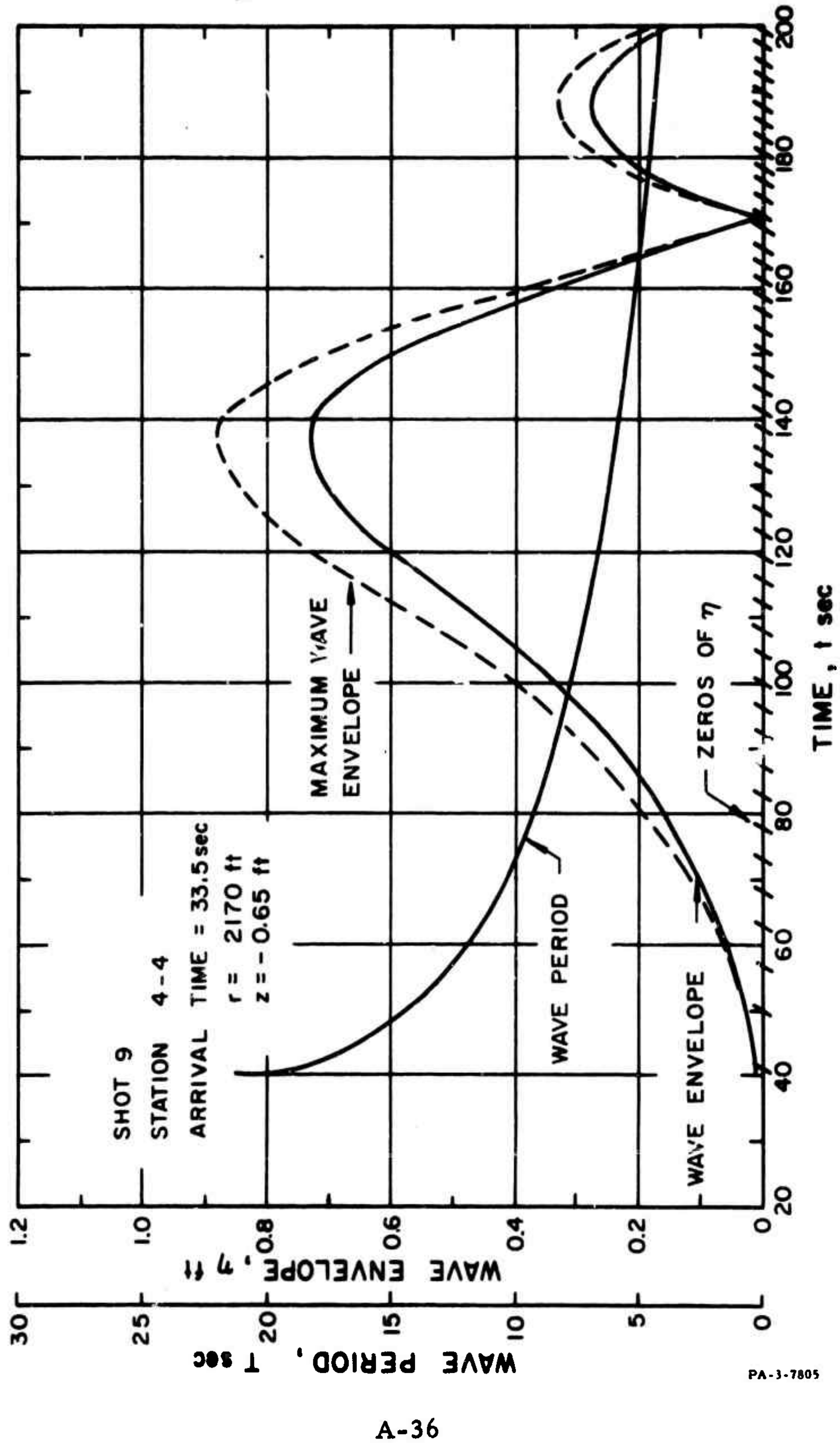
SHOT 9
STATION 4-4
ARRIVAL TIME = 33.5 sec
r = 2170 ft
z = -0.65 ft
MAXIMUM WAVE ENVELOPE
WAVE PERIOD
WAVE ENVELOPE
ZEROS OF η
TIME, t sec
WAVE ENVELOPE, η ft
WAVE PERIOD, T sec
20
40
60
80
100
120
140
160
180
200
0
0.2
0.4
0.6
0.8
1.0
1.2
0
5
10
15
20
25
30

PA-3-7805

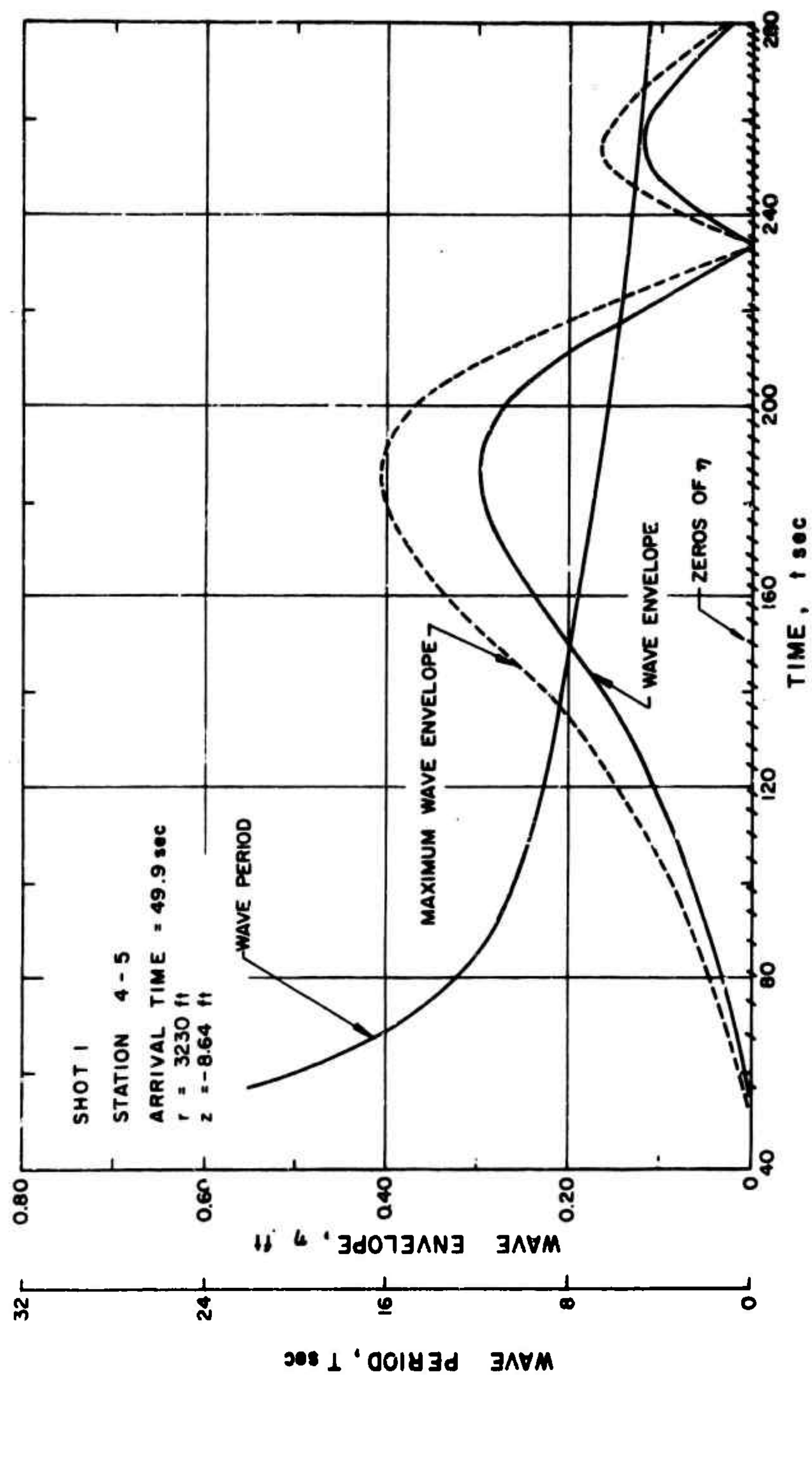
SHOT I
STATION 4 - 5
ARRIVAL TIME = 49.9 sec
r = 3230 ft
z = -8.64 ft
WAVE PERIOD
MAXIMUM WAVE ENVELOPE
WAVE ENVELOPE
ZEROS OF η
40
80
120
160
200
240
280
TIME, t sec
0
0.20
0.40
0.60
0.80
WAVE ENVELOPE, η ft
0
8
16
24
32
WAVE PERIOD, T sec

PB-3-7806

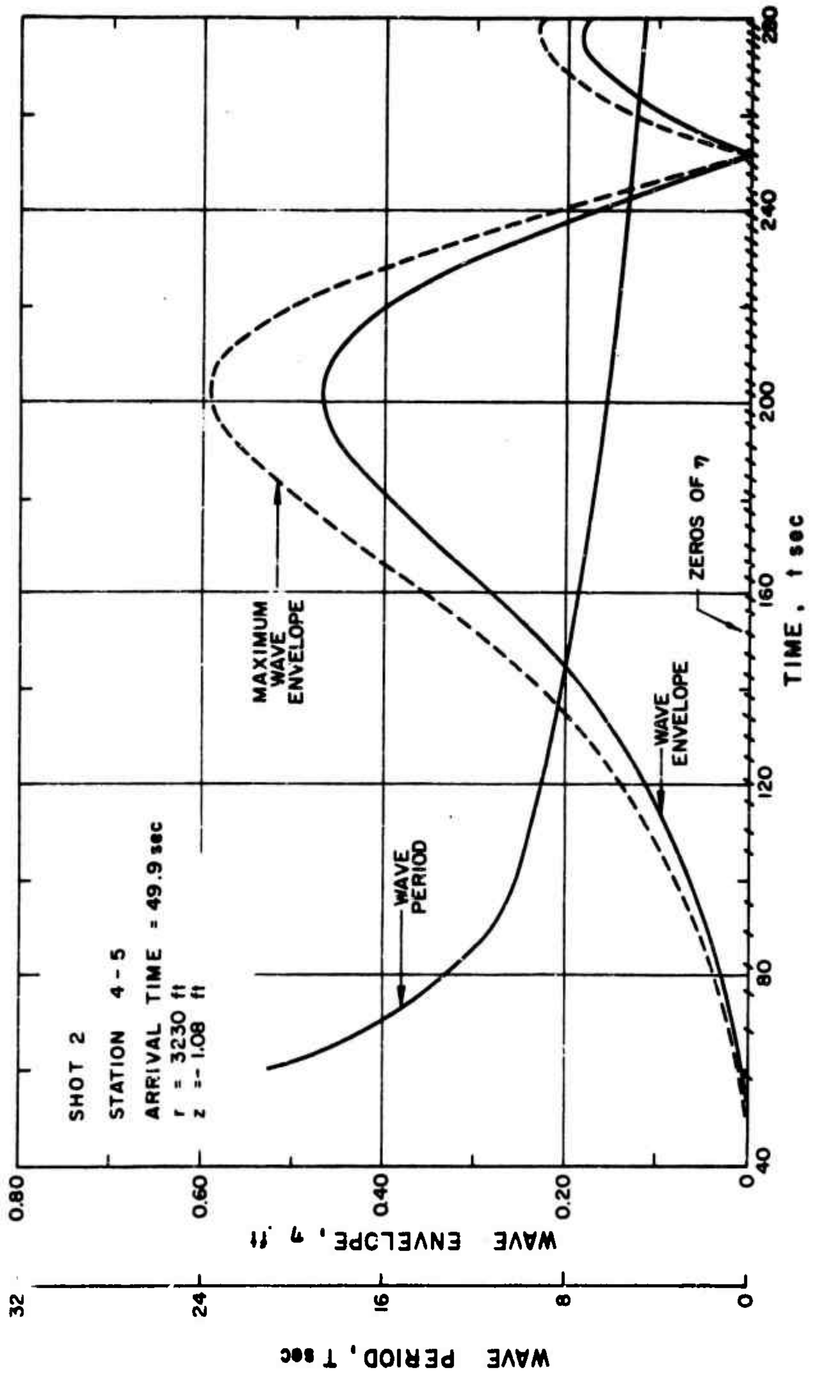
SHOT 2
STATION 4 - 5
ARRIVAL TIME = 49.9 sec
r = 3230 ft
z =- 1.08 ft
WAVE PERIOD
WAVE ENVELOPE
MAXIMUM WAVE ENVELOPE
ZEROS OF η
TIME, t sec
40
80
120
160
200
240
280
WAVE ENVELOPE, η ft
0
0.20
0.40
0.60
0.80
WAVE PERIOD, T sec
0
8
16
24
32

PB-3-7807

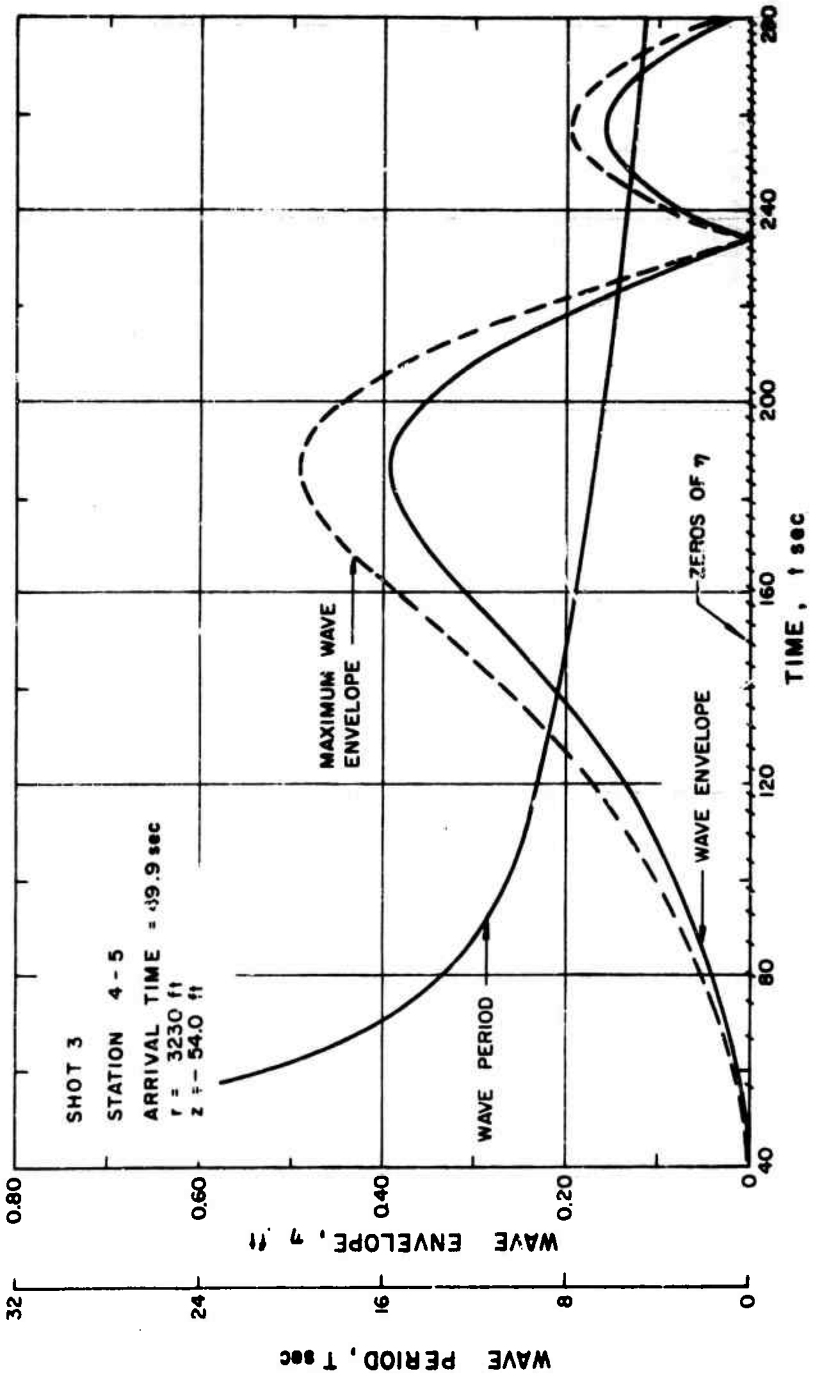
SHOT 3
STATION 4 - 5
ARRIVAL TIME = 39.9 sec
r = 3230 ft
z = - 54.0 ft
WAVE PERIOD
MAXIMUM WAVE ENVELOPE
WAVE ENVELOPE
ZEROS OF η
TIME, t sec
40
80
120
160
200
240
280
WAVE ENVELOPE, η ft
0
0.20
0.40
0.60
0.80
WAVE PERIOD, T sec
0
8
16
24
32

PB-3-7808

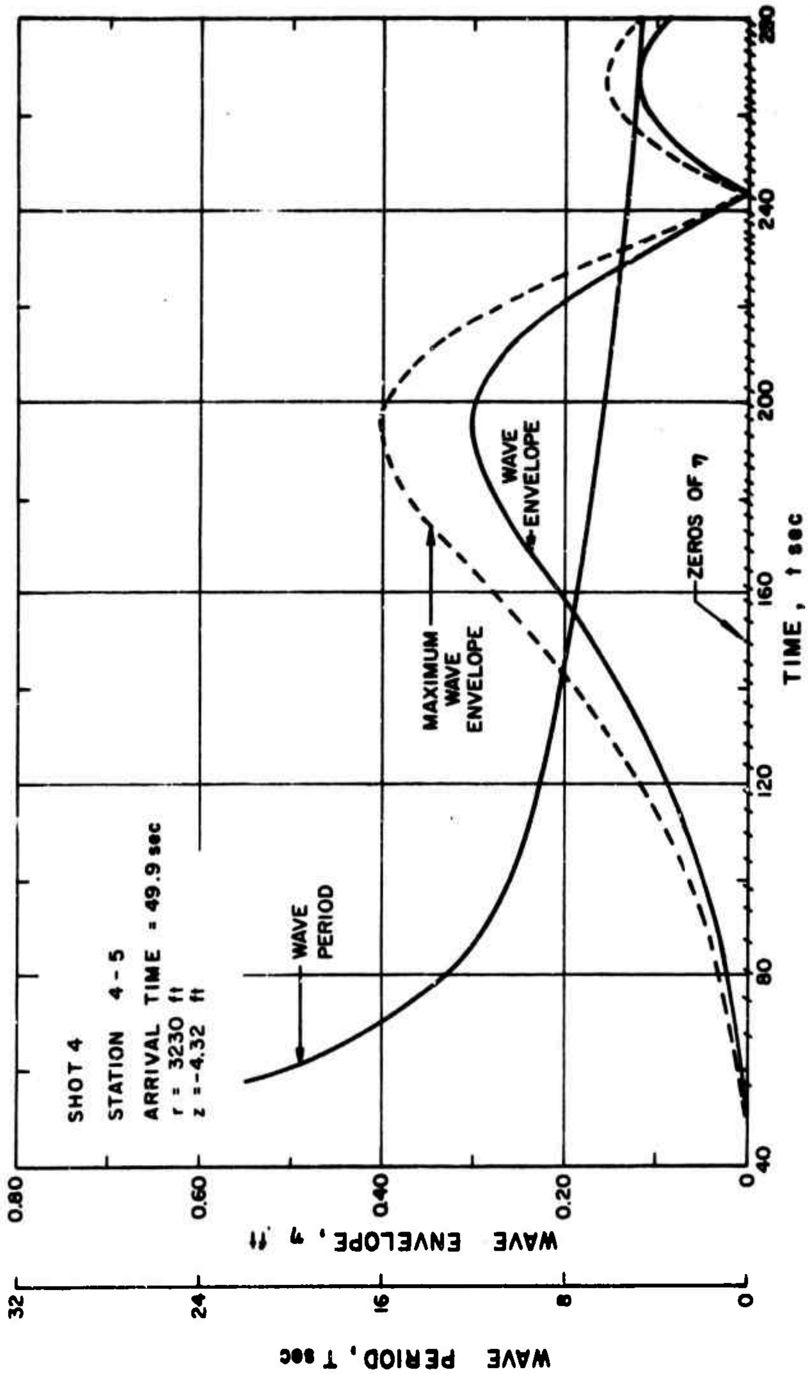
SHOT 4
STATION 4-5
ARRIVAL TIME = 49.9 sec
r = 3230 ft
z = -4.32 ft
WAVE PERIOD
MAXIMUM WAVE ENVELOPE
WAVE ENVELOPE
ZEROS OF η
TIME, t sec
WAVE ENVELOPE, η, ft
WAVE PERIOD, T sec
40
80
120
160
200
240
280
0
0.20
0.40
0.60
0.80
0
8
16
24
32

PB-3-7809

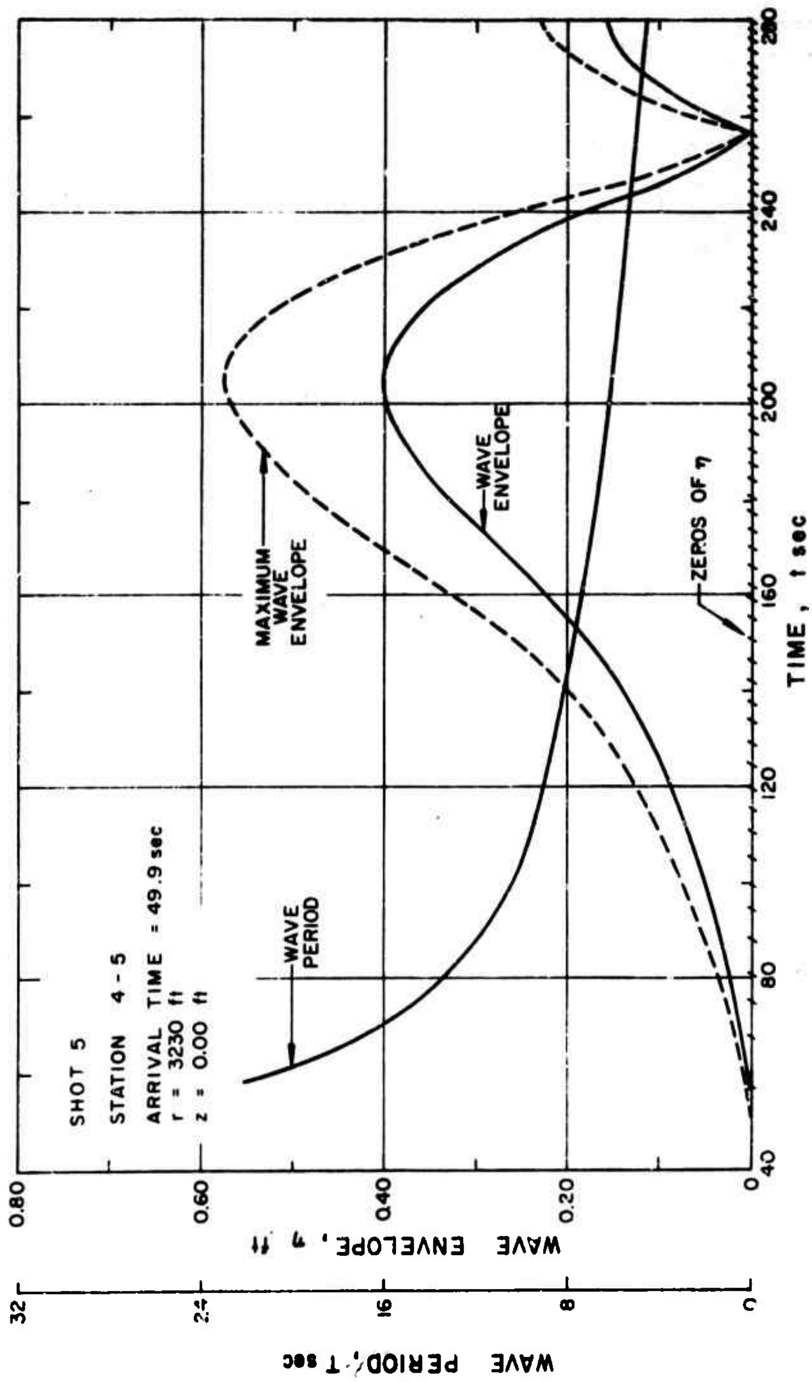
SHOT 5
STATION 4 - 5
ARRIVAL TIME = 49.9 sec
r = 3230 ft
z = 0.00 ft
WAVE PERIOD
MAXIMUM WAVE ENVELOPE
WAVE ENVELOPE
ZEROS OF η
TIME, t sec
WAVE ENVELOPE, η ft
WAVE PERIOD, T sec
0 40 80 120 160 200 240 280
0 0.20 0.40 0.60 0.80
0 8 16 24 32

PB-3-7810

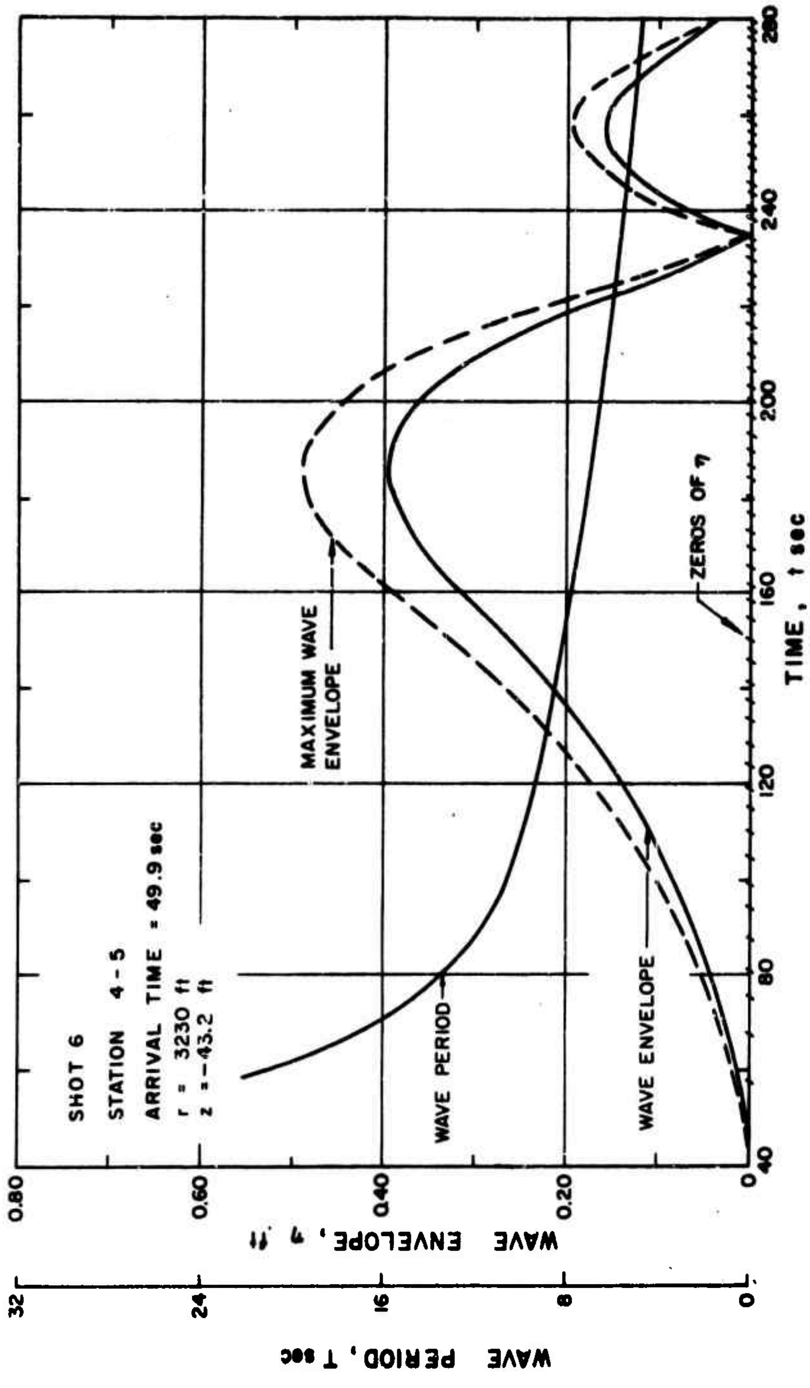

SHOT 6
STATION 4-5
ARRIVAL TIME = 49.9 sec
r = 3230 ft
z = -43.2 ft
MAXIMUM WAVE ENVELOPE
WAVE PERIOD
WAVE ENVELOPE
ZEROS OF η
TIME, t sec
WAVE ENVELOPE, η ft
WAVE PERIOD, T sec
0.80
0.60
0.40
0.20
0
32
24
16
8
0
40
80
120
160
200
240
280

PB-3-7811

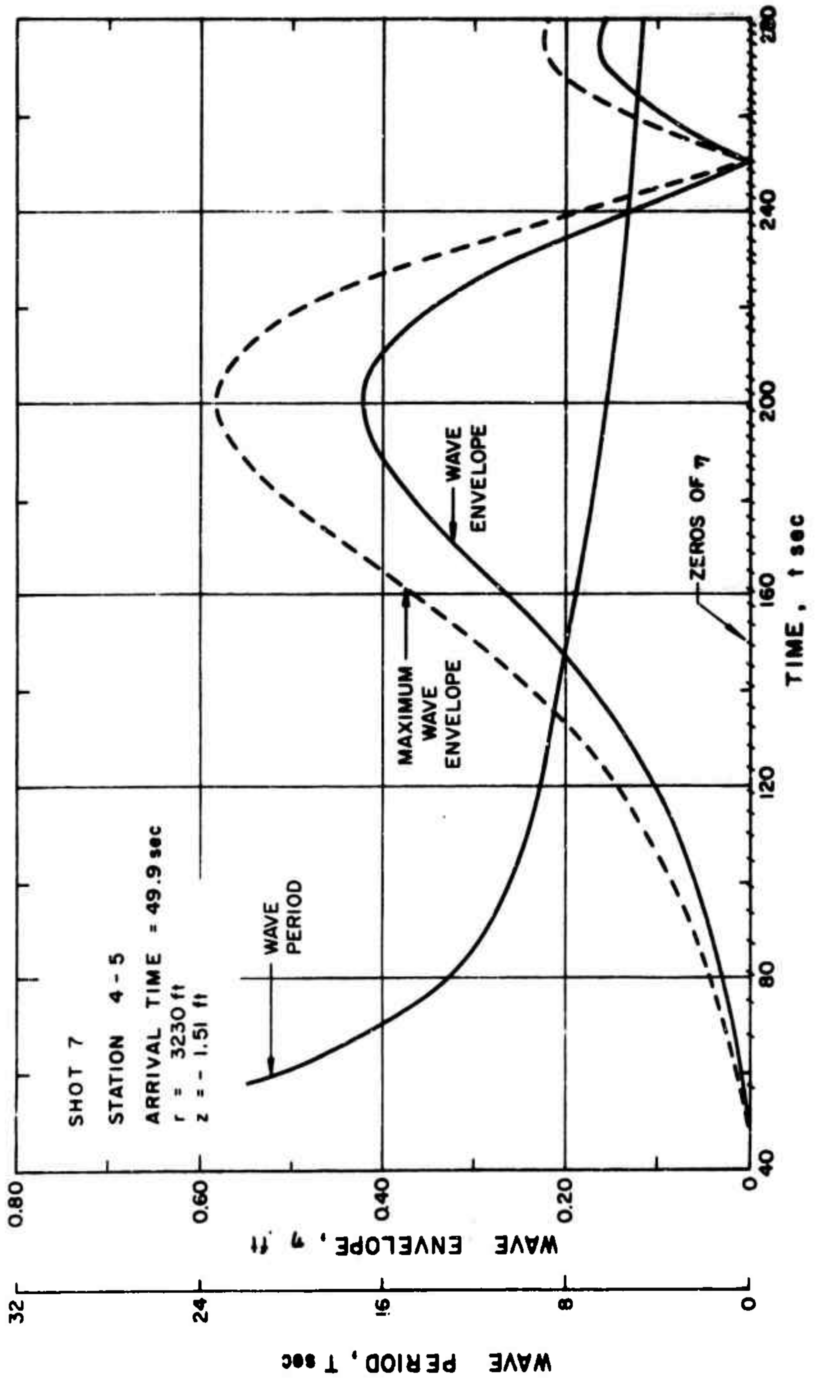
SHOT 7
STATION 4 - 5
ARRIVAL TIME = 49.9 sec
r = 3230 ft
z = - 1.51 ft
WAVE PERIOD
MAXIMUM WAVE ENVELOPE
WAVE ENVELOPE
ZEROS OF η
TIME, t sec
40
80
120
160
200
240
280
WAVE ENVELOPE, η ft
0
0.20
0.40
0.60
0.80
WAVE PERIOD, T sec
0
8
16
24
32

PB-3-7812

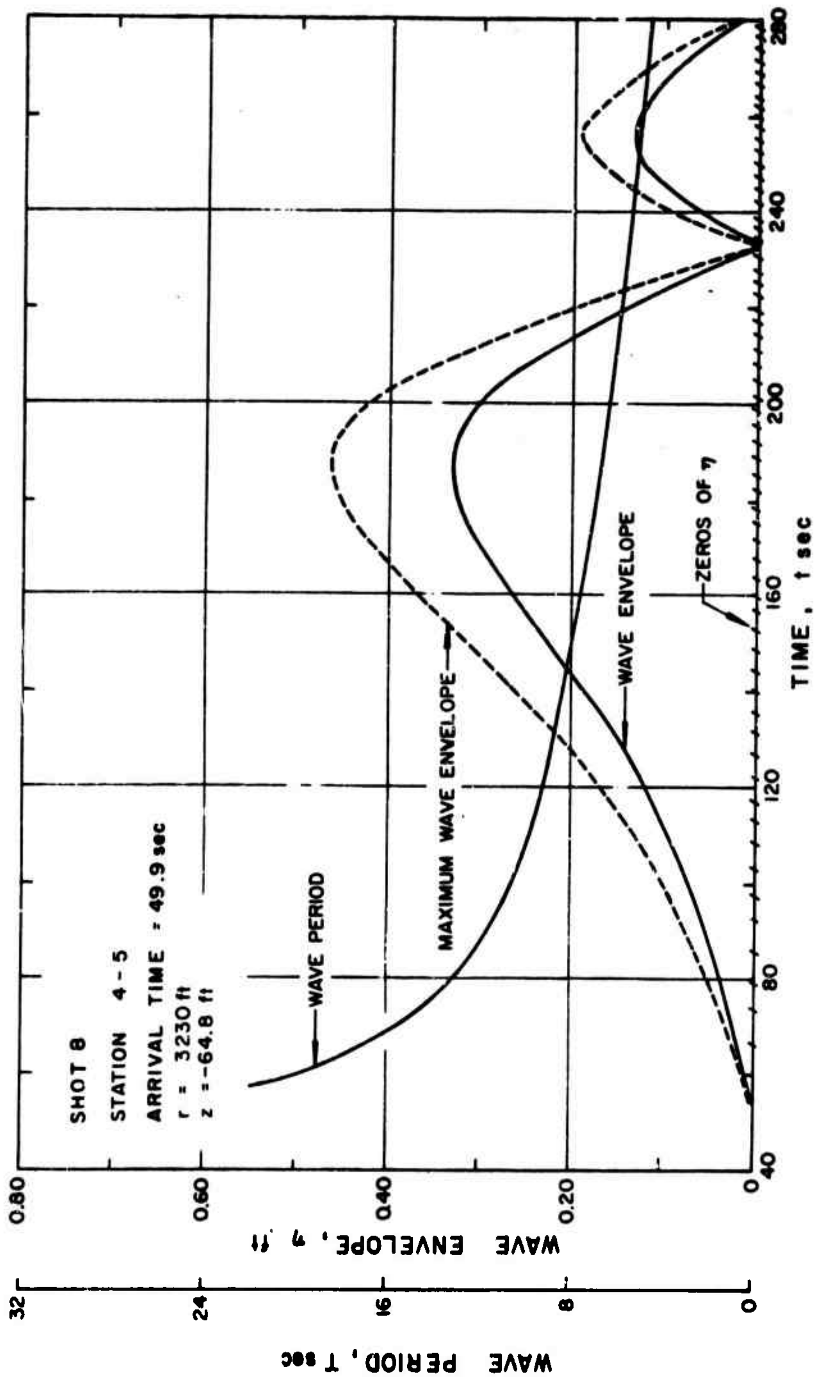
SHOT 8
STATION 4-5
ARRIVAL TIME = 49.9 sec
r = 3230 ft
z = -64.8 ft
WAVE PERIOD
MAXIMUM WAVE ENVELOPE
WAVE ENVELOPE
ZEROS OF η
TIME, t sec
40 80 120 160 200 240 280
WAVE ENVELOPE, η, ft
0 0.20 0.40 0.60 0.80
WAVE PERIOD, T sec
0 8 16 24 32

PB-3-7813

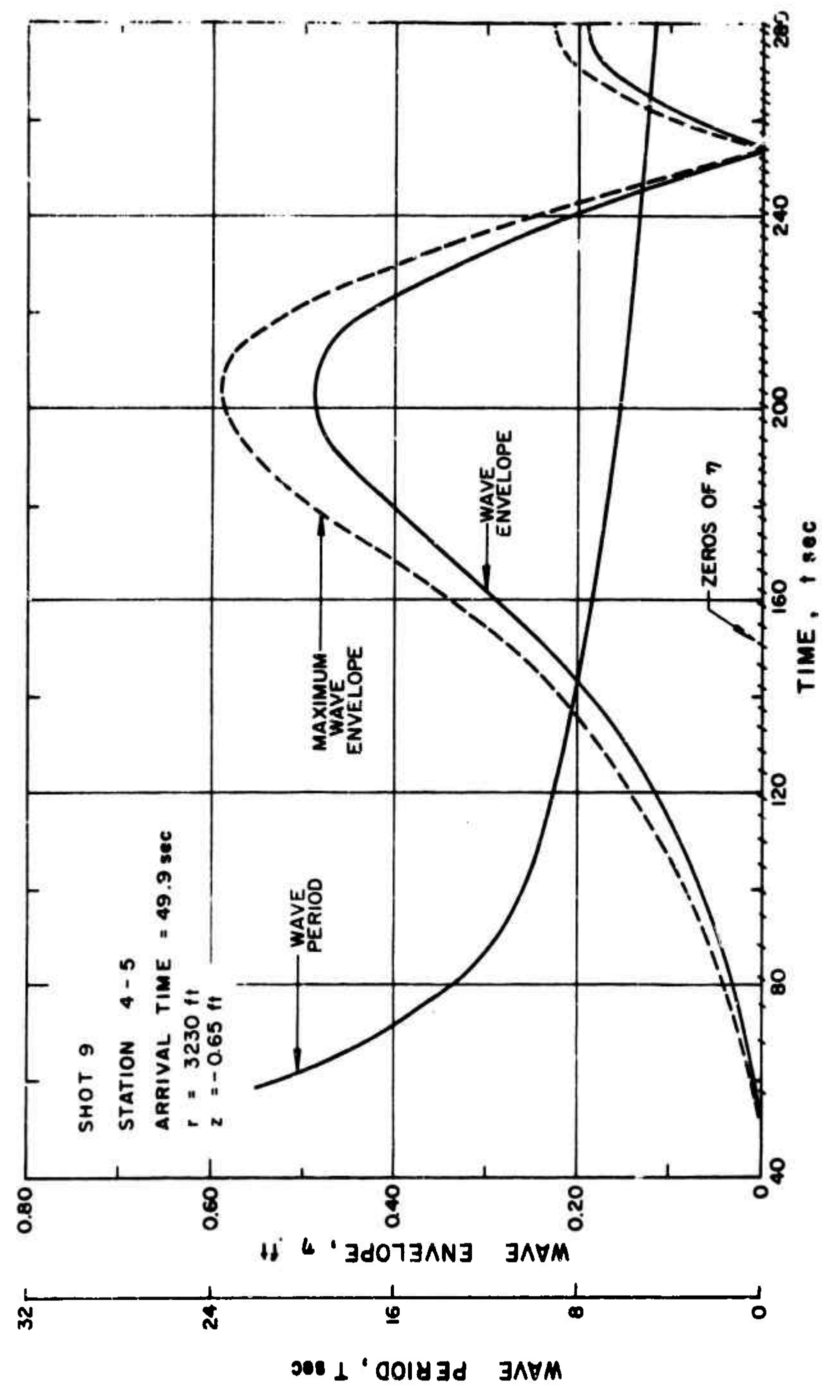
SHOT 9
STATION 4-5
ARRIVAL TIME = 49.9 sec
r = 3230 ft
z = -0.65 ft
WAVE PERIOD
MAXIMUM WAVE ENVELOPE
WAVE ENVELOPE
ZEROS OF η
TIME, t sec
WAVE ENVELOPE, η ft
WAVE PERIOD, T sec
0
0.20
0.40
0.60
0.80
8
16
24
32
40
80
120
160
200
240
280

PB-3-7814

APPENDIX B

PREDICTIONS AT STATIONS NEAR THE EDGE OF THE SHELF

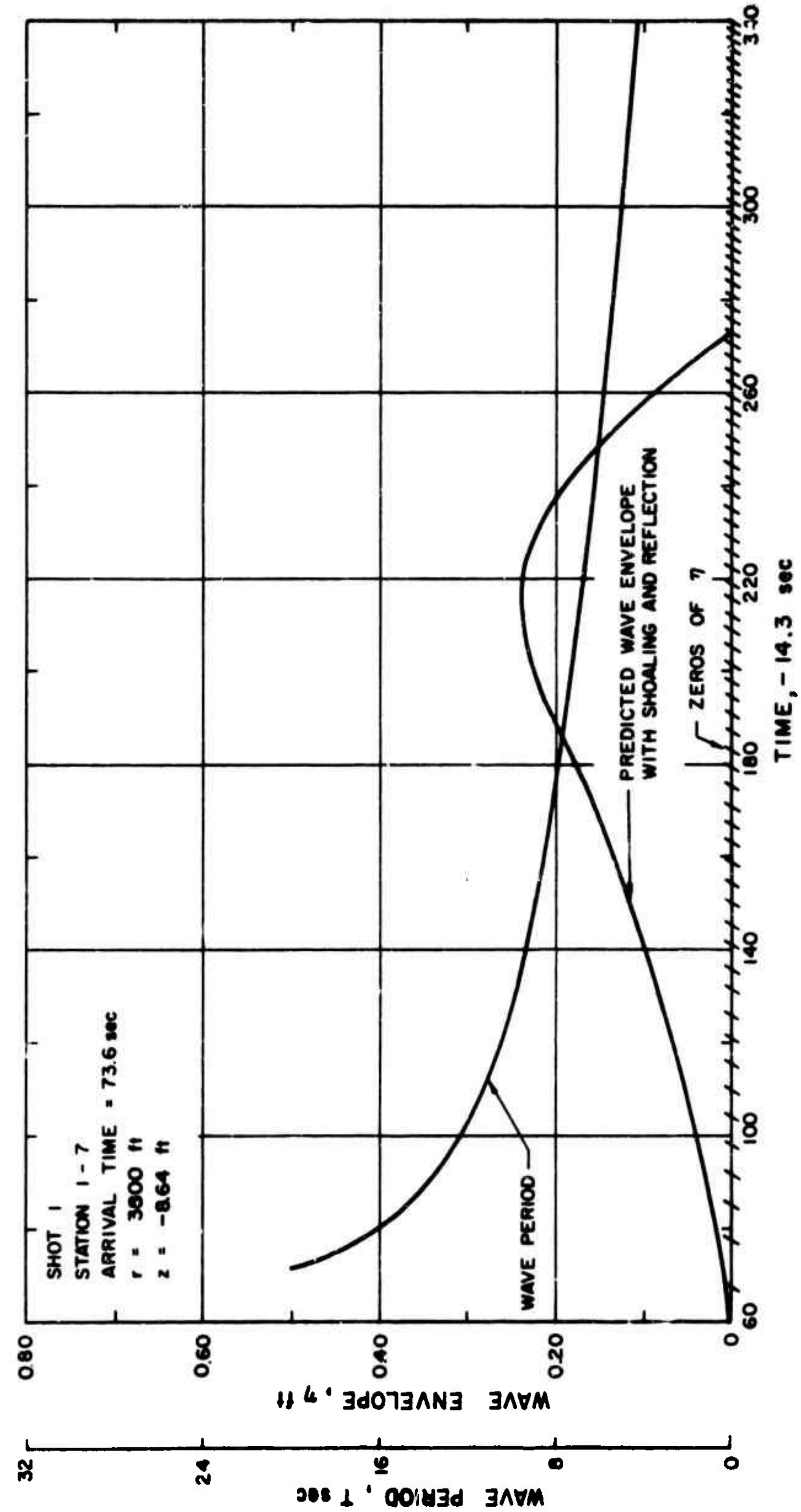
SHOT I
STATION I - 7
ARRIVAL TIME = 73.6 sec
r = 3800 ft
z = -8.64 ft
WAVE PERIOD
PREDICTED WAVE ENVELOPE WITH SHOALING AND REFLECTION
ZEROS OF η
TIME, - 14.3 sec
WAVE ENVELOPE, η ft
WAVE PERIOD, T sec
60
100
140
180
220
260
300
330
0
0.20
0.40
0.60
0.80
8
16
24
32

PB-3-7815

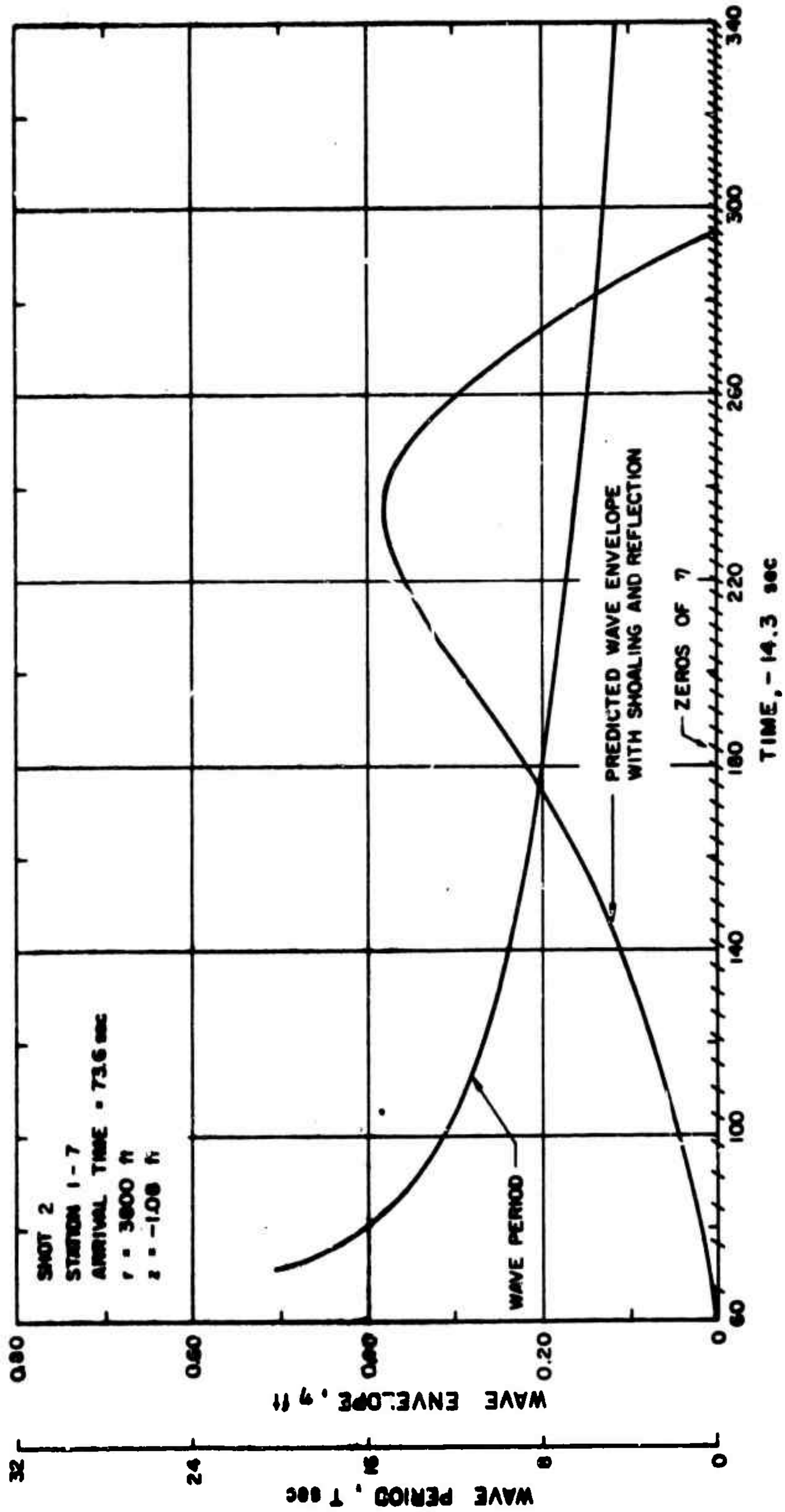
SHOT 2
STATION I-7
ARRIVAL TIME = 73.6 sec
r = 3800 ft
z = -1.08 ft
WAVE PERIOD
PREDICTED WAVE ENVELOPE
WITH SHOALING AND REFLECTION
ZEROS OF η
TIME, - 14.3 sec
WAVE ENVELOPE, η ft
WAVE PERIOD, T sec
0.80
0.60
0.40
0.20
0
32
24
16
8
0
60
100
140
180
220
260
300
340

PB-3-7816

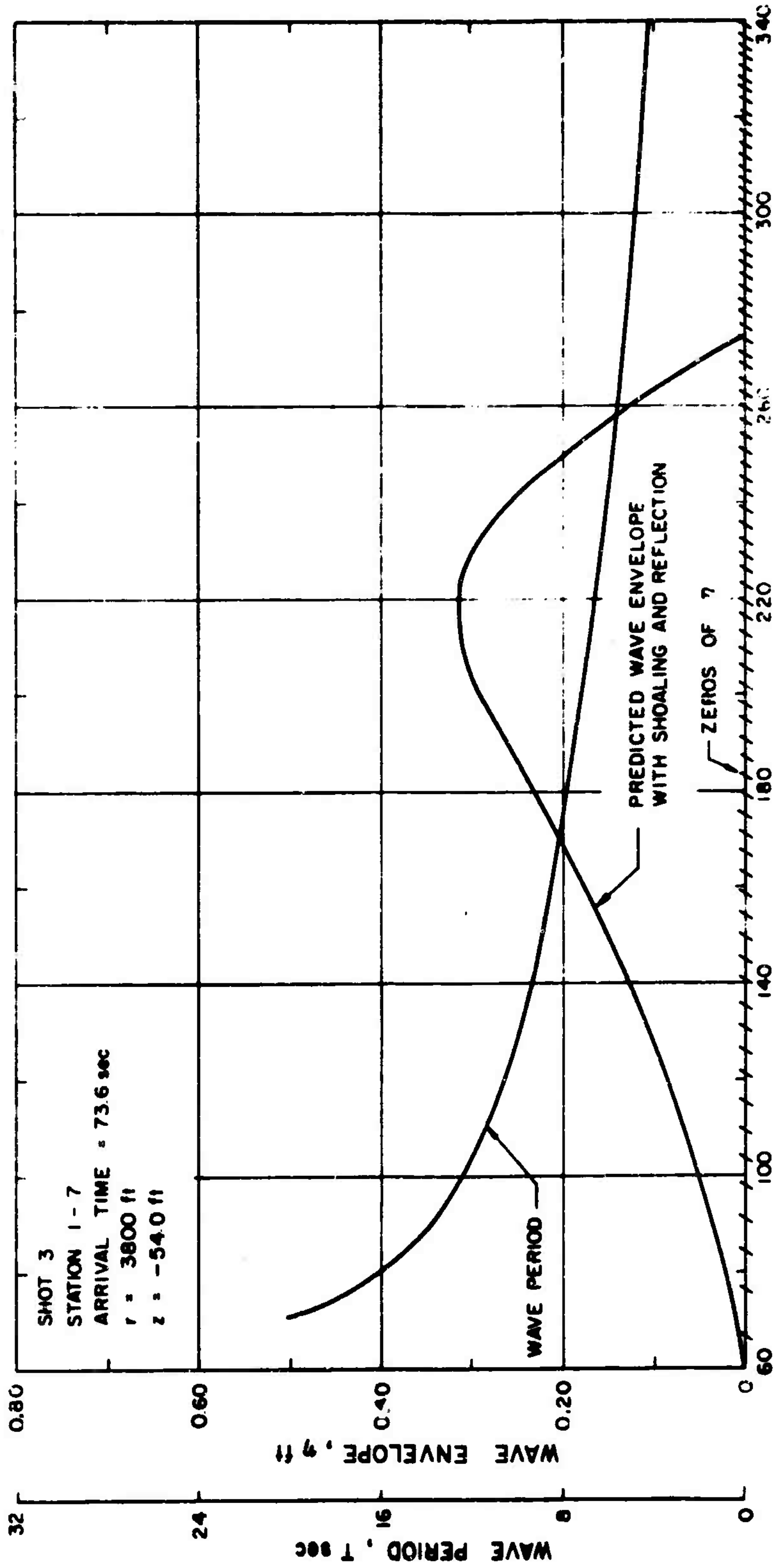
SHOT 3
STATION I - 7
ARRIVAL TIME = 73.6 sec
r = 3800 ft
z = -54.0 ft
WAVE PERIOD
PREDICTED WAVE ENVELOPE WITH SHOALING AND REFLECTION
ZEROS OF η
WAVE ENVELOPE , η ft
WAVE PERIOD , T sec
0.80
0.60
0.40
0.20
0
32
24
16
8
0
60
100
140
180
220
300
340

PB-3-7817

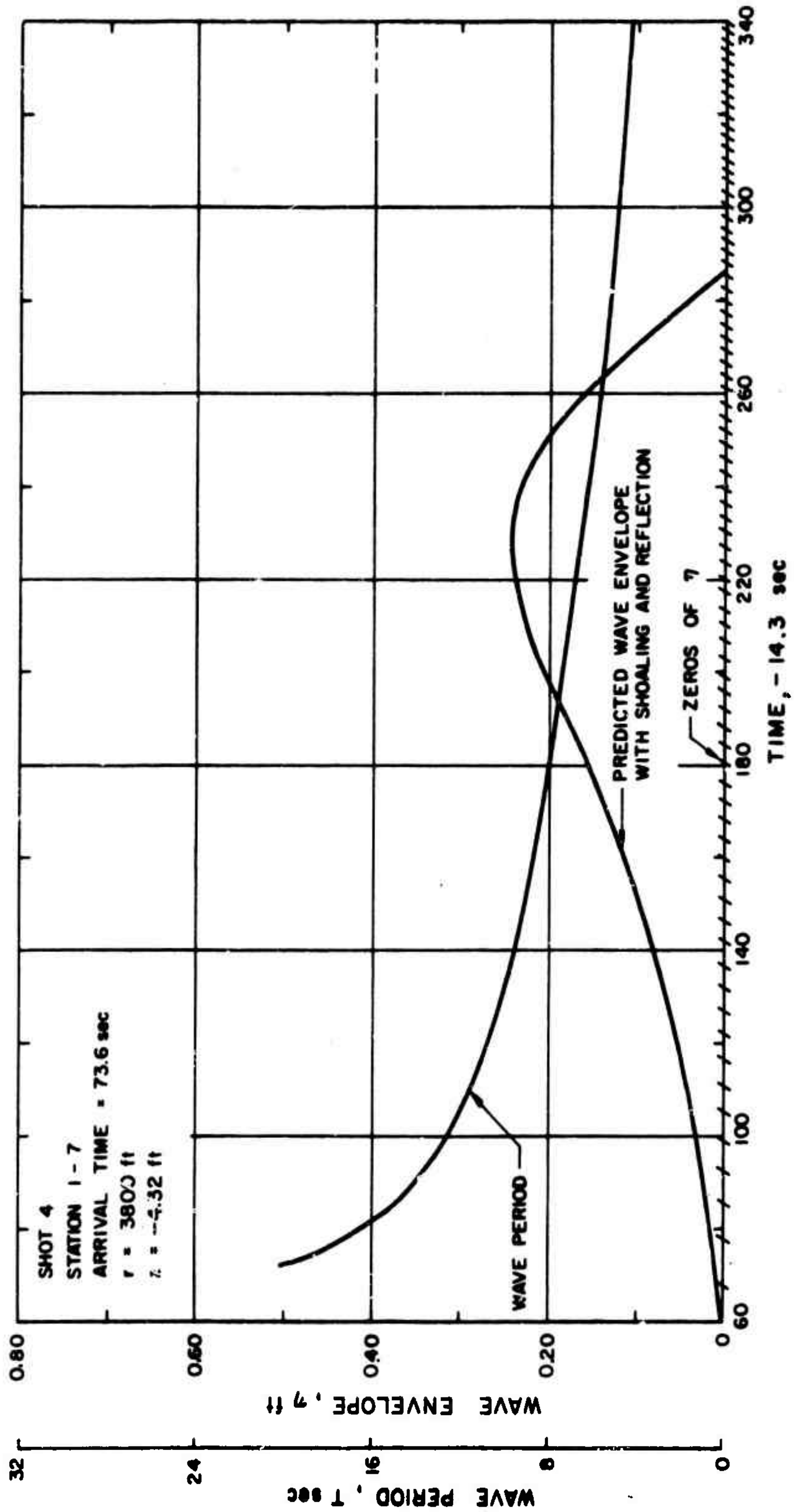
SHOT 4
STATION I - 7
ARRIVAL TIME = 73.6 sec
r = 3800 ft
h = -4.32 ft
WAVE PERIOD
PREDICTED WAVE ENVELOPE WITH SHOALING AND REFLECTION
ZEROS OF η
TIME, - 14.3 sec
60
100
140
180
220
260
300
340
WAVE ENVELOPE, η ft
0
0.20
0.40
0.60
0.80
WAVE PERIOD, T sec
0
8
16
24
32

PB-3-7818

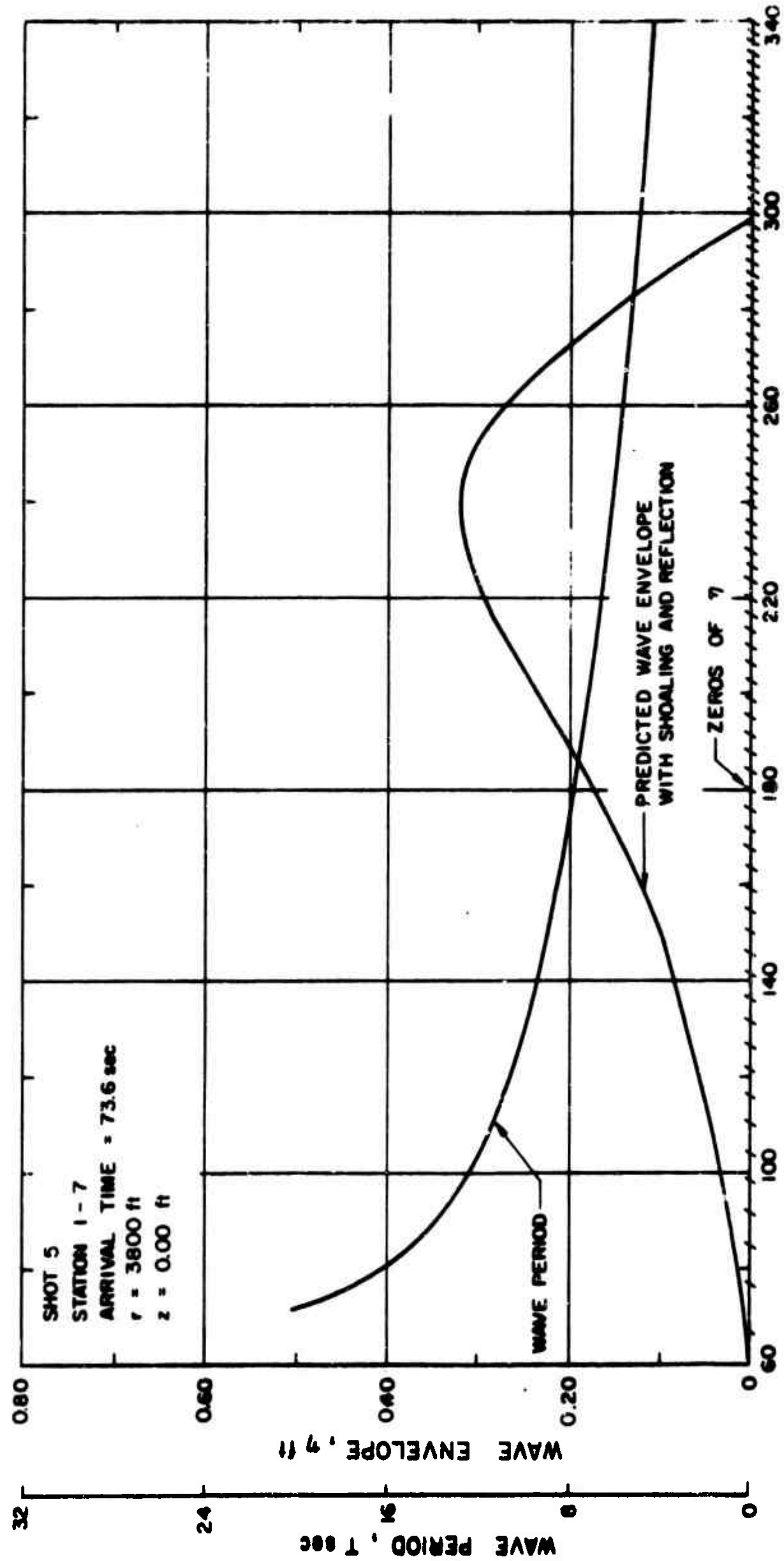
SHOT 5
STATION I-7
ARRIVAL TIME = 73.6 sec
r = 3800 ft
z = 0.00 ft
WAVE PERIOD
PREDICTED WAVE ENVELOPE WITH SHOALING AND REFLECTION
ZEROS OF η
TIME, - 14.3 sec
60
100
140
180
220
260
300
340
WAVE ENVELOPE, η ft
0
0.20
0.40
0.60
0.80
WAVE PERIOD, T sec
0
8
16
24
32

PB-3-7819

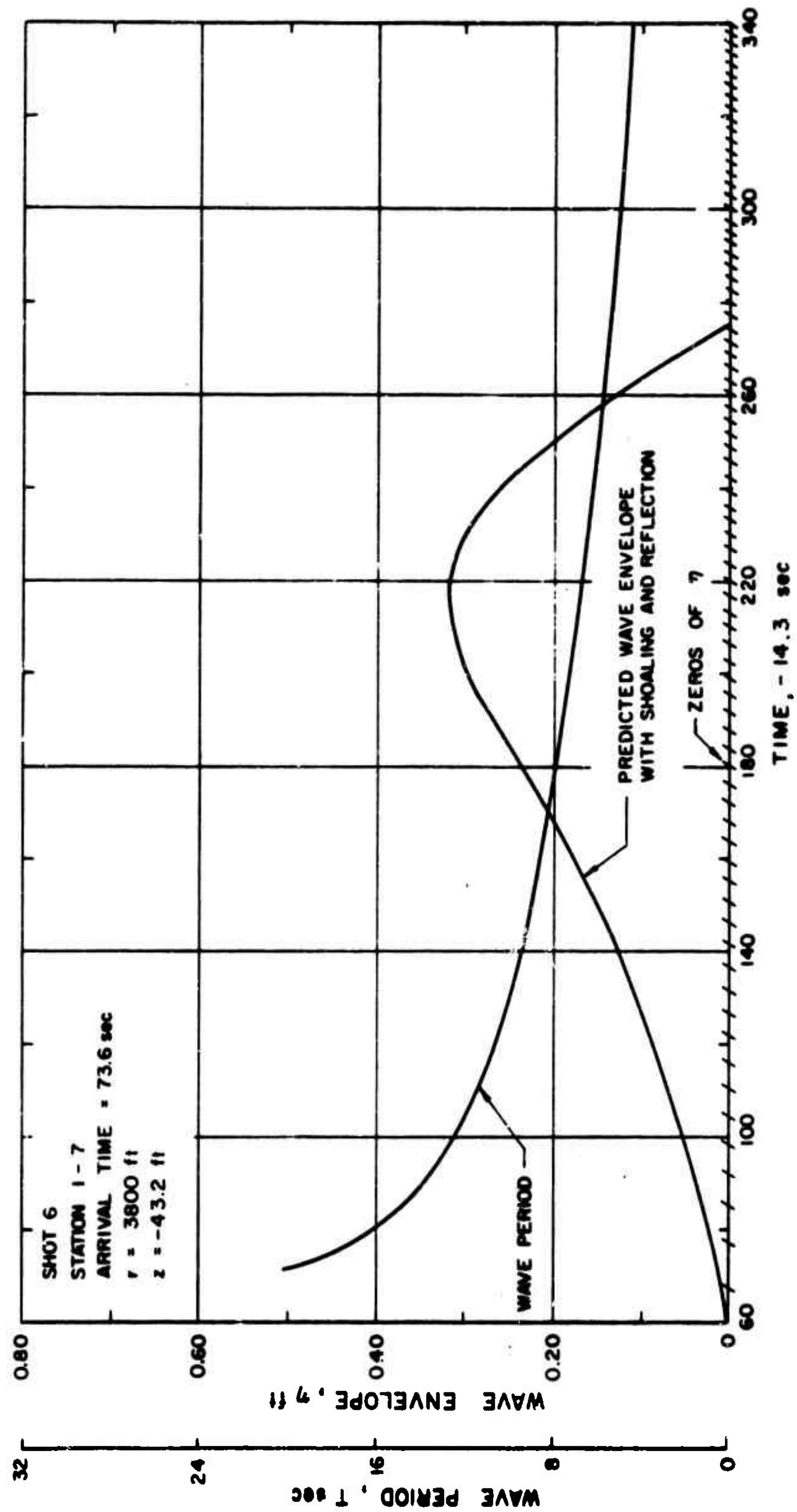
SHOT 6
STATION I-7
ARRIVAL TIME = 73.6 sec
r = 3800 ft
z = -43.2 ft
WAVE PERIOD
PREDICTED WAVE ENVELOPE
WITH SHOALING AND REFLECTION
ZEROS OF η
TIME, - 14.3 sec
60
100
140
180
220
260
300
340
WAVE ENVELOPE, η ft
0
0.20
0.40
0.60
0.80
WAVE PERIOD, T sec
0
8
16
24
32

PB-3-7820

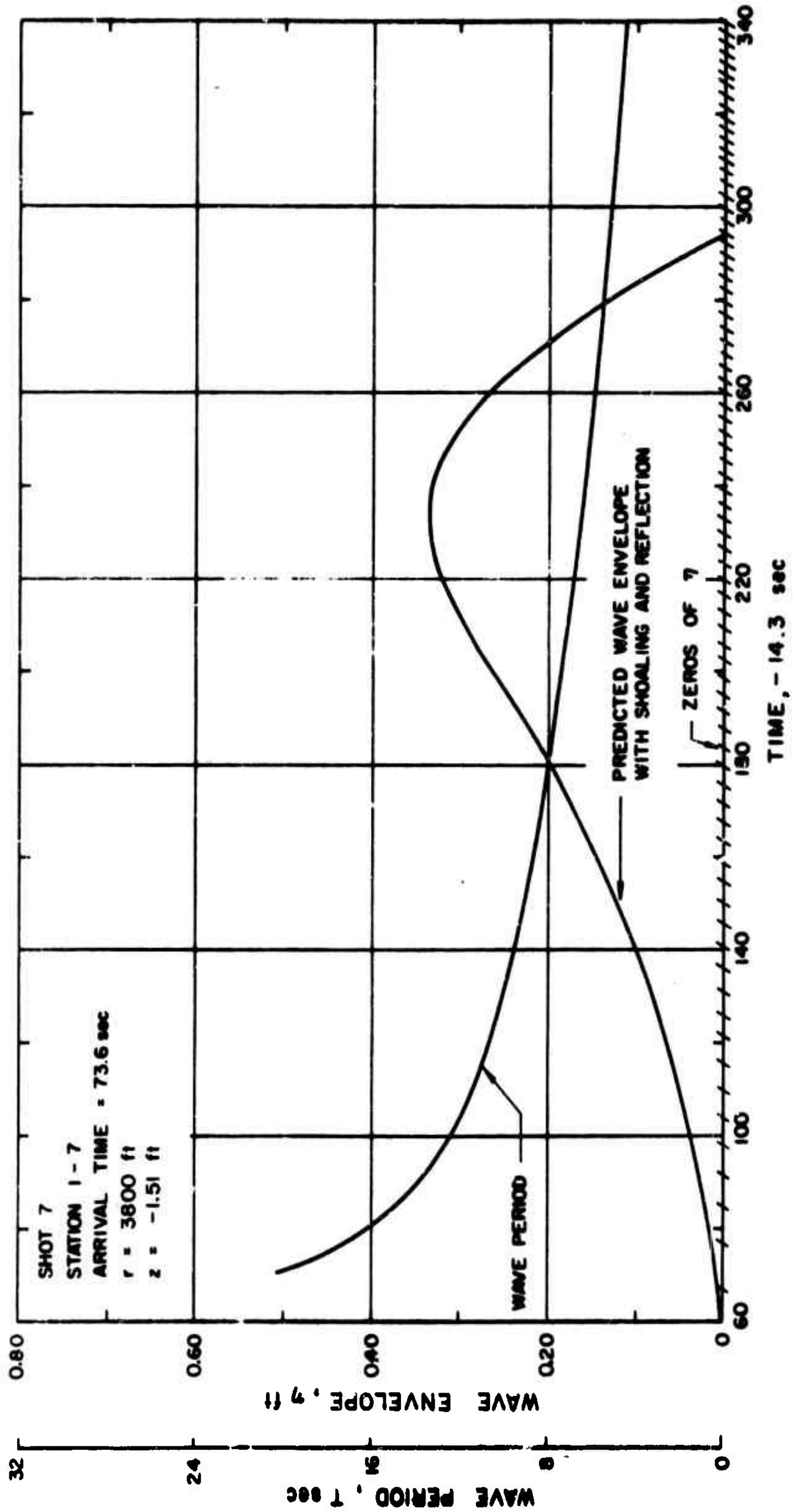
SHOT 7
STATION I - 7
ARRIVAL TIME = 73.6 sec
r = 3800 ft
z = -1.51 ft
WAVE PERIOD
PREDICTED WAVE ENVELOPE
WITH SHOALING AND REFLECTION
ZEROS OF η
TIME, - 14.3 sec
60
100
140
180
220
260
300
340
WAVE ENVELOPE, η ft
0
0.20
0.40
0.60
0.80
WAVE PERIOD, T sec
0
8
16
24
32

PB-3-7821

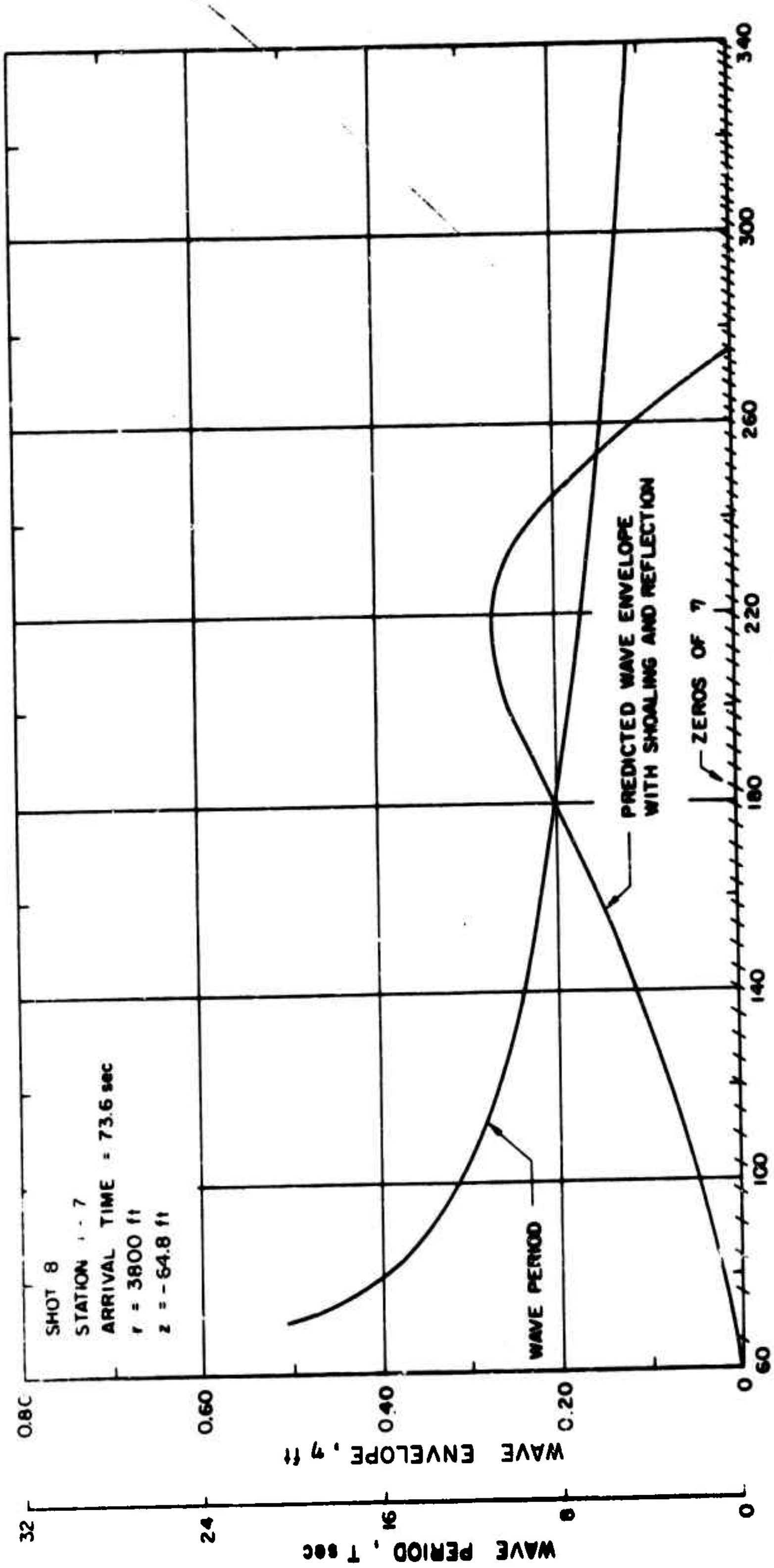
SHOT 8
STATION - 7
ARRIVAL TIME = 73.6 sec
r = 3800 ft
z = -64.8 ft
WAVE PERIOD
PREDICTED WAVE ENVELOPE WITH SHOALING AND REFLECTION
ZEROS OF η
TIME, - 14.3 sec
60
100
140
180
220
260
300
340
WAVE ENVELOPE, η ft
0
0.20
0.40
0.60
0.8C
WAVE PERIOD, T sec
0
8
16
24
32

PB-3-7H22

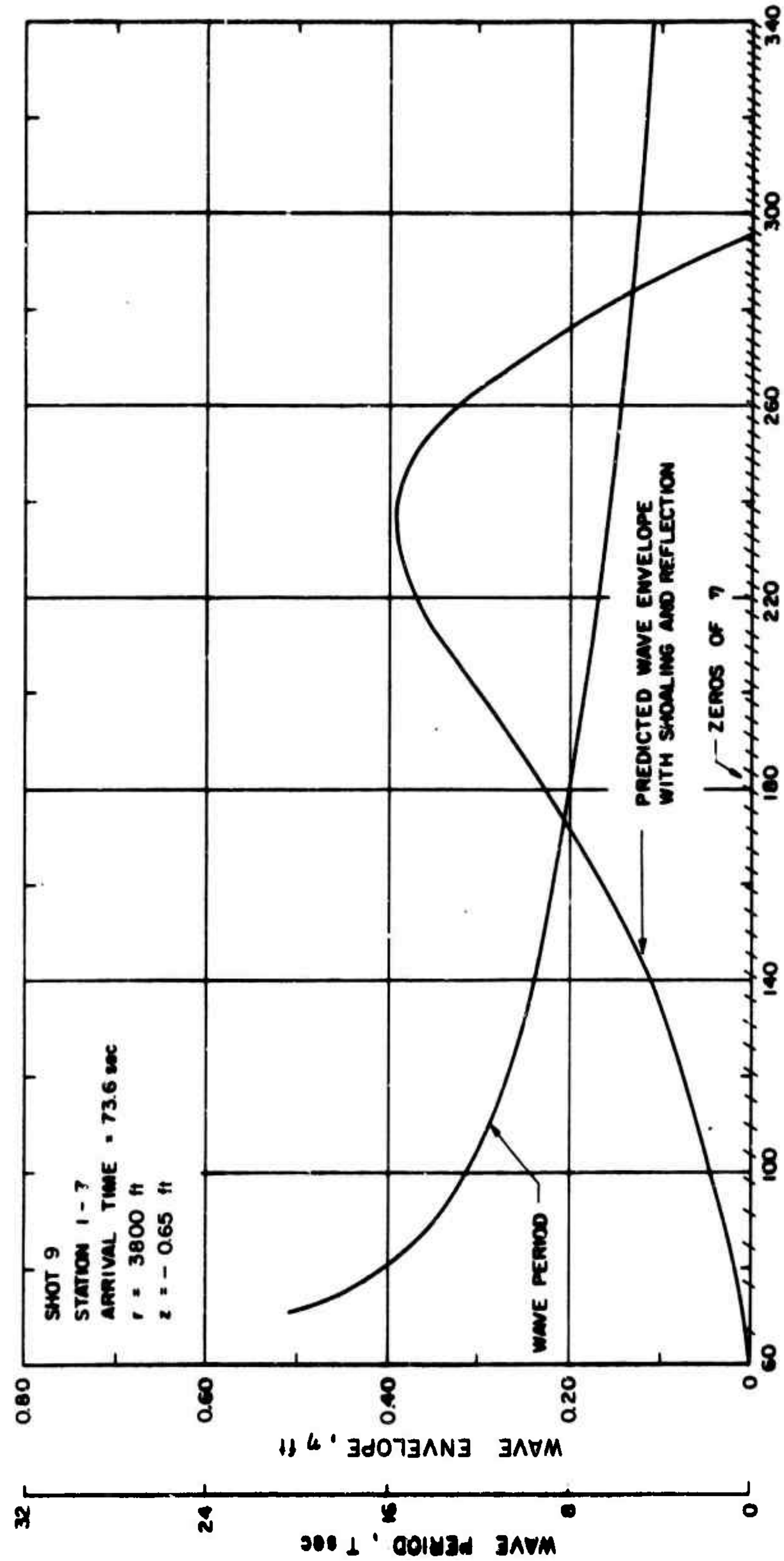
SHOT 9
STATION I - 7
ARRIVAL TIME = 73.6 sec
r = 3800 ft
z = - 0.65 ft
WAVE PERIOD
PREDICTED WAVE ENVELOPE WITH SHOALING AND REFLECTION
ZEROS OF η
TIME, - 14.3 sec
60
100
140
180
220
260
300
340
WAVE ENVELOPE, η ft
0
0.20
0.40
0.60
0.80
WAVE PERIOD, T sec
0
8
16
24
32

PB-3-7823

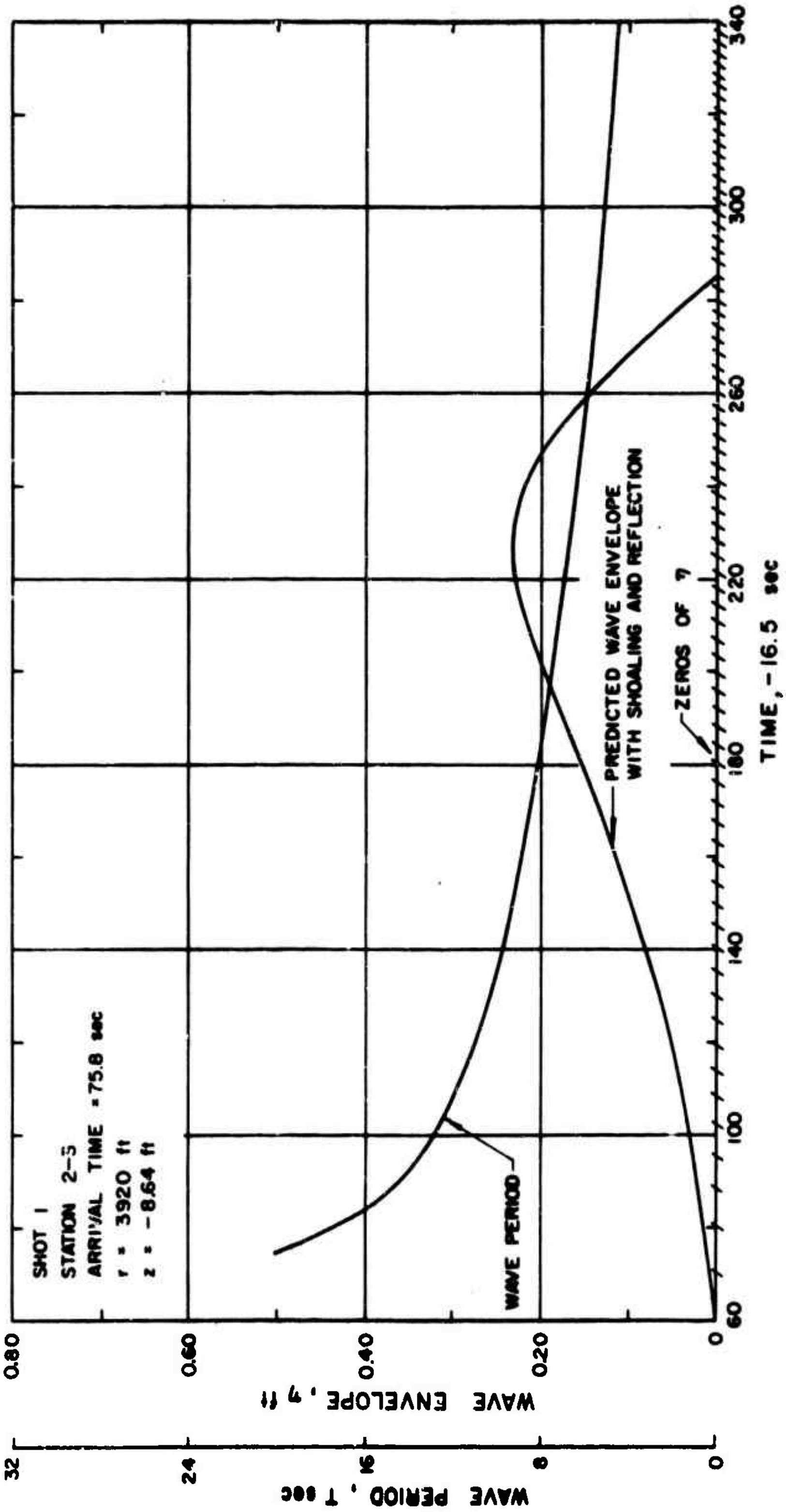

SHOT I
STATION 2-5
ARRIVAL TIME =75.8 sec
r = 3920 ft
z = -8.64 ft
WAVE PERIOD
PREDICTED WAVE ENVELOPE WITH SHOALING AND REFLECTION
ZEROS OF η
TIME, -16.5 sec
60
100
140
180
220
260
300
340
WAVE ENVELOPE, η ft
0
0.20
0.40
0.60
0.80
WAVE PERIOD, T sec
0
8
16
24
32

PB-3-7824

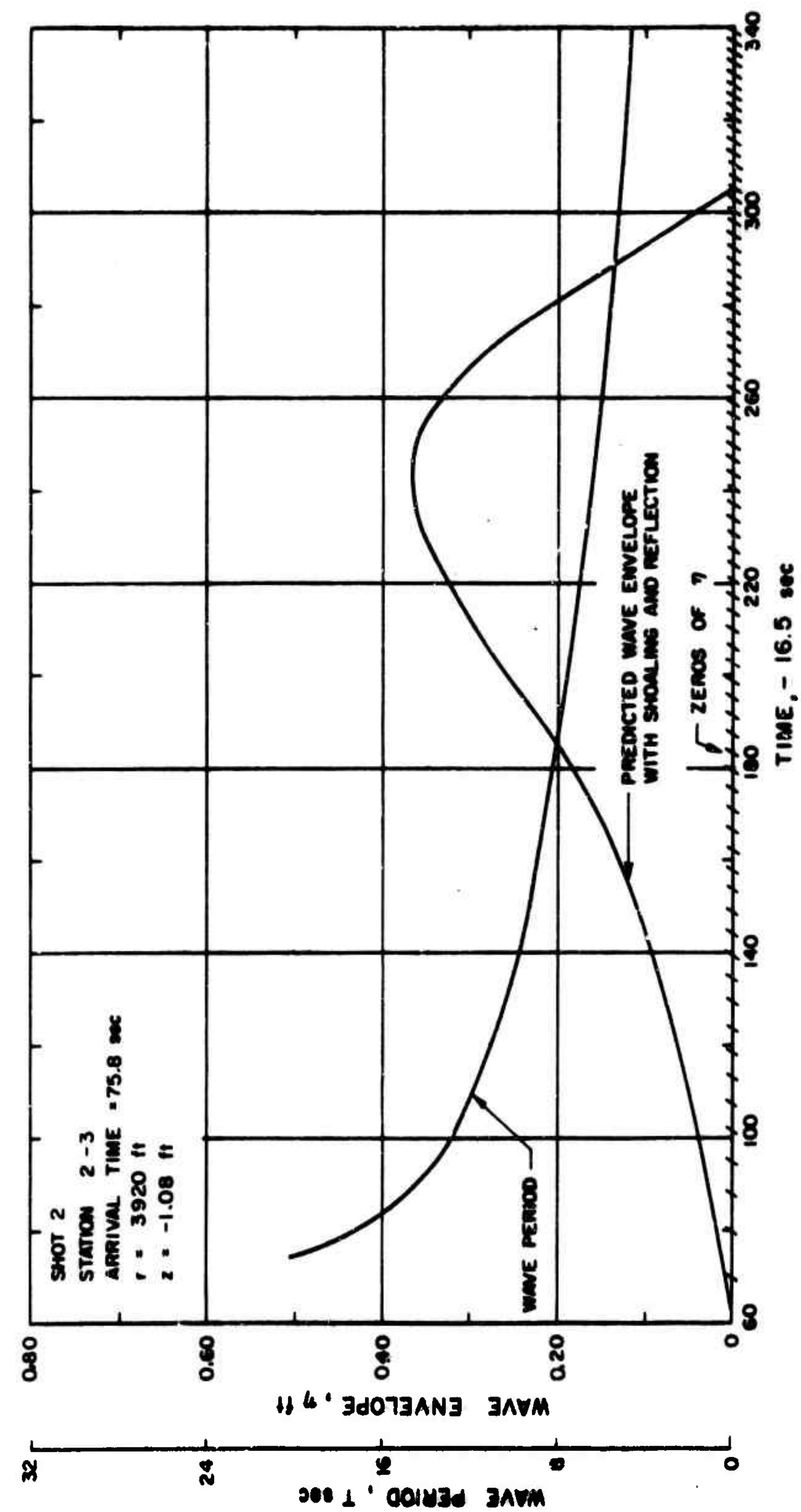
SHOT 2
STATION 2-3
ARRIVAL TIME =75.8 sec
r = 3920 ft
z = -1.08 ft
WAVE PERIOD
PREDICTED WAVE ENVELOPE
WITH SHOALING AND REFLECTION
ZEROS OF η
TIME, - 16.5 sec
60
100
140
180
220
260
300
340
WAVE ENVELOPE, η ft
0
0.20
0.40
0.60
0.80
WAVE PERIOD, T sec
0
8
16
24
32

PB-3-7825

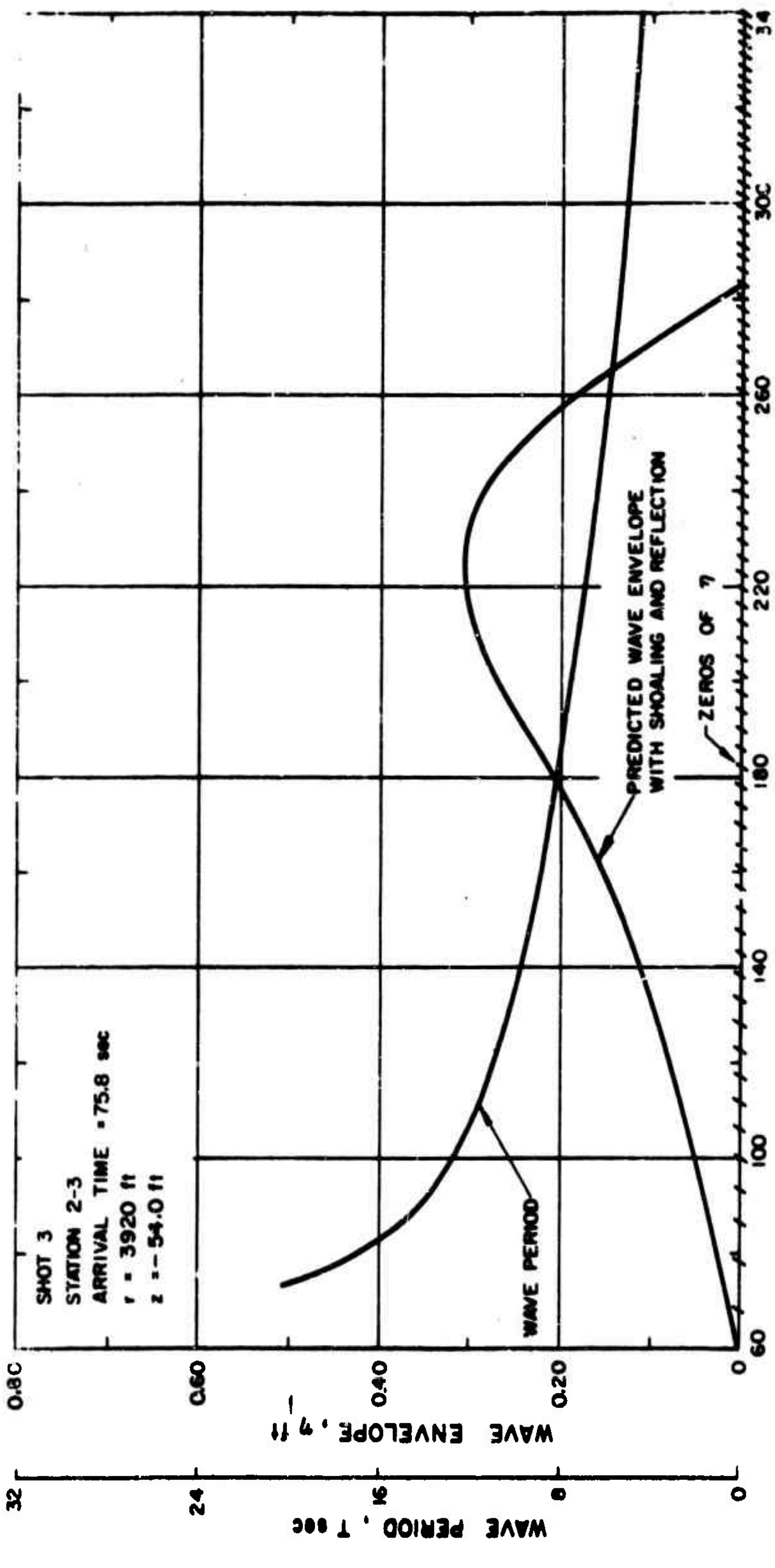
SHOT 3
STATION 2-3
ARRIVAL TIME = 75.8 sec
r = 3920 ft
z = -54.0 ft
WAVE PERIOD
PREDICTED WAVE ENVELOPE WITH SHOALING AND REFLECTION
ZEROS OF η
TIME -16.5 sec
WAVE ENVELOPE, η ft
WAVE PERIOD, T sec
0.80
0.60
0.40
0.20
0
32
24
16
8
0
60
100
140
180
220
260
300
340

PB-3-7826

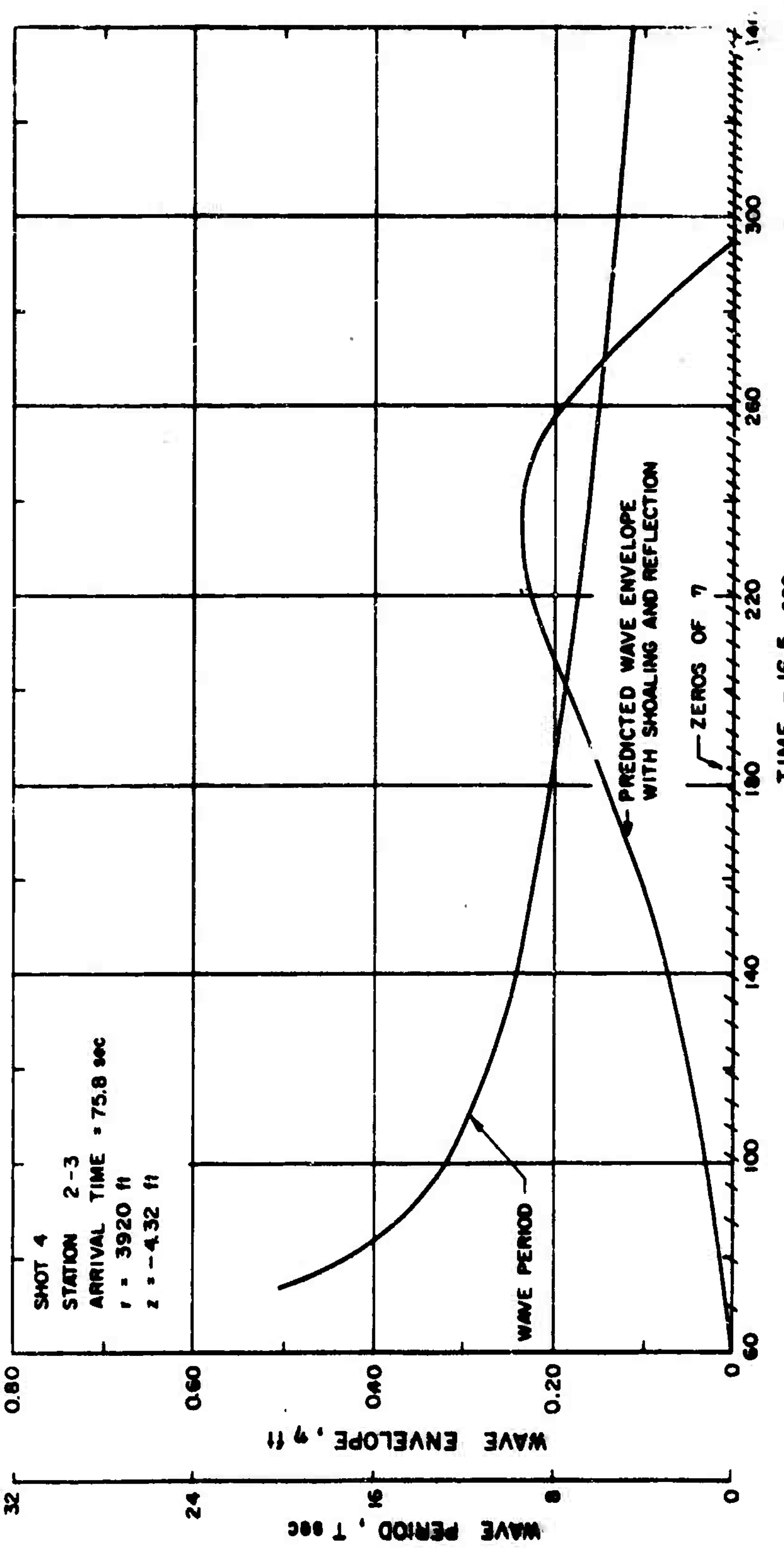
SHOT 4
STATION 2-3
ARRIVAL TIME = 75.8 sec
r = 3920 ft
z = -4.32 ft
WAVE PERIOD
PREDICTED WAVE ENVELOPE WITH SHOALING AND REFLECTION
ZEROS OF η
TIME, - 16.5 sec
60
100
140
180
220
260
300
340
WAVE ENVELOPE, η ft
0
0.20
0.40
0.60
0.80
WAVE PERIOD, T sec
0
8
16
24
32

PB-3-7821

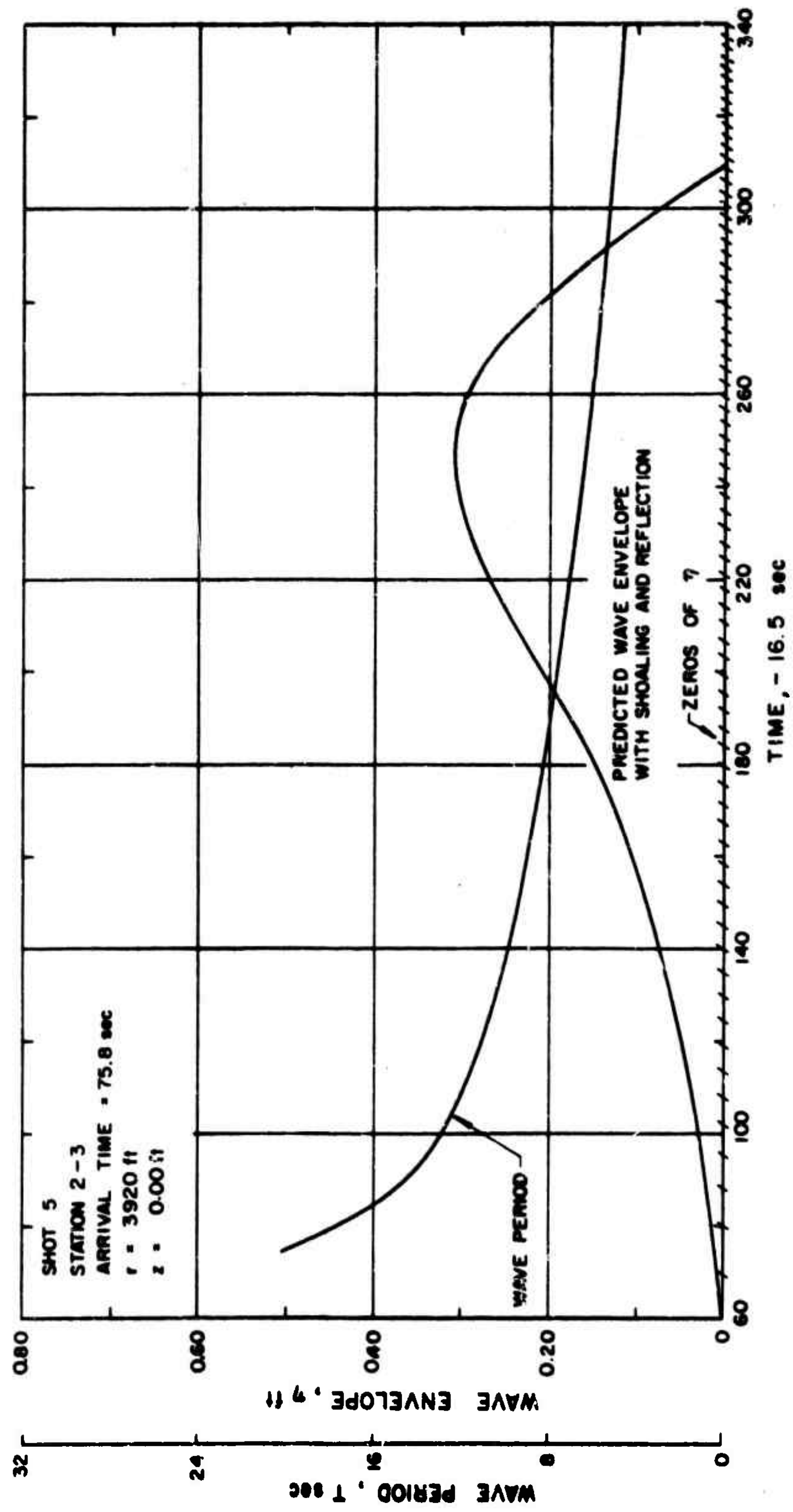
SHOT 5
STATION 2-3
ARRIVAL TIME = 75.8 sec
r = 3920 ft
z = 0.00 ft
WAVE PERIOD
PREDICTED WAVE ENVELOPE
WITH SHOALING AND REFLECTION
ZEROS OF η
TIME, - 16.5 sec
WAVE ENVELOPE, η ft
WAVE PERIOD, T sec
0
0.20
0.40
0.60
0.80
0
8
16
24
32
60
100
140
180
220
260
300
340

PB-3-7828

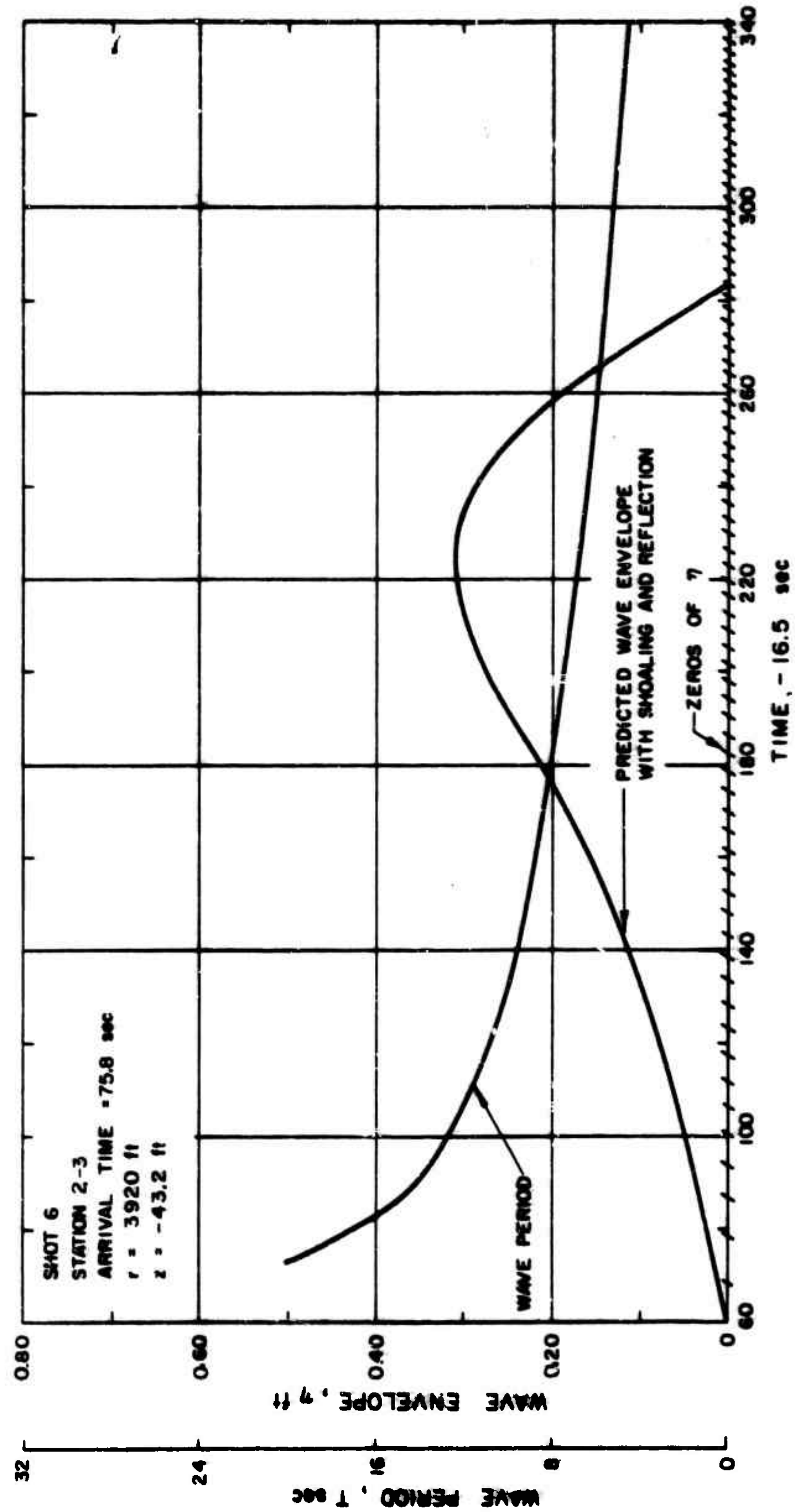
SHOT 6
STATION 2-3
ARRIVAL TIME =75.8 sec
r = 3920 ft
z = -43.2 ft
WAVE PERIOD
PREDICTED WAVE ENVELOPE WITH SHOALING AND REFLECTION
ZEROS OF η
TIME, - 16.5 sec
60
100
140
180
220
260
300
340
WAVE ENVELOPE, η ft
0
0.20
0.40
0.60
0.80
WAVE PERIOD, T sec
0
8
16
24
32

PB-3-7829

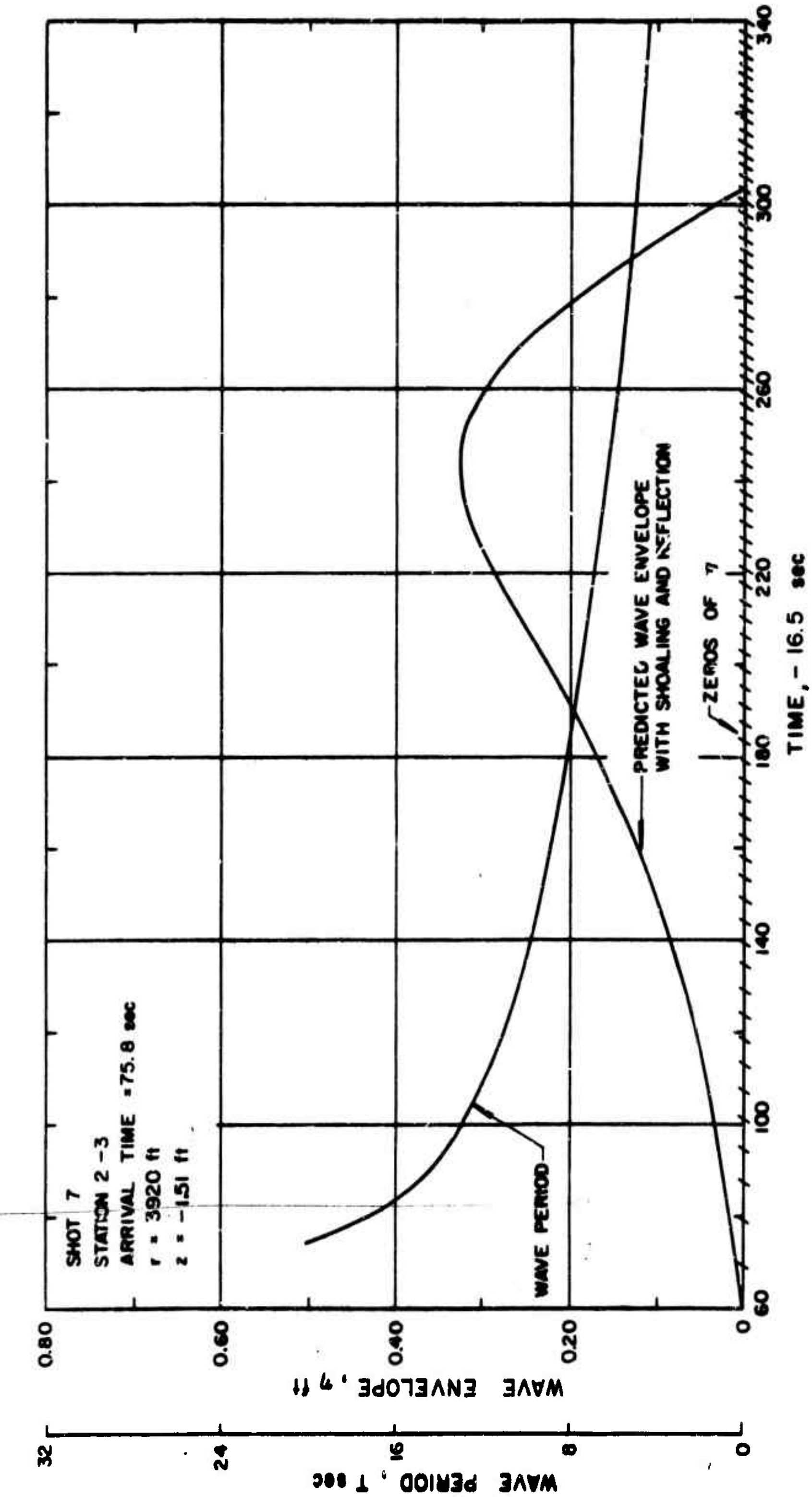
SHOT 7
STATION 2-3
ARRIVAL TIME =75.8 sec
r = 3920 ft
z = -1.51 ft
WAVE PERIOD
PREDICTED WAVE ENVELOPE WITH SHOALING AND REFLECTION
ZEROS OF η
TIME, - 16.5 sec
WAVE ENVELOPE, η ft
WAVE PERIOD, T sec
0.80
0.60
0.40
0.20
0
32
24
16
8
0
60
100
140
180
220
260
300
340

PB-3-7830

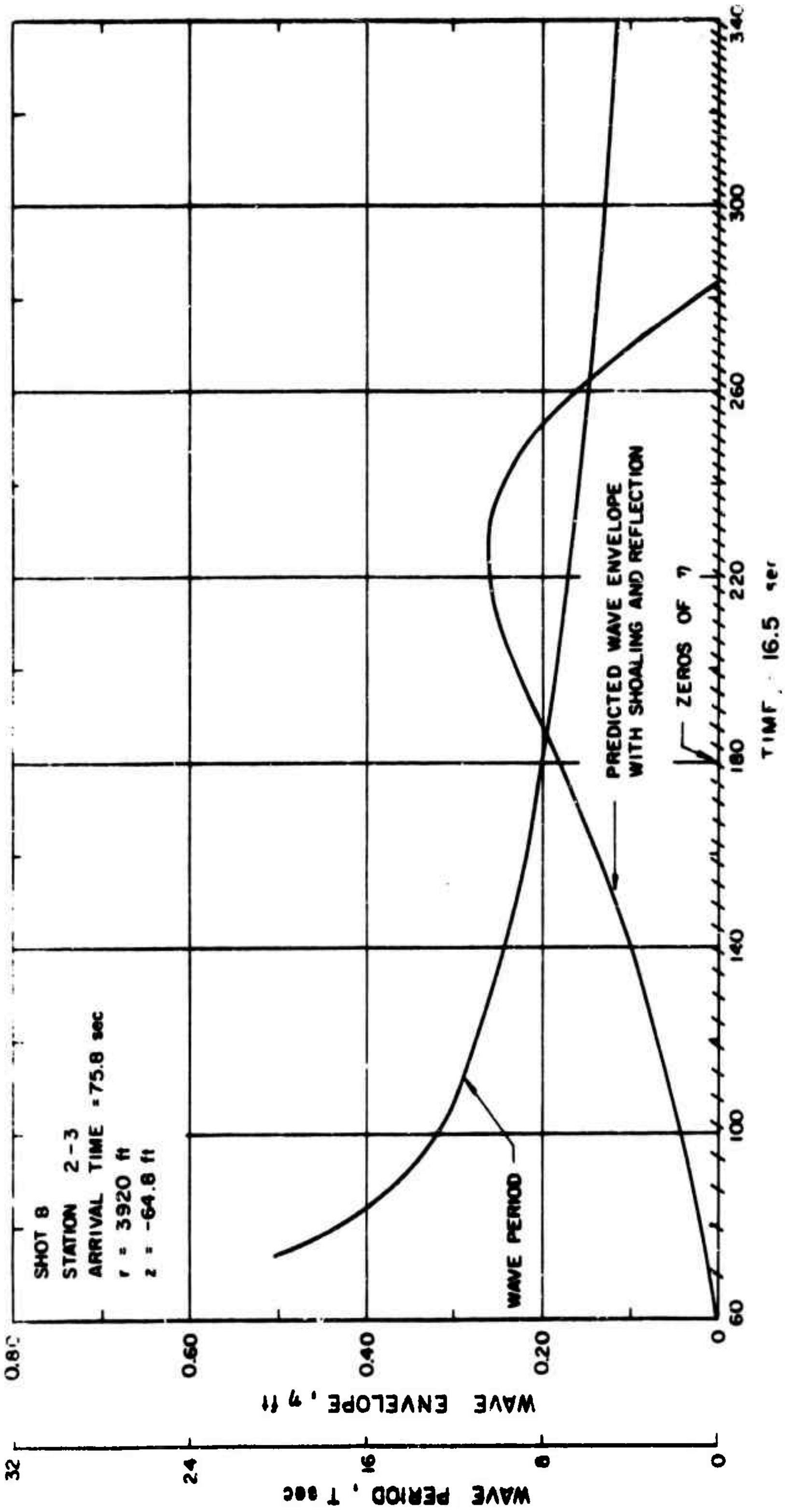
SHOT 8
STATION 2-3
ARRIVAL TIME =75.8 sec
r = 3920 ft
z = -64.8 ft
WAVE PERIOD
PREDICTED WAVE ENVELOPE
WITH SHOALING AND REFLECTION
ZEROS OF η
TIME
16.5
60
100
140
180
220
260
300
340
0.80
0.60
0.40
0.20
0
WAVE ENVELOPE , η ft
32
24
16
8
0
WAVE PERIOD , T sec

PB-3-7831

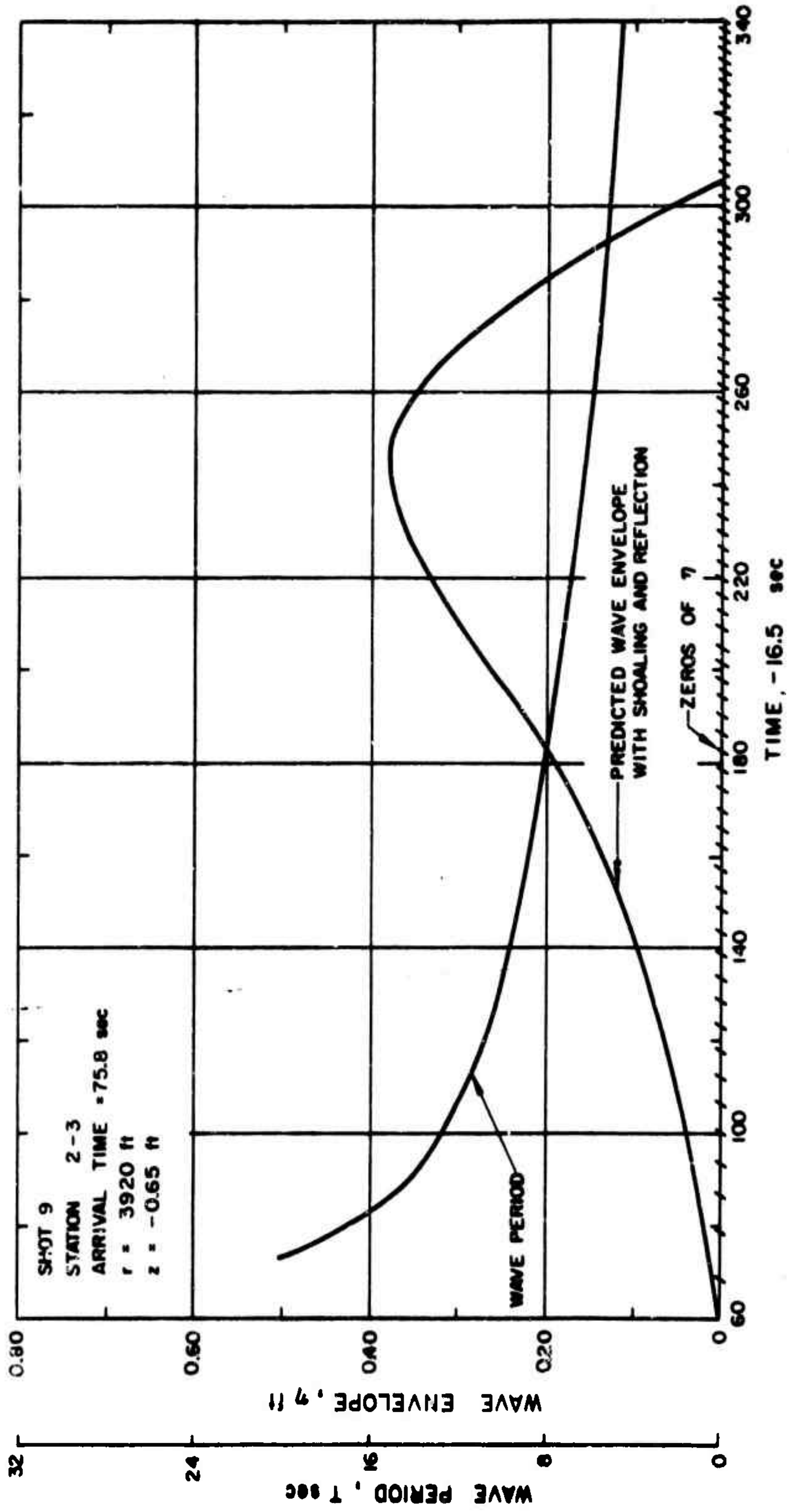
SHOT 9
STATION 2-3
ARRIVAL TIME =75.8 sec
r = 3920 ft
z = -0.65 ft
WAVE PERIOD
PREDICTED WAVE ENVELOPE WITH SHOALING AND REFLECTION
ZEROS OF η
TIME, -16.5 sec
60
100
140
180
220
260
300
340
WAVE ENVELOPE, η ft
0
0.20
0.40
0.60
0.80
WAVE PERIOD, T sec
0
8
16
24
32

PB-3-7832

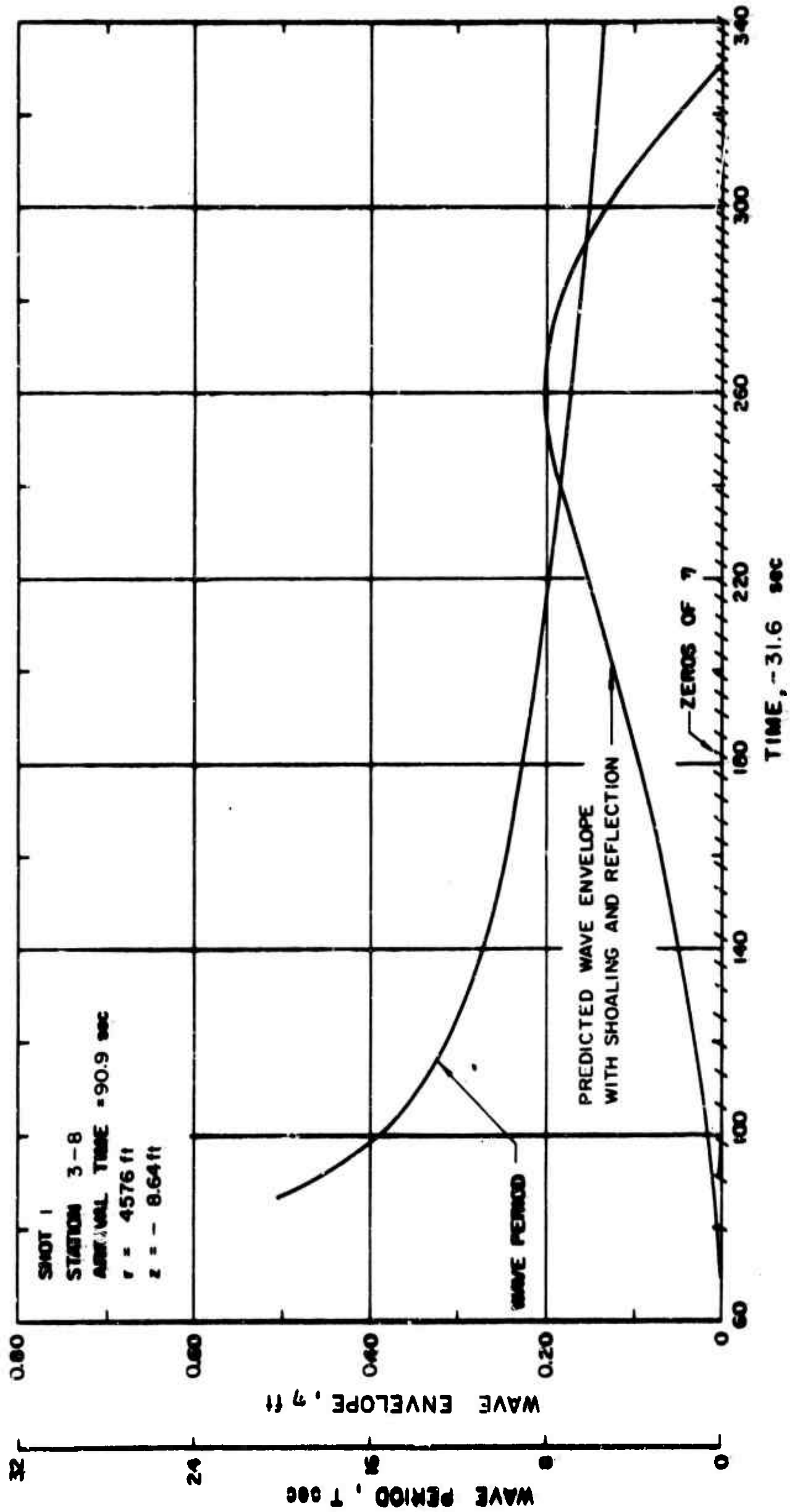

SHOT I
STATION 3-8
ARRIVAL TIME =90.9 sec
r = 4576 ft
z = - 8.64 ft
WAVE PERIOD
PREDICTED WAVE ENVELOPE
WITH SHOALING AND REFLECTION
ZEROS OF η
TIME, -31.6 sec
60
100
140
180
220
260
300
340
WAVE ENVELOPE, η ft
0
0.20
0.40
0.60
0.80
WAVE PERIOD, T sec
0
8
16
24
32

PB-3-7833

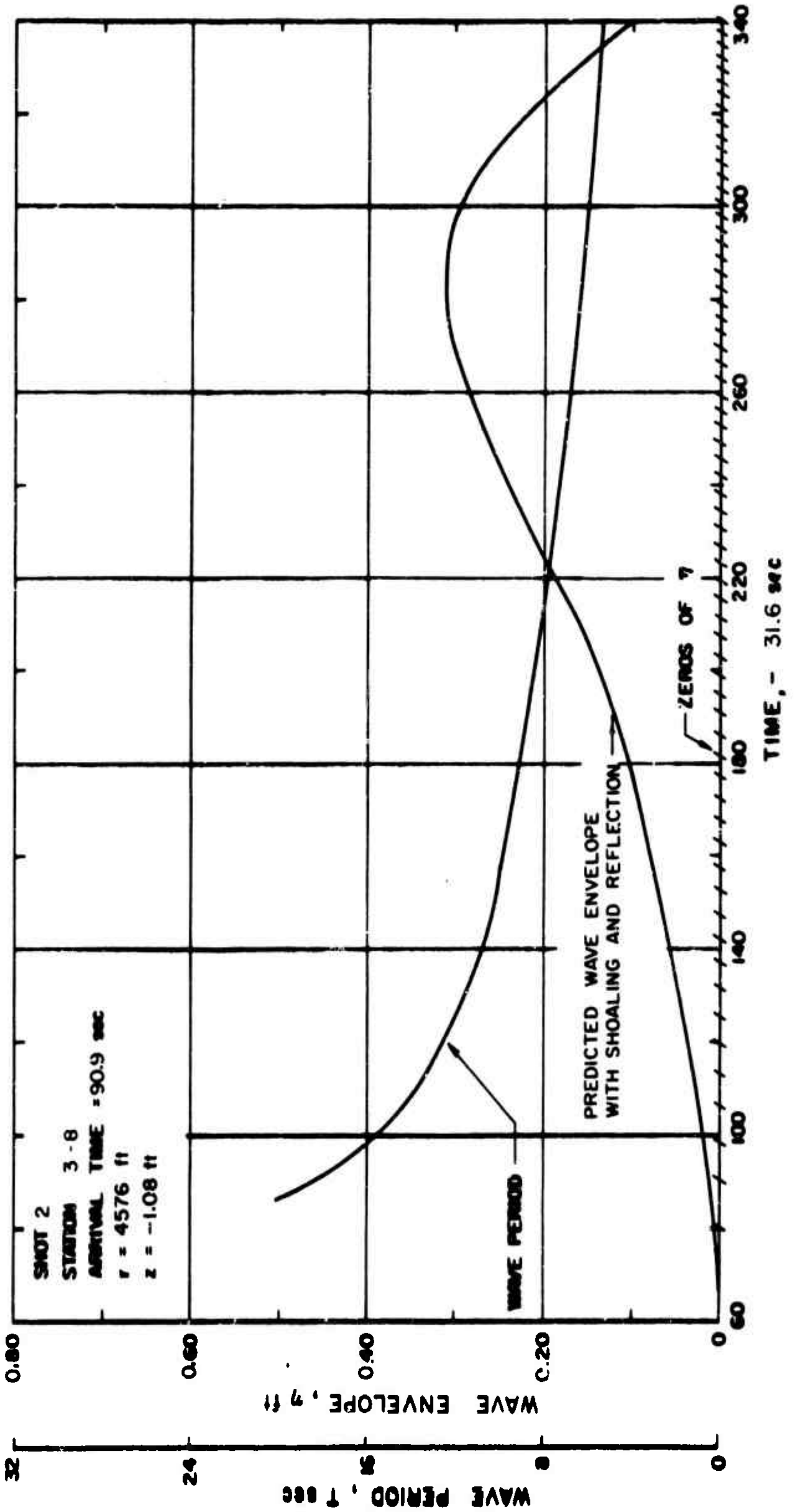

SHOT 2
STATION 3-8
ARRIVAL TIME =90.9 sec
r = 4576 ft
z = -1.08 ft
WAVE PERIOD
PREDICTED WAVE ENVELOPE
WITH SHOALING AND REFLECTION
ZEROS OF η
TIME, - 31.6 sec
60
100
140
180
220
260
300
340
WAVE ENVELOPE , η ft
0
0.20
0.40
0.60
0.80
WAVE PERIOD , T sec
0
8
16
24
32

PB-3-7834

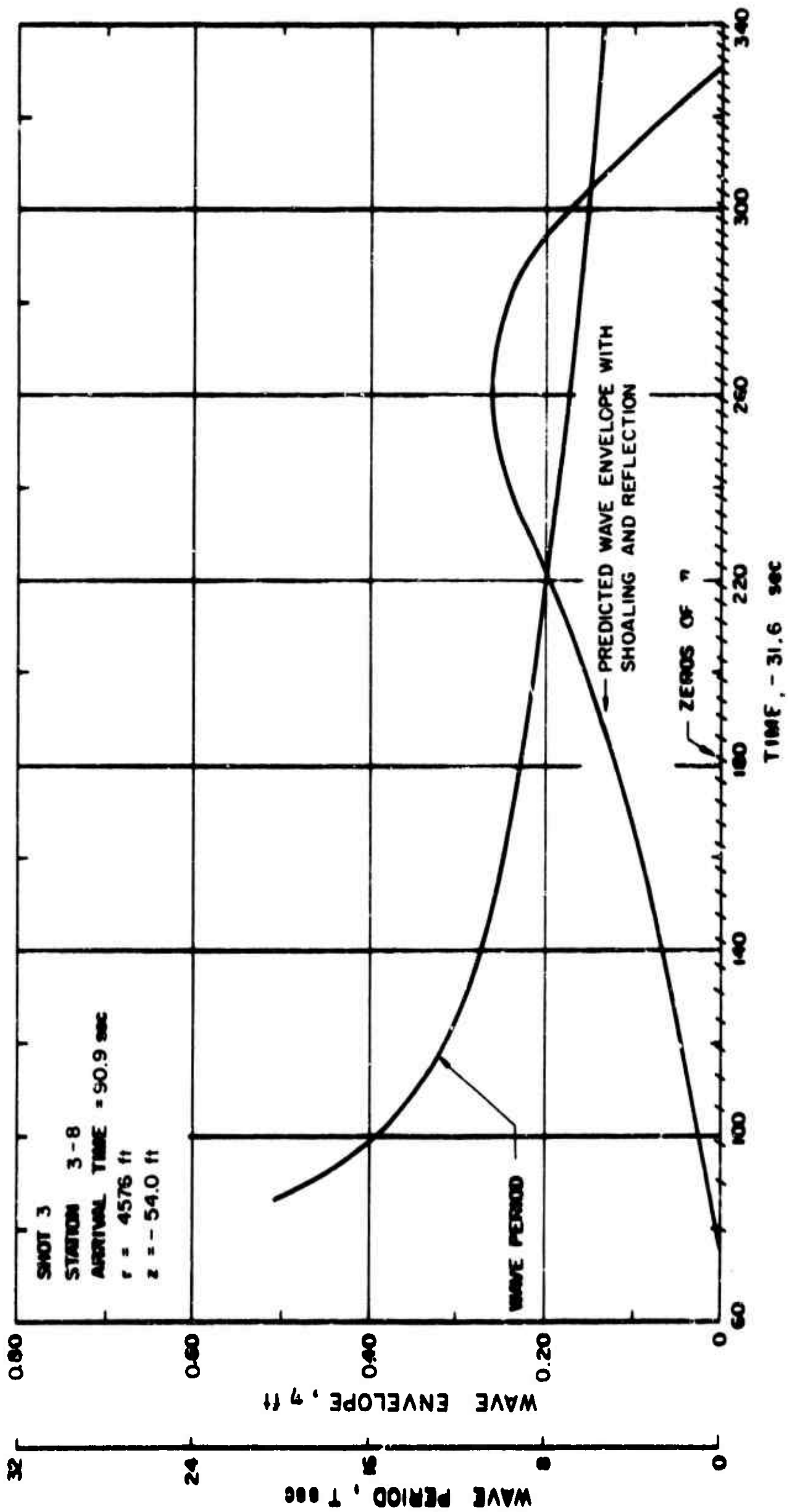
SHOT 3
STATION 3-8
ARRIVAL TIME = 90.9 sec
r = 4576 ft
z = - 54.0 ft
WAVE PERIOD
PREDICTED WAVE ENVELOPE WITH SHOALING AND REFLECTION
ZEROS OF η
TIME, - 31.6 sec
60
100
140
180
220
260
300
340
WAVE ENVELOPE, η ft
0.80
0.60
0.40
0.20
0
WAVE PERIOD, T sec
32
24
16
8
0

PR-3-7435

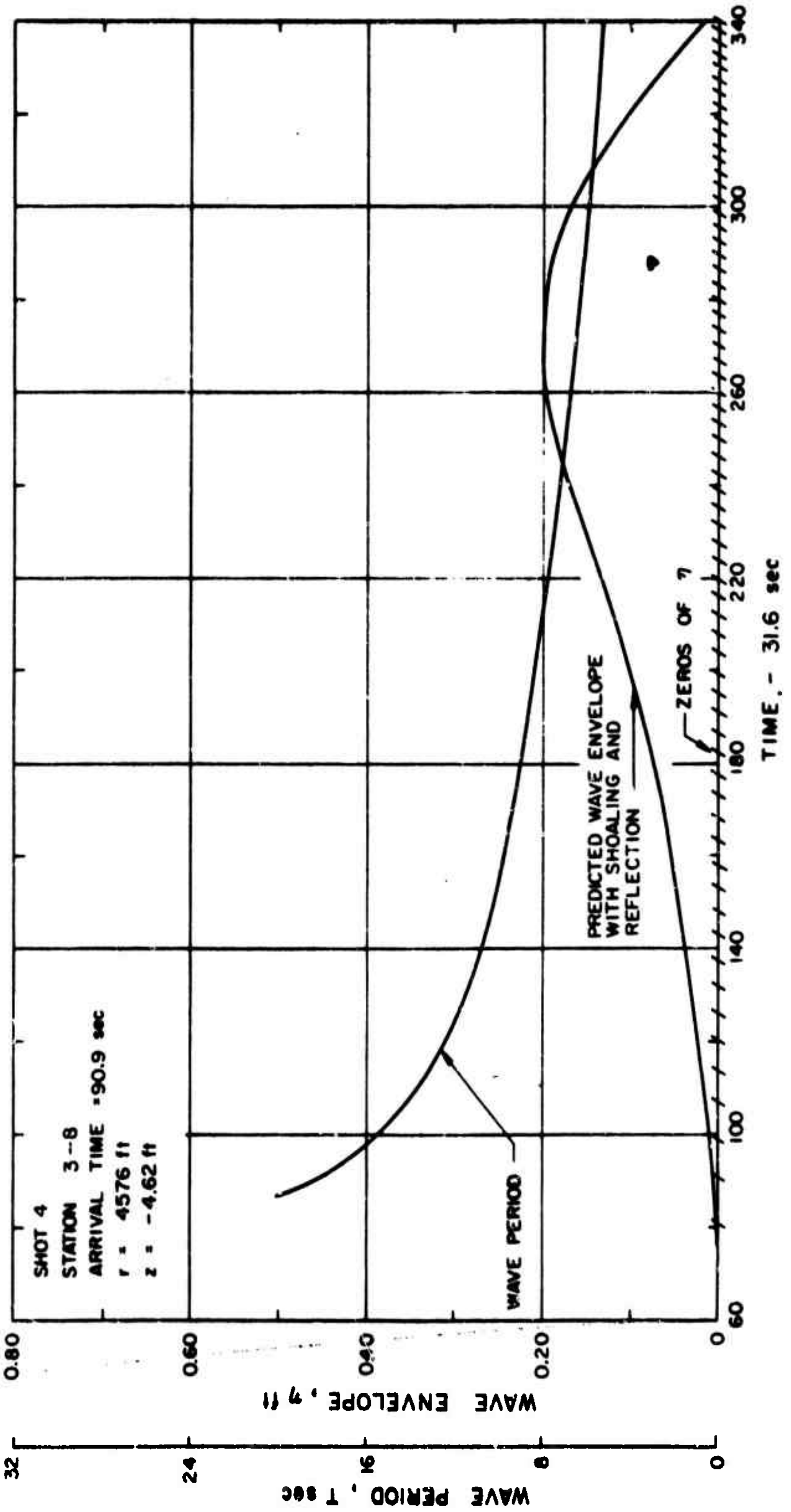
SHOT 4
STATION 3-8
ARRIVAL TIME =90.9 sec
r = 4576 ft
z = -4.62 ft
WAVE PERIOD
PREDICTED WAVE ENVELOPE WITH SHOALING AND REFLECTION
ZEROS OF η
TIME, - 31.6 sec
WAVE ENVELOPE, η ft
WAVE PERIOD, T sec
0
0.20
0.40
0.60
0.80
8
16
24
32
60
100
140
180
220
260
300
340

PB-3-7836

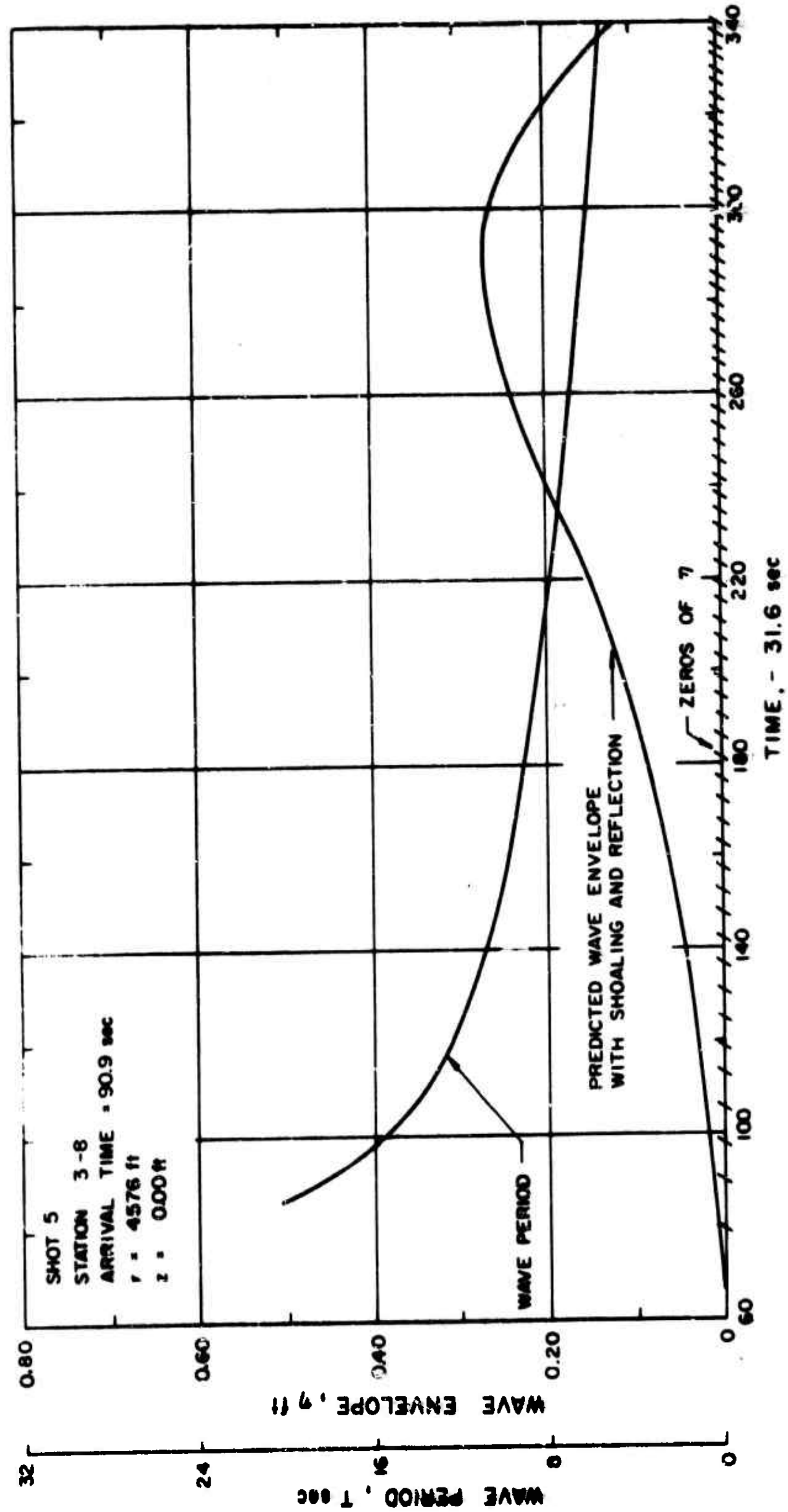
SHOT 5
STATION 3-8
ARRIVAL TIME = 90.9 sec
r = 4576 ft
z = 0.00 ft
WAVE PERIOD
PREDICTED WAVE ENVELOPE
WITH SHOALING AND REFLECTION
ZEROS OF η
TIME, - 31.6 sec
60
100
140
180
220
260
300
340
WAVE ENVELOPE, η ft
0
0.20
0.40
0.60
0.80
WAVE PERIOD, T sec
0
8
16
24
32

PB-3-7837

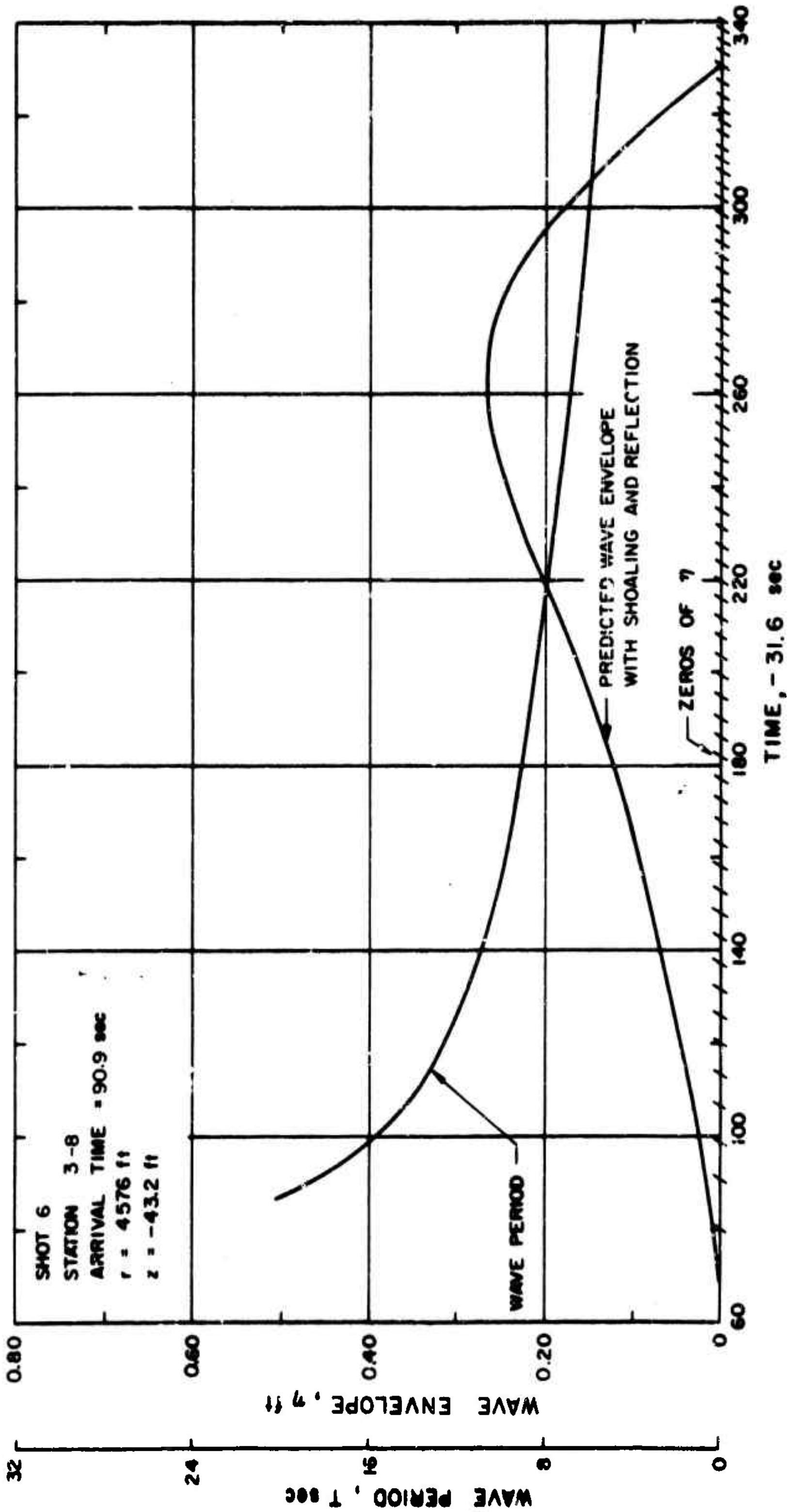
SHOT 6
STATION 3-8
ARRIVAL TIME = 90.9 sec
r = 4576 ft
z = -43.2 ft
WAVE PERIOD
PREDICTED WAVE ENVELOPE
WITH SHOALING AND REFLECTION
ZEROS OF η
TIME, - 31.6 sec
WAVE ENVELOPE, η ft
WAVE PERIOD, T sec
60
100
140
180
220
260
300
340
0
0.20
0.40
0.60
0.80
0
8
16
24
32

PB-3-7838

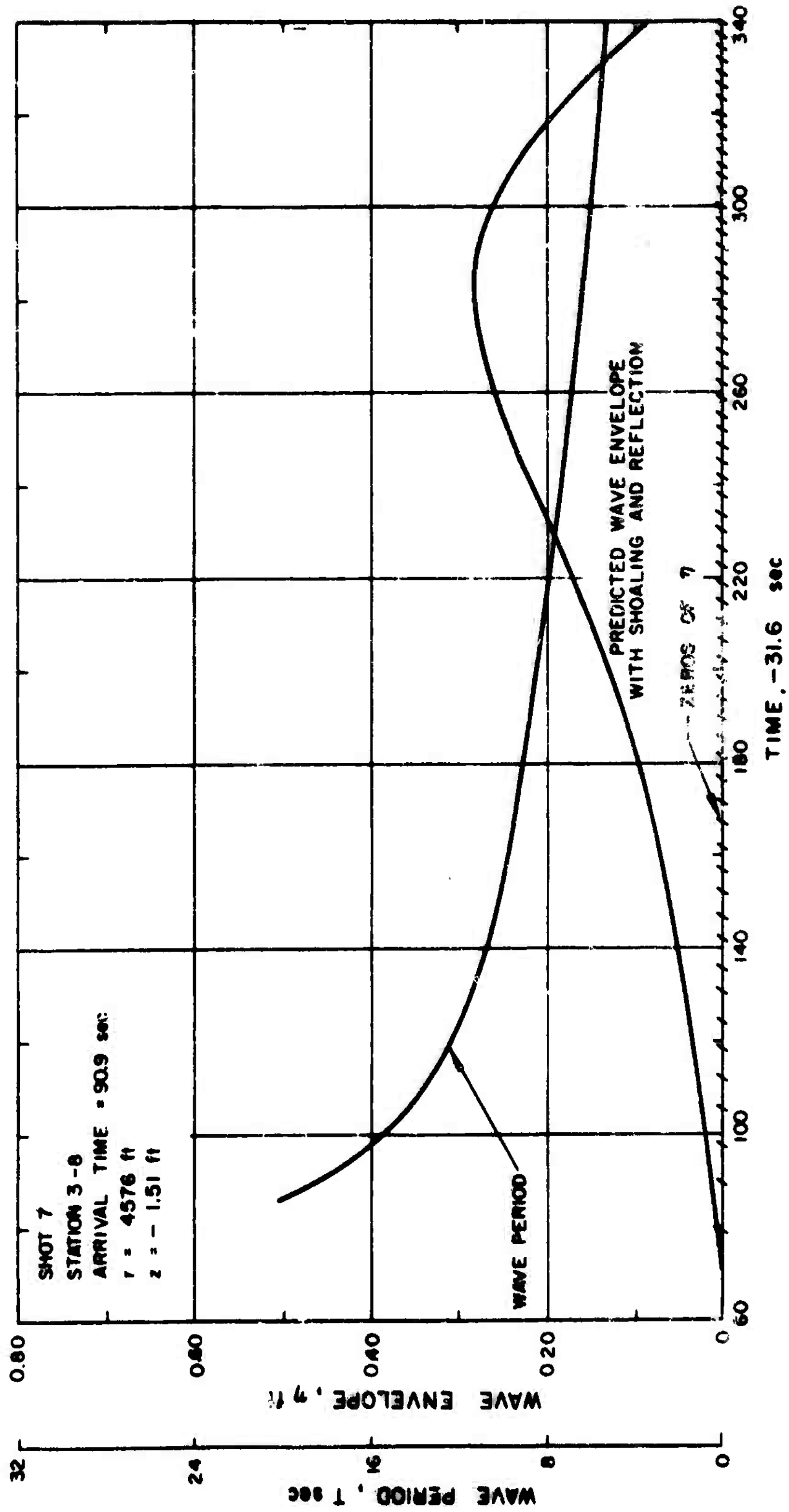
SHOT 7
STATION 3-8
ARRIVAL TIME = 90.9 sec
r = 4576 ft
z = - 1.51 ft
WAVE PERIOD
PREDICTED WAVE ENVELOPE
WITH SHOALING AND REFLECTION
ZEROS OF η
TIME, -31.6 sec
60
100
140
180
220
260
300
340
WAVE ENVELOPE, η ft
0.80
0.60
0.40
0.20
0
WAVE PERIOD, T sec
32
24
16
8
0

PB-3-7839

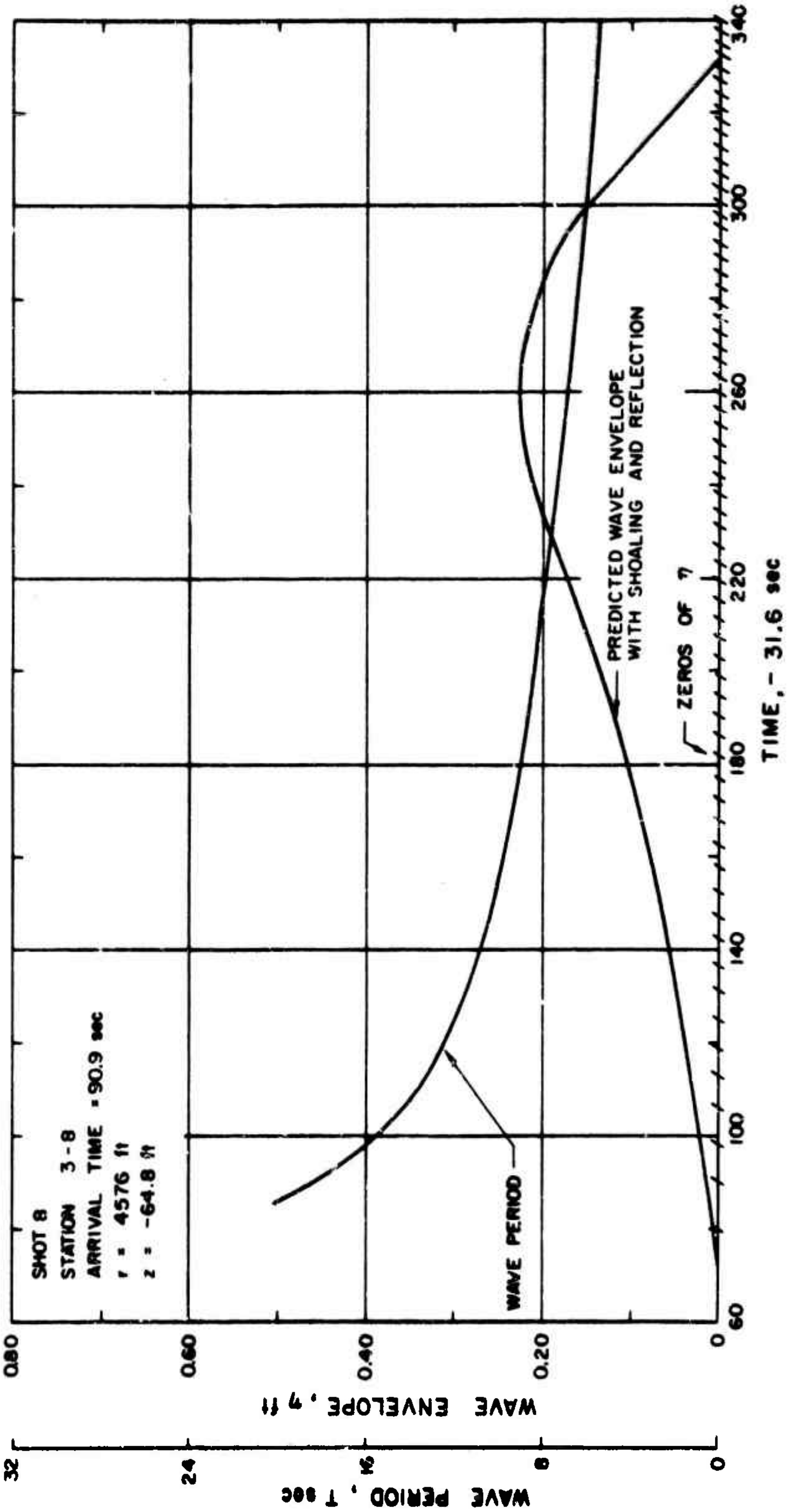
SHOT 8
STATION 3-8
ARRIVAL TIME = 90.9 sec
r = 4576 ft
z = -64.8 ft
WAVE PERIOD
PREDICTED WAVE ENVELOPE WITH SHOALING AND REFLECTION
ZEROS OF η
TIME, - 31.6 sec
WAVE ENVELOPE, η ft
WAVE PERIOD, T sec
60
100
140
180
220
260
300
340
0
0.20
0.40
0.60
0.80
8
16
24
32

PB-3-7840

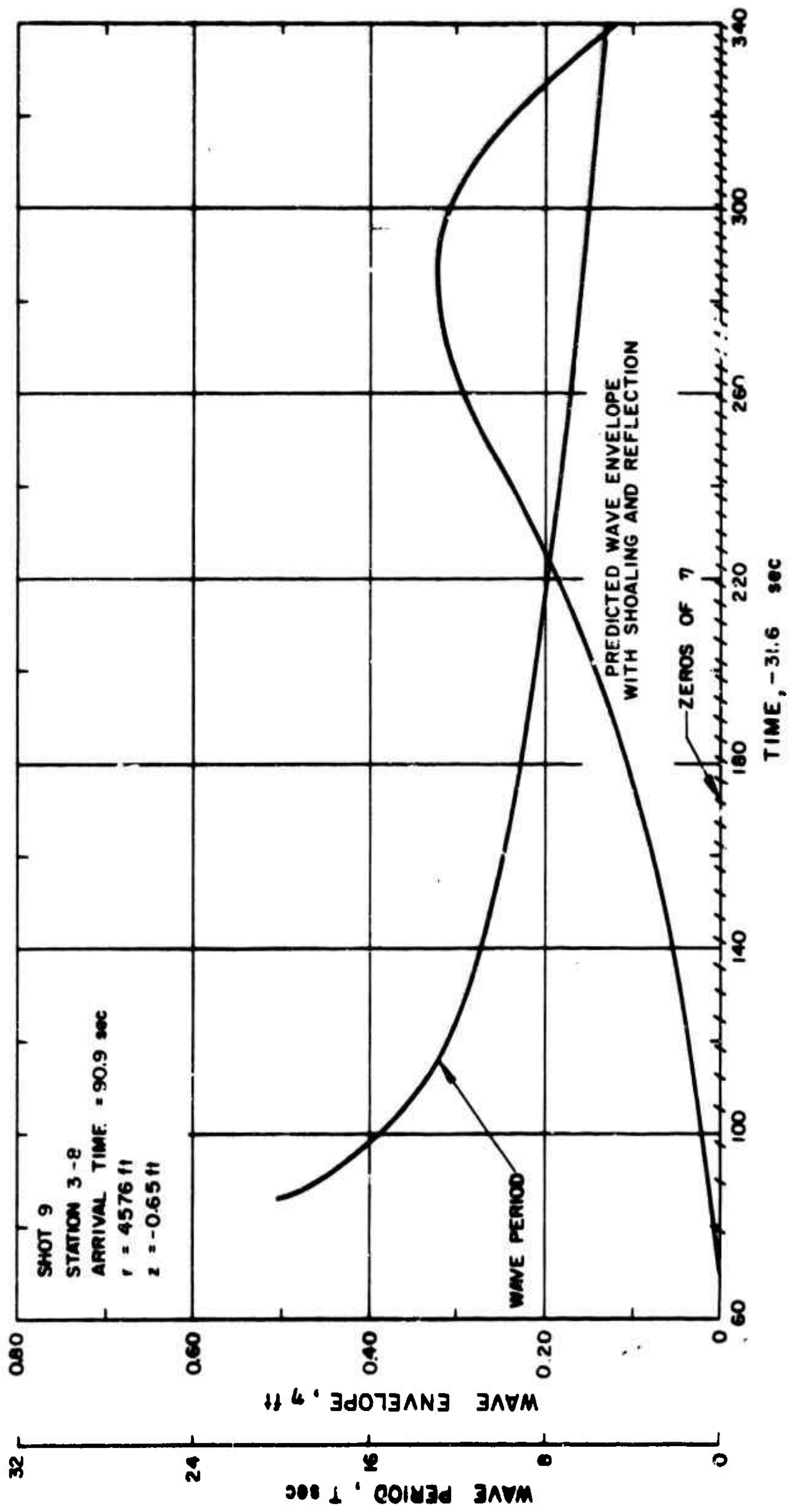

SHOT 9
STATION 3-8
ARRIVAL TIME = 90.9 sec
r = 4576 ft
z = -0.65 ft
WAVE PERIOD
PREDICTED WAVE ENVELOPE
WITH SHOALING AND REFLECTION
ZEROS OF η
TIME, -31.6 sec
WAVE ENVELOPE, η ft
WAVE PERIOD, T sec
0.80
0.60
0.40
0.20
0
32
24
16
8
0
60
100
140
180
220
260
300
340

PB-1 7841

UNCLASSIFIED

Security Classification

DOCUMENT CONTROL DATA - R&D

(Security classification of title, body of abstract and indexing annotation must be entered when the overall report is classified)

1. ORIGINATING ACTIVITY *(Corporate author)*

National Engineering Science Company
Pasadena, California 91105

2a. REPORT SECURITY CLASSIFICATION

Unclassified

2b. GROUP

N/A

3. REPORT TITLE

Contributions to the Mono Lake Experiments

4. DESCRIPTIVE NOTES *(Type of report and inclusive dates)*

Final Report

5. AUTHOR(S) *(Last name, first name, initial)*

Le Méhauté, B. J.
Whalin, R. W.
Webb, L. M.

6. REPORT DATE	7a. TOTAL NO. OF PAGES	7b. NO. OF REFS
October, 1965	193	51

8a. CONTRACT OR GRANT NO.

Nonr 5006(00)

b. PROJECT NO.

c.

d.

9a. ORIGINATOR'S REPORT NUMBER(S)

S 256-2

9b. OTHER REPORT NO(S) *(Any other numbers that may be assigned this report)*

10. AVAILABILITY/LIMITATION NOTICES

Qualified requesters may obtain copies of this report from DDC.

11. SUPPLEMENTARY NOTES

12. SPONSORING MILITARY ACTIVITY

Department of the Navy
Office of Naval Research
Washington, D.C. 20360

13. ABSTRACT

Gravity waves generated by underwater explosions and the wave run-up are predicted for a series of tests to be performed in Mono Lake (California). The time histories of the wave profiles are given at various locations in the lake in deep and shallow water where wave recorders will be installed. The times of arrival and heights of wave run-up are determined at three locations on the shoreline of Mono Lake.

This prediction is done by making use of the most advanced theories and all available information in that field, and some new theoretical developments are presented in Volumes II and III, namely:

1) A linear theory for waves generated by explosions, making use of a symmetric and asymmetric time dependent surface disturbance.

2) A linear theory for the propagation of periodic waves over the continental slope.

DD FORM 1 JAN 64 1473

UNCLASSIFIED

Security Classification

UNCLASSIFIED
Security Classification

14. KEY WORDS	LINK A		LINK B		LINK C	
	ROLE	WT	ROLE	WT	ROLE	WT
Water waves						
Underwater explosions						
Wave run-up						
Waves on a slope						

INSTRUCTIONS

1. ORIGINATING ACTIVITY: Enter the name and address of the contractor, subcontractor, grantee, Department of Defense activity or other organization *(corporate author)* issuing the report.

2a. REPORT SECURITY CLASSIFICATION: Enter the overall security classification of the report. Indicate whether "Restricted Data" is included. Marking is to be in accordance with appropriate security regulations.

2b. GROUP: Automatic downgrading is specified in DoD Directive 5200.10 and Armed Forces Industrial Manual. Enter the group number. Also, when applicable, show that optional markings have been used for Group 3 and Group 4 as authorized.

3. REPORT TITLE: Enter the complete report title in all capital letters. Titles in all cases should be unclassified. If a meaningful title cannot be selected without classification, show title classification in all capitals in parenthesis immediately following the title.

4. DESCRIPTIVE NOTES: If appropriate, enter the type of report, e.g., interim, progress, summary, annual, or final. Give the inclusive dates when a specific reporting period is covered.

5. AUTHOR(S): Enter the name(s) of author(s) as shown on or in the report. Enter last name, first name, middle initial. If military, show rank and branch of service. The name of the principal author is an absolute minimum requirement.

6. REPORT DATE: Enter the date of the report as day, month, year, or month, year. If more than one date appears on the report, use date of publication.

7a. TOTAL NUMBER OF PAGES: The total page count should follow normal pagination procedures, i.e., enter the number of pages containing information.

7b. NUMBER OF REFERENCES: Enter the total number of references cited in the report.

8a. CONTRACT OR GRANT NUMBER: If appropriate, enter the applicable number of the contract or grant under which the report was written.

8b, 8c, & 8d. PROJECT NUMBER: Enter the appropriate military department identification, such as project number, subproject number, system numbers, task number, etc.

9a. ORIGINATOR'S REPORT NUMBER(S): Enter the official report number by which the document will be identified and controlled by the originating activity. This number must be unique to this report.

9b. OTHER REPORT NUMBER(S): If the report has been assigned any other report numbers *(either by the originator or by the sponsor)*, also enter this number(s).

10. AVAILABILITY/LIMITATION NOTICES: Enter any limitations on further dissemination of the report, other than those imposed by security classification, using standard statements such as:

(1) "Qualified requesters may obtain copies of this report from DDC."

(2) "Foreign announcement and dissemination of this report by DDC is not authorized."

(3) "U. S. Government agencies may obtain copies of this report directly from DDC. Other qualified DDC users shall request through
_______________."

(4) "U. S. military agencies may obtain copies of this report directly from DDC. Other qualified users shall request through
_______________."

(5) "All distribution of this report is controlled. Qualified DDC users shall request through
_______________."

If the report has been furnished to the Office of Technical Services, Department of Commerce, for sale to the public, indicate this fact and enter the price, if known.

11. SUPPLEMENTARY NOTES: Use for additional explanatory notes.

12. SPONSORING MILITARY ACTIVITY: Enter the name of the departmental project office or laboratory sponsoring *(paying for)* the research and development. Include address.

13. ABSTRACT: Enter an abstract giving a brief and factual summary of the document indicative of the report, even though it may also appear elsewhere in the body of the technical report. If additional space is required, a continuation sheet shall be attached.

It is highly desirable that the abstract of classified reports be unclassified. Each paragraph of the abstract shall end with an indication of the military security classification of the information in the paragraph, represented as *(TS)*, *(S)*, *(C)*, or *(U)*.

There is no limitation on the length of the abstract. However, the suggested length is from 150 to 225 words.

14. KEY WORDS: Key words are technically meaningful terms or short phrases that characterize a report and may be used as index entries for cataloging the report. Key words must be selected so that no security classification is required. Identifiers, such as equipment model designation, trade name, military project code name, geographic location, may be used as key words but will be followed by an indication of technical context. The assignment of links, rules, and weights is optional.

UNCLASSIFIED
Security Classification